ENTRAINMENT OF FINE SEDIMENTS BY TURBULENT FLOWS

Thesis by

Alexander James Sutherland

In Partial Fulfillment of the Requirements

For the Degree of

Doctor of Philosophy

California Institute of Technology

Pasadena, California

1966

(Submitted May 13, 1966)

ACKNOWLEDGMENTS

For his encouragement and invaluable advice the author expresses his sincere appreciation to Professor Vito A. Vanoni, who served as advisor during the course of this research. The author is also indebted to Professor Norman H. Brooks for his continuing interest in the work and for his willingness to discuss all aspects of it.

For advice and assistance with all phases of the photographic work during the experimental program the author is indebted to Mr. Carl Eastvedt. For their assistance in the preparation of the final draft of this thesis the author extends his gratitude to Patricia Rankin, who so ably typed the manuscript, and to Ron Handy who prepared many of the figures.

Special thanks are due to my wife Judith, to whom this thesis is dedicated, for the innumerable contributions that she made towards the completion of the research program and to the preparation of the manuscript.

The research was performed with the support of National Science Foundation Grants G19194 and GK89. Financial assistance provided by the California Institute of Technology in the form of Graduate Teaching and Research Assistantships is also gratefully acknowledged.

ABSTRACT

A study was made of the means by which turbulent flows entrain sediment grains from alluvial stream beds. Entrainment was considered to include both the initiation of sediment motion and the suspension of grains by the flow. Observations of grain motion induced by turbulent flows led to the formulation of an entrainment hypothesis. It was based on the concept of turbulent eddies disrupting the viscous sublayer and impinging directly onto the grain surface. It is suggested that entrainment results from the interaction between fluid elements within an eddy and the sediment grains.

A pulsating jet was used to simulate the flow conditions in a turbulent boundary layer. Evidence is presented to establish the validity of this representation. Experiments were made to determine the dependence of jet strength, defined below, upon sediment and fluid properties. For a given sediment and fluid, and fixed jet geometry there were two critical values of jet strength: one at which grains started to roll across the bed, and one at which grains were projected up from the bed. The jet strength, K, is a function of the pulse frequency, ω, and the pulse amplitude, A, defined by

$$K = A\omega^{-s}$$

where s is the slope of a plot of log A against log ω. Pulse amplitude is equal to the volume of fluid ejected at each pulse divided by the cross sectional area of the jet tube.

Dimensional analysis was used to determine the parameters by which the data from the experiments could be correlated. Based on this, a method was devised for computing the pulse amplitude and frequency necessary either to move or project grains from the bed for any specified fluid and sediment combination.

Experiments made in a laboratory flume with a turbulent flow over a sediment bed are described. Dye injection was used to show the presence, in a turbulent boundary layer, of two important aspects of the pulsating jet model and the impinging eddy hypothesis. These were the intermittent nature of the sublayer and the presence of velocities with vertical components adjacent to the sediment bed.

A discussion of flow conditions, and the resultant grain motion, that occurred over sediment beds of different form is given. The observed effects of the sediment and fluid interaction are explained, in each case, in terms of the entrainment hypothesis.

The study does not suggest that the proposed entrainment mechanism is the only one by which grains can be entrained. However, in the writer's opinion, the evidence presented strongly suggests that the impingement of turbulent eddies onto a sediment bed plays a dominant role in the process.

TABLE OF CONTENTS

TABLE OF CONTENTS (Cont'd)

TABLE OF CONTENTS (Cont'd)

LIST OF FIGURES

LIST OF FIGURES (Cont'd)

LIST OF FIGURES (Cont'd)

LIST OF FIGURES (Cont'd)

LIST OF FIGURES (Cont'd)

LIST OF FIGURES (Cont'd)

LIST OF FIGURES (Cont'd)

LIST OF FIGURES (Cont'd)

LIST OF TABLES

CHAPTER I

INTRODUCTION

A. INTRODUCTORY NOTE.

Even the most casual observer can see that alluvial streams transport sediment particles. The ability of flowing water to suspend and transport solid particles presents an intriguing problem to those who would seek to explain it. That the majority of the suspended particles have their origin in the boundary of the stream, has been well established. However, the means by which they are removed from the boundary and transferred into the main flow is not so clear. A satisfactory explanation of the mechanics of the entrainment process has not yet been presented. This lack of understanding is one of the reasons why, today, there is still some uncertainty in predictions made about the behavior of alluvial streams.

In the past, many hydraulic engineering works have been built on sediment bearing streams, without adequate consideration being given to the effects of sedimentation on the project. Costly maintenance, and in some cases complete destruction of important engineering works, have resulted from filling of reservoirs by sediment, filling or scouring of canals and channels, and erosion or gullying of adjacent lands. Such experiences have caused hydraulic engineers to consider rivers in a wider sense, that of sediment streams as well as water streams.

The boundaries of an alluvial stream, in particular the bed, are composed of discrete particles which as a result of forces arising

from the flow over them, can be set in motion. To do this the stream must exert some finite force on the particle; that force which is just sufficient to initiate motion may be termed a critical force. It will be a function not only of the particle properties, but also of the arrangement of the particles in the bed. Particles which project above the mean bed level may be expected to have a lower critical force than those which are imbedded in the surface layers. If this critical force is exceeded at any time the particle will move, presumably with a rolling or sliding motion, across the bed. At some stage during this motion a transfer from the bed to the main flow can take place. The particle is then said to be entrained or suspended. A clarification of the mechanism involved in this lifting of the grains from the bed is required. It is a necessary step that will have to be made before the relation between hydrodynamic conditions at the stream bed and the transportation of sediment can be understood.

In recent years much research has been done with the practical objective of obtaining such a relation. Assuming its existence and that it can be formulated in a tractable way, it would be an expression relating sediment discharge to hydraulic parameters and sediment properties. Obtaining such an expression would be a major step in the prediction of such important phenomena as scouring or aggradation of channels, reservoir silting and likelihood of flooding.

Surprisingly few writers have engaged in speculation about the nature of the forces which remove particles from the bed. Many writers are satisfied with the concept of shearing stress being the only important quantity on which to base their analysis. The possibility of

lift forces acting on the grains is seldom considered. A number of ways in which lift forces may arise are easily recognized; the existence of a velocity gradient in the flow, the possibility of stagnation pressure existing under the grains and the existence of upward velocity components adjacent to the bed as a result of turbulence. Analytical studies by Jeffreys (1)*, and experimental studies by Chepil (2), and Einstein and El-Samni (3) tend to confirm the presence of lift forces.

Lift forces must contribute substantially to the ease with which a given drag force can move a particle. If the lift were approximately equal to the weight, then even small drag forces would be sufficient to initiate rolling or sliding. Thus, to be realistic, a model or theory for entrainment should make provision for lift forces as well as shearing forces. Few writers have done so.

In sediment transportation, as in other phenomena of like complexity, many theories and different approaches to the problem have been presented. In the next section a brief historical summary is given which outlines the main contributions to the subject of entrainment and transportation.

B. HISTORICAL SUMMARY

Man has been aware of sedimentation problems for centuries. Records of ancient civilizations in China and Egypt indicate that even in the earliest of times difficulties were encountered. However it was

---

* Numbers in parentheses refer to publications listed in the Bibliography.

not until the eighteenth century that a scientific investigation was made of the problem. Leliavsky (4) presents an account of the early work which was largely of an empirical nature. By contrast, Jeffreys (1), in 1929, presented a theoretical account of grain motion. He was the first to attempt an explanation of the lift exerted on a grain.

Assuming potential flow and using the methods of classical hydrodynamics, Jeffreys computed the upward force exerted on an infinite cylinder lying on the flat bed of a stream with its axis perpendicular to the flow. If the upward force exceeded the cylinder's weight, then the cylinder would be lifted into the flow. For sand and water this criterion implied $U^2 > 1.19\ ga$, where U is the free stream velocity, g is the acceleration due to gravity and a is the grain radius. The relative density of fluid and grain is included in the numerical factor. It is interesting to note that this is actually the "sixth power law" of Brahms and Airy, which was first proposed in 1753, (see Leliavsky page 34). Jeffreys claimed order of magnitude agreement with the experimental results available at that time. Actually the observed values were 3 or 4 times larger than those calculated, which was explained by noting that the calculation referred to a cylinder and not to a grain.

Jeffrey's description of a grain's motion after leaving the bed is intriguing. According to the classical theory, there would be a position above the bed at which lift would balance weight and the particle would remain stationary as the fluid moved past it. In a real fluid, viscosity would cause the flow to lose its irrotationality and the particle would accelerate. Jeffreys continues ..... "Viscous drag

between the solid and the bottom may prevent the ultimate velocity of the solid from being that of the fluid, and some lift may remain, but in any case the solid cannot be permanently suspended..... and in a violent one (current) over a rough bed the transported particles will strike projections on the bed and undergo sudden reductions in their velocity. In either case the jerk when the particle hits the bed again will restore the condition of streaming past a stationary obstacle and the classical flow will begin afresh."

At this stage according to Jeffreys the particle would be lifted, accelerated and deposited again as in a saltating motion. Jeffreys points out that this agrees with observations made by Gilbert (5). The possibility of other than potential flow apparently did not occur to Jeffreys or was considered to be inconsequential.

Other analyses of the initiation of motion have been developed, the two most significant and widely known being those of A. Shields (6) and C. M. White (7). By considering the disturbing forces to be restricted to shear forces, each author derived an expression for a critical shear stress which if exceeded will cause motion. Shields developed a relation

$$\frac{\tau_c}{(\gamma_s - \gamma) d_s} = f\left(\frac{U_* d_s}{\nu}\right)$$

where τ_c is the critical shear stress at the bed, γ_s and γ are the specific weights of the sediment and fluid respectively, d_s is the grain size, ν is the kinematic viscosity of the fluid and U_* is the critical

shear velocity. The function f was presented as a shaded area on what has become known as Shields diagram, a plot of $\frac{\tau_c}{(\gamma_s - \gamma)d_s}$ against $\frac{U_* d_s}{\nu}$. These data were obtained from flume experiments with fully developed turbulent flows over artificially flattened sediment beds. The value of the critical shear stress was determined by Shields from a graph of observed sediment discharge versus shear stress, by extrapolating back to zero sediment discharge.

White (7) obtained a relation for flows in which motion around the grain was laminar, viz $\frac{\tau_c}{(\gamma_s - \gamma)d_s} = 0.18 \tan \theta$, where θ is the angle of repose of the sediment immersed in the fluid. The form of the equation was found by considering the interaction of the drag and weight forces on a grain. The numerical constant was determined experimentally. For turbulent flows he found that the critical shear stress was about one half of that for laminar flows. He attributed the difference to velocity fluctuations in the turbulent flow, which cause fluctuations in the boundary shear stress and in the forces acting on the grain. In pointing this out, White was one of the first researchers to recognize the importance of turbulent fluctuations in the sediment entrainment problem. Neither of these theories, however, sheds any real light on the mechanism whereby grains are plucked from the bed and transferred into the main flow.

In 1933 O'Brien (8) made a substantial contribution by formulating a satisfactory approach to the problem of suspended load. He assumed a state of equilibrium between the rate at which particles fall under their own weight, and the rate at which the fluid lifts the particles by the process of turbulent mixing. This can be expressed

analytically by the equation

$$C w = \epsilon_s \frac{dC}{dy} \tag{1}$$

where C is the concentration of sediment at elevation y above the bed, w is the settling velocity of the sediment and ϵ_s is a diffusion coefficient for sediment. Rouse (9), using a system in which ϵ_s was constant throughout the flow field, was able to obtain agreement between observed sediment concentration profiles and those predicted by integration of equation (1). This established the validity of O'Brien's formulation of the suspension problem in terms of a diffusion equation.

For a stream of depth d in which ϵ_s is not constant everywhere, Rouse (10) presented a solution to equation (1) in the form

$$\frac{C}{C_a} = \left[\frac{d-y}{y}\,\frac{a}{d-a}\right]^z \tag{2}$$

where C_a is the concentration of sediment with a settling velocity w at the level y = a, and $z = \frac{w}{\beta k U_*}$. Both β and k are numerical constants; $\beta \doteq 1.0$ and the von Karman constant, $k \doteq 0.4$. In 1942 Anderson (11), in natural streams, and Vanoni (12), in a laboratory flume, were able to show that equation (2) was of the correct form. However, it did not agree quantitatively with the experimental measurements. Since that time the reasons for these discrepancies have been investigated, and the effect of suspended sediment on flow characteristics has been well documented. The reader is referred to the Progress Report of the Task Committee on Preparation of Sedimentation Manual section D,

"Suspension of Sediment", published in the Journal of the Hydraulics Division, Proc. A. S. C. E. Volume 89, (1963). A quote from a discussion of Kalinske and Pien's 1943 paper (13) by J. W. Johnson, which appears immediately following the paper, sums up the feeling about this portion of the sedimentation problem. "The author's experimental data in addition to the data of other investigators taken in recent years appear to verify, for all practical purposes, the general theory of the vertical distribution of suspended sediment in a turbulent stream of water. This theory permits the total suspended sediment load transported in a vertical section to be estimated from a determination of the concentration and the particle size distribution of the sediment at a single point in the vertical, and the hydraulic characteristics of the stream".

The theory of suspended load must fail in the region close to the bed because Equation (2) predicts concentrations approaching infinity as y tends to zero. This is a physical impossibility. Another restriction on the theory is revealed when the total sediment load is computed. The boundary condition at the bed is unknown in the sense that the choice of the reference level, a, can be made arbitrarily. A significant portion of the total sediment load is transported close to the bed, which suggests a need for a theory applicable to this region.

Many equations have been suggested for the prediction of the rate of bed load transportation as a function of flow conditions and sediment properties. Some of the later ones may correctly be termed total load relations because they do account explicitly for the suspended load. Most of these formulae are empirical, being derived from

limited sets of experimental data. A summary of the more noteworthy ones is given in Chapter 6 of reference (14). Figure 7.4 of that report shows that the results obtained by using them, are just as dissimilar as the appearance of the formulae themselves.

Recently two bed load equations, which may be termed theoretical, have been presented. Kalinske (15) and Einstein (43) both derived, from different sets of explicit assumptions, relationships which allow a prediction of the bed load to be made. Kalinske's development is interesting because of the manner in which he allowed for the fact that the forces acting on a grain are not constant, but are fluctuating. He treated these variations by assuming that the velocity fluctuations followed the Gaussian frequency law. Some of the assumptions that he made in his analysis are difficult to accept. For example, he equated the number of particles in motion to the number of particles on the bed, which seems to imply that regardless of the transport rate the number of particles in motion is constant. Einstein also recognized the influence of turbulence on bed load movement, but his physical model of grain motion is questionable. He visualized the movement of a sediment grain as a series of jumps, the mean length and frequency of which are functions only of its size. Observations by the writer of grain motion in a laboratory flume show this concept to be unrealistic.

All of these approaches suffer from the same defect, that of not understanding the entrainment mechanism. Many do not even attempt to define the conditions existing in what may be called the interchange region between the bed and the main flow. In order to examine conditions adjacent to the bed, measurements have been made

of the forces exerted on rough boundaries by a flowing fluid. The most informative are those of Einstein and El-Samni (3), in water, and Chepil (2),(16),(17), in air.

The former measured the forces exerted by a turbulent flow on plastic hemispheres, 2.7 in. in diameter, glued in a hexagonal pattern onto a flat surface. By assuming a theoretical wall at 0.2 sphere diameters below the tops of the spheres, the authors found that all velocity distributions plotted as straight lines on semi-logarithmic paper. The slope of these lines is equal to $\frac{2.3U_*}{k}$ from which the boundary shear stress $\tau_o = \rho U_*^2$, can be determined. A value of 0.4 was assumed for k , the von Karman constant. The lift force was determined from measurements of the pressure difference, Δp, between the top and the base of the hemispheres. They found that

$$\Delta p = C_L \frac{\rho U^2}{2}$$

where C_L was constant and equal to 0.178 if U was the flow velocity measured at 0.35 sphere diameters from the theoretical wall. With these results and using the friction formula for flow over a rough boundary, one can show that the lift force is approximately equal to three times the drag force. They extended their experiments to natural gravels and found that to have the theoretical wall at 0.2D below the upper surface of the grains, where D is a representative grain size, it was necessary to choose D_{67} as being representative of the sample. By definition, 67% by weight of the grains are smaller in

size than D_{67}. For the lift on natural gravels, they again found

$$\Delta p = 0.178 \frac{\rho U^2}{2}$$

with U measured at 0.35 grain diameters from the theoretical wall. Here, the representative diameter had to be taken as D_{35}. This is considerably different from that describing roughness, D_{67}, but equals that size which Einstein (43) found to be the size required to describe the sediment mixture in his bed load equation. This agreement would seem to be significant, if indeed lift is a factor in sediment transportation. Einstein describes it as "a major moving force of bed load". The writer agrees with this statement.

Chepil, (2),(16),(17), has published three interesting papers on the lift force due to a horizontal wind, experienced by grains resting on the surface of the ground. By both direct and indirect methods, the latter being measurements of pressure distributions, he found in reference (2) that the average lift on hemispheres ranging from 0.16 cm to 5.08 cm in diameter, was equal to about 85% of the drag. This figure was apparently unaffected by the shear velocity, size of the hemispheres, or thickness of the boundary layer. He concludes that lift is an important feature in the initiation of grain motion. An interesting part of this paper is the comparison made with Einstein and El-Samni's work which was done in water. By introducing a scaling factor, determined from experiments, to compensate for the different methods used in obtaining the pressure differences, he found

$C_L = \frac{\Delta p}{1/2 \rho U^2} = 0.062$ for Einstein and El-Samni and $C_L = 0.068$ for Chepil. This would indicate, he claims, that the mechanism by which lift is produced is the same in both cases. The writer feels that the conclusion is too strong because the correction factor appears to be arbitrary and the two sets of experiments were made at very different Reynolds numbers.

In 1959 Chepil published the results of a study designed to evaluate the effects of turbulent fluid motion on the grains. By using a system of strain gages attached to a sediment grain, a record of the instantaneous values of lift and drag was obtained. The mean values agreed well with his previous study. The ratio of maximum to mean lift and drag was found to be approximately 2.5 which is the figure used by both White (7) and Kalinske (15) in their theoretical treatments.

In reference (17), Chepil measured the lift and drag on spheres at different heights above the surface. Pressure measurements were the only data taken, lift being computed from the pressure distribution. He found that lift decreased with elevation, becoming virtually zero at 3 to 4 grain diameters above the bed. Increased shear velocity and ground roughness both resulted in increased lift. Chepil draws two main conclusions: "....lift is caused by a steep velocity gradient near the ground....", and "....lift alone is too small to cause saltating grains to rise as they do, essentially vertically."

The experimental arrangement used to measure pressures, which was an inclined tube manometer, was such that the pressures recorded were mean values. Thus a time average value of the lift was obtained. For a grain in a fluid it is the instantaneous value of

the lift that is important; when it is large the grain rises and when it is small or negative it will sink. The mean value going to zero away from the wall is not an indication of zero lift, but indicates that there are as many positive lifts as negative lifts. This must be true in a turbulent flow region where the effect of the wall is becoming less pronounced. The writer must disagree with Chepil's conclusions as he has stated them. A fair conclusion would be that lift is aided by a steep velocity gradient.

Since 1960 there have been many more sophisticated investigations into the flow structure beneath a boundary layer. Some of these are discussed in Section II-B.

C. PURPOSE AND SCOPE OF THIS INVESTIGATION.

The aim of the present research is to obtain an insight into the mechanism by which sediment grains are first moved and subsequently entrained by a flowing stream. Interest is concentrated on the interchange region between the flow and the sediment bed, for it must be the conditions in this region that control the entrainment process. These conditions are those existing in a turbulent boundary layer.

There are many reports of both experimental and theoretical work on turbulent boundary layer flow over rigid walls. However the sediment entrainment problem is further complicated by the presence of a boundary composed of particles. If the forces applied by the fluid exceed a critical value the particles move and the boundary changes shape. The apparent complexity of the fluid and grain interactions precludes the use of an analytical treatment. Consequently, the

research reported here is based entirely upon observations made of the manner in which sediment grains are moved by a turbulent fluid flowing over them.

In Chapter II observations of grain movement, at the bed, under the action of turbulent fluctuations are described, and a brief literature survey on flow conditions adjacent to a boundary is presented. An entrainment theory based on the ability of turbulent bursts to impinge upon the boundary is then presented. Chapter IV deals with an experimental study of a pulsating jet acting on a sediment bed. This jet provided a simple model which simulated the impact of turbulent bursts on a sediment bed. Two aspects of the jet are investigated. Corresponding values of jet amplitude and frequency, which produced grain motion, are determined for a wide variety of conditions. Jet amplitude is defined as the volume of fluid ejected at each pulse, divided by the cross-sectional area of the tube from which the jet issued. A study is then made of the flow field of the jet. Flow visualization techniques are used in conjunction with still photography and motion pictures.

Chapter V outlines experiments, performed in a laboratory flume with a sediment covered bed, which sought to obtain evidence substantiating the entrainment hypothesis put forward in Chapter II.

CHAPTER II

BASIS FOR ENTRAINMENT HYPOTHESIS

A. INITIAL EXPERIMENTS.

In a study of sediment entrainment the most important region of flow is that adjacent to the sediment bed. The flow conditions in this interchange region must govern the exchange of sediment particles between the moving fluid and the boundary. It is imperative that careful observations be made of both the movement of sediment particles and of the subsequent deformation undergone by the bed. In a flowing fluid it is extremely difficult to make observations of this nature. Some broad conclusions can however be arrived at by watching the flow through transparent panels in the sides of laboratory flumes; this has been done by previous investigators.

Deacon (18) made observations of sand movement in water in a glass-sided trough. His sand was obtained from the estuary of the Mersey River but no details are given as to its mean size or size distribution. From his remarks it can be deduced that the base of his trough was completely covered with grains. He noted that the first movement of isolated sand particles was observed at a water surface velocity of 1.3 ft/sec. These grains arranged themselves in bands like "ripples on the sea shore." He continues ..."At this velocity the profile of each sand ripple had a very slow motion of translation caused by sand particles running up the flatter slope and tumbling over the crest. ...A critical velocity was reached when the surface of the water moved at 2.125 ft/sec, when the sand ripples became very

irregular, indicating greatly increased unsteadiness of motion of the water. At about this critical velocity the particles were occasionally carried by the water direct to the next crest; and as the velocity of the water was gradually increased an increasing bombardment of each crest from the one behind it took place. At about 2.5 ft/sec, another critical velocity was reached and many of the little projectiles cleared the top of the first, or even of the second crest ahead of that from which they were fired." The scour thereafter, he states, was a different phenomenon; sand and water being mixed in a constant process of lifting, carrying and deposition. The average height that the grains reached appeared to depend on the velocity.

It is unfortunate that Deacon did not report some more details about his flow; for example, the flow depth and the slope of his trough. The velocities mentioned are meaningless without the corresponding depth being given. His statements on the formation and movement of ripples are substantially correct, but the reference to projectiles being fired from crest to crest is a little misleading.

Gilbert (5) also an early worker, made similar observations, but recorded the details of the flow more accurately. He states:-

"Streams of water carry forward debris in various ways. The simplest is that in which the particles are slidden or rolled. Sliding rarely takes place except where the bed of the channel is smooth. Pure rolling, in which the particle is continuously in contact with the bed, is also of small relative importance. If the bed is uneven, the particle usually does not retain continuous contact but makes leaps, and the process is then called saltation. With swifter currents leaps

are extended and if a particle thus freed from the bed be caught by an ascending portion of a swirling current its excursion may be indefinitely prolonged. Thus borne it is said to be suspended."

It is not specifically mentioned in either of these statements, that the sand grain movement is discontinuous. The grains move sporadically and not always in the direction of the main flow. By observing a sand bed under the action of a flow which is just sufficient to disturb the grains, this intermittent motion is very easily detected. It occurs in bursts over a small area. At each burst grains move simultaneously, and then the area remains undisturbed for a period until another short burst occurs. Gusts produced by turbulence near the bed must be responsible for this effect. That the movement of bed material in general is greatly influenced by the presence of the turbulent bursts, is by now generally acknowledged. As bursts increase in intensity, usually as a result of an increase in flow velocity, the motion of the particles becomes more violent and after a certain point they are projected into the flow as suspended load.

If a sand bed is allowed to deform under the action of a fluid flowing over it, the bed will eventually reach a stage in which those parameters characterizing its geometry become constant. The time required for this equilibrium state to be reached is dependent on the properties of both the sediment and the flow and particularly on the transport rate of the sediment. It is usually of the order of a few hours in a laboratory flume for low and moderate transport rates.

Since an equilibrium state is reached by the fluid and the bed, one may expect that a relationship exists among the several variables

involved. These include particle and fluid properties, sediment concentration in the bed and adjacent to it, together with the flow and turbulence characteristics. An attempt to determine the important parameters of the problem was made using a turbulence jar. This jar, used by Rouse (9) in his investigation of the mechanics of sediment suspension, is essentially a cylindrical glass jar, 12 inches in diameter and 24 inches high, inside of which is a lattice structure which can be made to oscillate vertically in simple harmonic motion. The chief advantage offered by the jar is that a turbulent flow can be reproduced and maintained at will, a necessity for this study. Other advantages obtained by its use include good control of bed material of which only a limited quantity is required, and various fluids of different viscosities and densities can easily be used.

After a few preliminary runs it became clear that an exhaustive investigation of flow parameters, although valuable, was not the most pertinent aspect of the experiments. Rather, the sequence of events at the bed under conditions of fixed stroke and increasing frequency of lattice oscillation, and thus turbulence intensity, was of greater interest.

At the start of the experiment a levelled sand bed approximately $\frac{1}{2}$ in. in thickness, was prepared on the base of the jar. The lattice was then inserted and a value for the stroke selected. At low frequencies the agitation had no observable effect on the sand grains. When the frequency was increased slowly, a point was reached at which isolated grains would rock slightly and then fall back into their original position. This occurred at many points on the sand bed.

If the frequency was increased again, some of the grains began to move. The motion was one of sliding and rolling across the bed in short bursts with no preferred direction. The bed took on a roughened appearance with slight depressions appearing, which did not persist. At this stage there were no grains leaving the bed and the fluid was clear throughout the jar. With further increase in frequency, the sand grains moved in an entirely different manner. They could be seen leaving the bed in gusts, i.e. a number of grains from a small area would suddenly leap vertically and go into suspension. A small crater was left on the bed. These craters appeared in a random array if one disregarded the lattice-caused regularities. The overall appearance of the bed at this stage was that of a moonscape. The impression was given, of a surface onto which a number of objects had impacted causing the crater-like depressions. At still higher frequencies violent scouring action took place, with the subsequent entrainment of many grains. It was impossible to observe any details of the motion at this stage, because of the high concentration of suspended grains near the bed. If the agitation was then reduced or stopped, the grains settled to the bed which then appeared as a highly disturbed surface of rounded hills and hollows. Again there was no obvious geometric pattern. A parallel can be noted between these observations and those of Gilbert (5) given previously.

The sequence of events just outlined is similar to the sequence which occurs on a bed composed of sand grains with mean sieve size in the range 0.1 to 2.0 mm as the flow velocity over it is increased. Observations made by the writer of sand movement in flumes will be

described in detail in Chapter V. Flow conditions slightly in excess of those required to initiate grain motion, result in a pattern of movement which bears a close resemblance to that observed in the jar at low frequencies. These similarities have led to the conjecture that the grain motion may be caused or affected greatly by jet-like bursts of flow impinging onto the bed. To explore this more fully it is necessary to consider the type of flow that can be expected adjacent to the boundary of a flowing stream. Stream flows will always be turbulent, and so turbulent flow near a wall is considered first.

B. TURBULENT FLOW NEAR A WALL.

The complexity of turbulent fluctuations has so far prevented the development of a completely theoretical formulation for the turbulent flow of a single phase fluid. With the addition of a boundary composed of discrete particles which are free to move, the problem is complicated even further. Some broad statements and conclusions can however be made.

In turbulent flows, the velocity and pressure at a fixed point in space do not remain constant with time, but perform very irregular fluctuations of high frequency. The fluid elements which perform such fluctuations are macroscopic fluid lumps of varying sizes. These fluid lumps have their own intrinsic motion which is superimposed upon the main flow. They move as a unit for a short period of time, before disintegrating and losing their identity in the surrounding fluid. With the exception of layers near the wall, the lumps or eddies are distributed throughout the flow field in some random manner.

Close to the wall the flow can be divided into two regions: a thin viscous sublayer where the velocity gradient is a maximum, and the adjacent region in which the turbulence intensity is a maximum. A boundary, any definition of which would necessarily be a little vague, must then exist between the turbulent region and the viscous sublayer. There will certainly be an exchange of fluid across the boundary. An eddy close to and moving towards this boundary, will persist as an eddy and penetrate into the viscous sublayer.

It is proposed that those eddies that have sufficient velocity to penetrate down to and impinge upon the sand bed, are responsible for the local disturbance of the surface layer of grains. This would imply that the viscous layer is actually an intermittent layer which is being continually disturbed and then reforms.

Evidence of velocity fluctuations at the boundary has been supplied by numerous investigators. Fage and Townend (19) in 1932, using an ultramicroscope to follow extremely small particles in water, made observations in the sublayer. They were able to record at values of $y^+ = y\frac{U_*}{\nu}$ of the order of 0.1. Here y is the distance from the wall, U_* the shear velocity and ν the kinematic viscosity. Their observations convinced them that, in their words, "the flow was indeed laminar like but the motion could not be called rectilinear." It appeared to be sinuous, and large lateral excursions were made by groups of particles, indicating perhaps, the intrusion of an eddy. They also noted that some fluid seemed to be ejected away from the wall. Nedderman (20), by using stereoscopic photography was able to show velocity fluctuations well within the sublayer at $y^+=1$. Runstadler (21),

after an exhaustive study using dye and hydrogen bubbles, concluded that the wall layer, $y^+<10$, had a regular structure of low and high longitudinal velocity streaks. The location of these streaks varied continually over the wall surface due to "the irregular break-up and ejection away from the wall layer of the low speed, momentum deficient streaks." The ejection must have been similar to that noted by Fage and Townend. They also noted that the ejected streaks followed a parabolic-like trajectory as they moved away from the wall layer and were carried downstream. This is perhaps what one would expect to occur after an eddy has impacted with the wall, and in effect, bounced back.

From a series of dye injections into the sublayer of a turbulent flow in a pipe, Einstein and Li (22) concluded that the flow in this region was inherently unstable. They postulated a model which visualized a periodic growth and rapid decay of the sublayer. However they did not indicate over how large an area the cycle takes place; whether it is very localized or whether it occurs simultaneously over a much larger area. From observations of sand grain movement in a boundary layer, the writer feels that the former possibility would be more realistic. Einstein and Li obtained very good results with their prediction of velocity profiles from their model. There is one arbitrary constant that was determined so that the best fit of their predictions and Laufer's data (23) was obtained. This was the number of boundary layer thicknesses above the boundary at which the representative velocity was measured. Values of 2.0 to 3.0 gave the best fit. This is an indication that the bulk flow parameters are the

important ones. Vanoni (24) has supplied some additional evidence to support this concept. From his observations of the time between successive bursts of sand grain movement, he was able to determine the period of breakdown of the sublayer. Using U as the flow velocity in the main flow, and Einstein's formula (22) for the period $T=\frac{4}{\pi}\frac{U^2\nu}{U_*^4}$ he found periods for conditions producing critical movement of from 2.6 to 3.8 secs. Observed values ranged from 1 to 3 secs, giving order of magnitude agreement.

The idea of an intermittent sublayer is not new. Chemical engineers have used it to explain diffusion and mass transfer from walls. Danckwerts (25) in 1951 appears to have been the first to propose that fluid at the boundary is continually being replaced with fluid from the main flow. Eddies, which are pictured as continually sweeping away the fluid adjacent to the wall, are assumed to be responsible for the intermittency. Hanratty (26) has taken this "discontinuous-film model", as he describes it, and put it into a mathematical form which predicts concentration and velocity profiles. Agreement with experimental results for both profiles is good. As in the theory of Einstein and Li (22), an arbitrary probability function for contact time with the wall is taken. It is shown however, that the particular form of the probability function does not greatly affect the calculated profiles. Einstein and Li's, and Hanratty's papers are important because they show that a flow model based on an unsteady sublayer can predict mean velocity and concentration profiles. A steady sublayer model can also predict velocity profiles, but it lacks the corroboration of experimental observation. Hanratty (27), (28) also investigated the

unsteady nature of the sublayer experimentally. From measurements of fluctuations in the mass transfer rate, he concludes that the flow disturbances are elongated in the direction of flow which, since the eddies will have a streamwise velocity, is physically reasonable. In the 1963 paper (27), a plot of Reynolds number based on pipe diameter and mean velocity, against the time average mass transfer coefficient is presented. At a Reynolds number of 2000 the curve shows an abrupt break which must be linked with the onset of turbulence in the pipe. Since, as Hanratty pointed out, the mass transfer rate is controlled by the conditions in the sublayer, the inference is that the onset of turbulence in the main flow has changed the nature of the sublayer. The change is thought to be the penetration of it by turbulent eddies. A further result that ties in with Vanoni's work,(24), is that the time scale of the fluctuating mass transfer process was dependent on the bulk flow parameters.

Lin, Moulton and Putman (29), who were also looking for evidence of eddies adjacent to the boundaries of a flow, performed a comprehensive set of experiments on mass transfer from walls. They conclude ..."The results prove definitely that the laminar type of film for molecular diffusion does not exist near the wall. Thus small amounts of eddies become very appreciable when the diffusivity is very low or the Schmidt group is very high." The first part of the statement is very sweeping and conclusive, and as such is open to debate. The second part is more interesting for the purposes of the writer because sand in water is an extreme case of high Schmidt number. The Schmidt number is defined as the ratio $\frac{\nu}{D^*}$ where ν is the kinematic viscosity

of the fluid, and D^* is the diffusivity of the diffusing substance. The value of D^* in sediment studies is zero.

Additional evidence of the importance of turbulent eddies on the flow at the boundary, is provided by Bacalso (30) from a different context. By using a lens system he was able to observe very carefully the initiation of motion of sand grains under a growing boundary layer in a flume. The boundary layer was laminar for approximately four feet from the inlet box; thereafter it went through a transition region and was turbulent for the rest of the flume. Near the critical conditions for movement, sediment motion was observed to occur only in the downstream section of the flume, i.e. under the transition and turbulent portions of the boundary layer. To illustrate this the following table has been extracted from Bacalso's results.

TABLE 2-1

Data on Grain Motion. Taken from Bacalso, (30).

Depth ft	Free Stream Velocity ft/sec	Station of Observation ft	Boundary Layer	Intensity of Grain Motion
0.269	0.656	2	lam	none
	0.662	5	trans	negligible
	0.686	7	turb	small
	0.707	9	turb	critical
	0.714	10	turb	critical

The sediment used in this run was glass beads with a mean size of 0.037 mm.

One concludes that the grain motion is facilitated by the presence of the turbulent flow over the sublayer. As the boundary layer changes from laminar to turbulent the nature of the sublayer evidently changes from continuous to intermittent, resulting in the observed differences in sediment behavior with distance from the flume entrance. This result is analogous to Hanratty's change in mass transfer rate with the onset of turbulent flow which was mentioned above.

Based on the experimentally observed effects just presented, namely the increased effectiveness of a turbulent flow in a mass transfer process and the ability of turbulent fluctuations to disrupt the viscous sublayer, an hypothesis for the mechanism of sediment entrainment is proposed in the next section.

C. ENTRAINMENT HYPOTHESIS.

Turbulent flow has been presented as a superposition of eddies of various sizes and vorticities. It is hypothesised that these eddies play an important part in the mechanism of grain motion and suspension by disrupting the viscous sublayer, adjacent to the boundary, and impinging directly onto the surface layer of grains.

Clearly the structure of the eddy is an important factor in this hypothesis. The eddy is a fluid region of macroscopic size moving through the surrounding fluid as a unit. Fluid within the eddy is also in motion. This will be a spinning motion which gives rise to the

vorticity associated with the eddy. A simple configuration to which an eddy can be likened, is Hill's spherical vortex (31). This consists of a combination of the potential flow due to a sphere moving through a fluid at rest, and of vortex motion within the sphere. The two motions can be matched so that there is no discontinuity in pressure or velocity across the sphere boundary. The eddy is thus pictured as a turbulent fluid region which exhibits some coherent motion and is capable of impinging upon the boundary.

Consider now a flat bed of sediment over which a turbulent stream is flowing. We assume that the conditions are such that the mean shear stress on the bed is not sufficient to cause grain motion. Assume also that an eddy approaches the bed. First, if it is a 'weak eddy', either because it breaks up before quite reaching the bed or it sweeps by at a finite distance from the bed, the grains will be unaffected by it.

If, however, it is a 'stronger eddy' it will reach the boundary, actually making contact with the sediment grains. As it nears the boundary, the eddy will be distorted in shape, resulting in a stretching of the vortex lines within the eddy. The velocity of the fluid particles making up the eddy must then be expected to increase. Depending upon the direction of rotation of these fluid particles, the boundary shear stress will be increased or decreased over an area comparable in size to that of the eddy. Observations of water flow over beds of fine sand with mean size in the range of 0.1 to 1.0 mm, near critical conditions for initiation of motion show this area to have a diameter of about one half to one inch. Under the action of the eddy the value

of the critical shear stress for grains may be exceeded for a short instant of time and the grains will be dragged across the bed. The size of the eddy is very much larger than the individual grains, and hence many grains will move. They will come to rest outside the area of influence of the eddy, or after disintegration of the eddy upon hitting the wall.

A small secondary effect that may be present under these conditions is the following. Fluid actually within the bed will be disturbed, and it is conceivable that fluid displaced from within the grain mass will be forced through the grains causing a loosening of the surface layers. This can merely act as an aid to grain motion and is certainly not the primary cause of motion.

If a still stronger eddy approaches the wall, where 'stronger' implies greater vorticity and thus kinetic energy present in the form of rotating fluid, the grain disturbance will be of a more violent nature. Consider the forces acting on a grain when it is under the influence of an eddy. There are two types of restraining forces; that force due to the grain's immersed weight and those forces due to interference of neighboring grains. These are opposed by the fluid drag and the forces arising from the pressure gradient which exists within the eddy. The fluid drag force, determined in part by the viscosity and relative velocity, will act in the direction of the local velocity. At the bed this will be a horizontal velocity and the grains will roll. Adjacent to the bed the velocity will be inclined at a small angle to the bed, as a result of the rotation within the eddy. The resultant force on a grain projecting above the mean bed level can thus

have two components, one horizontal and one vertical.

If the grains were the same density as the fluid there would be no weight force, and they would follow the trajectory of the fluid particles, viz a curved path away from the bed. With sand in water the density ratio is approximately 2.6, and hence with its greater inertia, the grain will follow a path of greater radius than the fluid particles in its vicinity. Since the grain has a weight force directed downwards, it cannot leave the bed unless the vertical component of the fluid forces is approximately equal to the grain weight. Factors such as interlocking of grains, particularly if they happen to be angular, and the possibility of a grain rolling up on top of another and being projected into the flow under the influence of its inertia, account for the above use of the word 'approximately'.

By assuming the effect of the forces arising from the pressure gradient within the eddy to be small, it can be said that an exposed grain will leave the bed when the vertical velocity component associated with the eddy is comparable with the fall velocity of the particle. If it is much less than the fall velocity, the particle will roll across the bed under the action of the horizontal velocity component. If it is much greater than the fall velocity, then a particle which projects above the mean bed level will move along a curved path leading away from the bed.

Figure 2-1 presents an idealized concept of eddy impingement. The eddy approaching the sediment bed is pictured as a region of flow in which the fluid motion is somewhat coherent. A rotating motion is indicated in the figure. The eddy is squashed upon impact with the bed

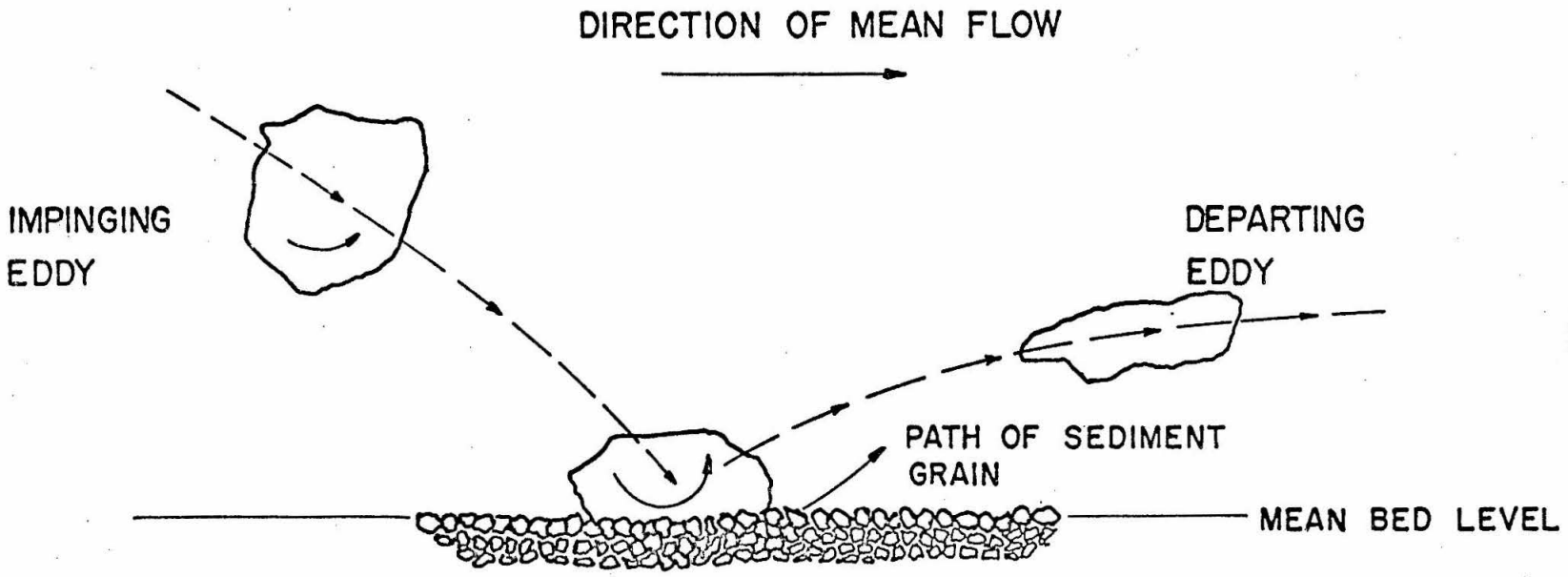

Fig. 2-1 Idealized concept of eddy impingement onto a sediment bed.

and leaves in a downstream direction. In accordance with the work of Runstadler (21), which is discussed fully in Chapter V, the fluid leaving the wall is drawn in the form of an elongated eddy. The path to be followed by the sediment grain is shown as a curve, leading away from the bed, and of radius greater than that followed by the fluid particles within the eddy. It is assumed that for the conditions shown in the figure, the vertical velocity component of the eddy motion exceeds the fall velocity of the grain. If this is not true then the grain will roll across the bed.

Once in motion away from the bed, the grain is susceptible to the influence of turbulent fluctuations which exist in the main flow. In laboratory flumes the sublayer thickness, defined as $\delta = 11.6\frac{\nu}{U_*}$, where ν is the kinematic viscosity of the fluid, and U_* is the shear velocity, is usually between 1.5 and perhaps 20 or 30 grain diameters. The former figure corresponds to coarse grains and the latter to fine grains. By being projected away from the bed a distance approximating the sublayer thickness, the chances of a grain being influenced by the turbulent fluctuations are great. Entrainment is then essentially a question of whether or not an upward velocity in excess of the grain's fall velocity occurs before the grain settles back to the bed.

So far the discussion has been concerned with the question of motion on a flat bed. At much higher flow velocities the sediment bed becomes rippled or dune covered, and other factors contribute to grain entrainment. One of the most effective factors is the presence of dune crests. Even weak eddies, if they cause particles to roll up to a dune crest, can be responsible for transferring grains from the bed to the

main flow. The crest is a region of high mean velocity and the grain, by virtue of its inertia, is launched from the crest. Once launched it is susceptible to the action of the free stream turbulence which can result in suspension. Many grains are entrained in this manner. Strong eddies will still cause entrainment as outlined previously, however the dune bed actually aids this process. On the back slopes of the dunes the flow is directed more towards the bed, while in the dune troughs there is a region of relative calm where the eddies can readily come into contact with the surface grains. A further discussion of how a dune bed aids in entrainment is presented in Chapter V.

In summary, the mechanism proposed in the entrainment hypothesis has two important features. Near the conditions of incipient motion it provides the necessary increase in the local shear stress to cause grain motion. It also provides a means by which a vertical velocity component can be induced adjacent to the bed.

The sequence of events that the entrainment hypothesis envisions as occurring at the bed can be listed as follows:

A. Near conditions of incipient motion.
    1. Turbulent eddies disrupt the viscous sublayer and impinge onto the surface layer of grains.
    2. The swirling motion of the fluid within the eddy increases the local shear stress, exceeding the critical value for grains and causing rolling.
    3. If the bed is dune covered, the motion will occur first in those regions where the most violent eddy action may be expected.

B. At higher rates of sediment transportation.

1. Turbulent eddies impinge onto the surface layer of grains.
2. The swirling motion within the eddy increases the drag force on the grains and accelerates them. Some, by virtue of their size or because they are rolled up and over neighboring grains, project above the mean bed level. In such a position they are susceptible to the vertical velocity component of the fluid motion within the eddy. If this velocity component exceeds their fall velocity, the resultant drag force on the grains will be inclined at a small positive angle to the bed. Under these conditions grains will leave the bed.
3. Other small effects can contribute to a grain's upward motion; e.g. the pressure gradient within the eddy and the possibility of it being projected into the flow as a result of collisions with neighboring grains.
4. If the sediment bed is dune covered, the bed features aid the entrainment process, the troughs and back slopes of the dunes being the most active regions.

To investigate these hypotheses a simple experimental model was built. It consisted of a device capable of producing a pulsating jet. The effects of this jet on numerous sediment beds were studied. The remainder of this thesis presents the results of these studies and some evidence showing the appropriateness of the pulsating jet model.

CHAPTER III

EXPERIMENTAL APPARATUS AND PROCEDURE

A. APPARATUS.

1. Pulsating Jet

A large part of the experimental program was aimed at investigating the effect of a pulse of fluid impacting on a bed of sediment grains. This was achieved by the use of a pulsating jet directed towards a sediment bed.

A distinct advantage that a pulsating jet has over a single pulse is that observations of grain movement are greatly facilitated by having the pulse repeated as many times as desired without interruption. A disadvantage that is incurred, is that the jet exit velocity is not as uniform during a pulse, as it might well be with a single shot, but is sinusoidal. It was thought that the details of the jet velocity at generation would not have any appreciable effect on the results produced at the sediment bed.

The equipment, which is shown in Figure 3-1, consisted of a motor-driven reciprocating pump which produced a series of pulses from the end of a brass tube. During the experiments this tube was placed vertically in a tank of still water. The dimensions of the tank were 14 in. by $8\text{-}\frac{1}{2}$ in., and it was filled to a depth of 9 in. The end of the tube, from which the pulse issued, was located near the center of the tank and approximately 2 or 3 in. above the base. Before each experiment, a sediment bed of loose grains was placed in the bottom of the tank and carefully levelled. Observations of grain movement under the action of the jet, were made through the glass walls of the tank.

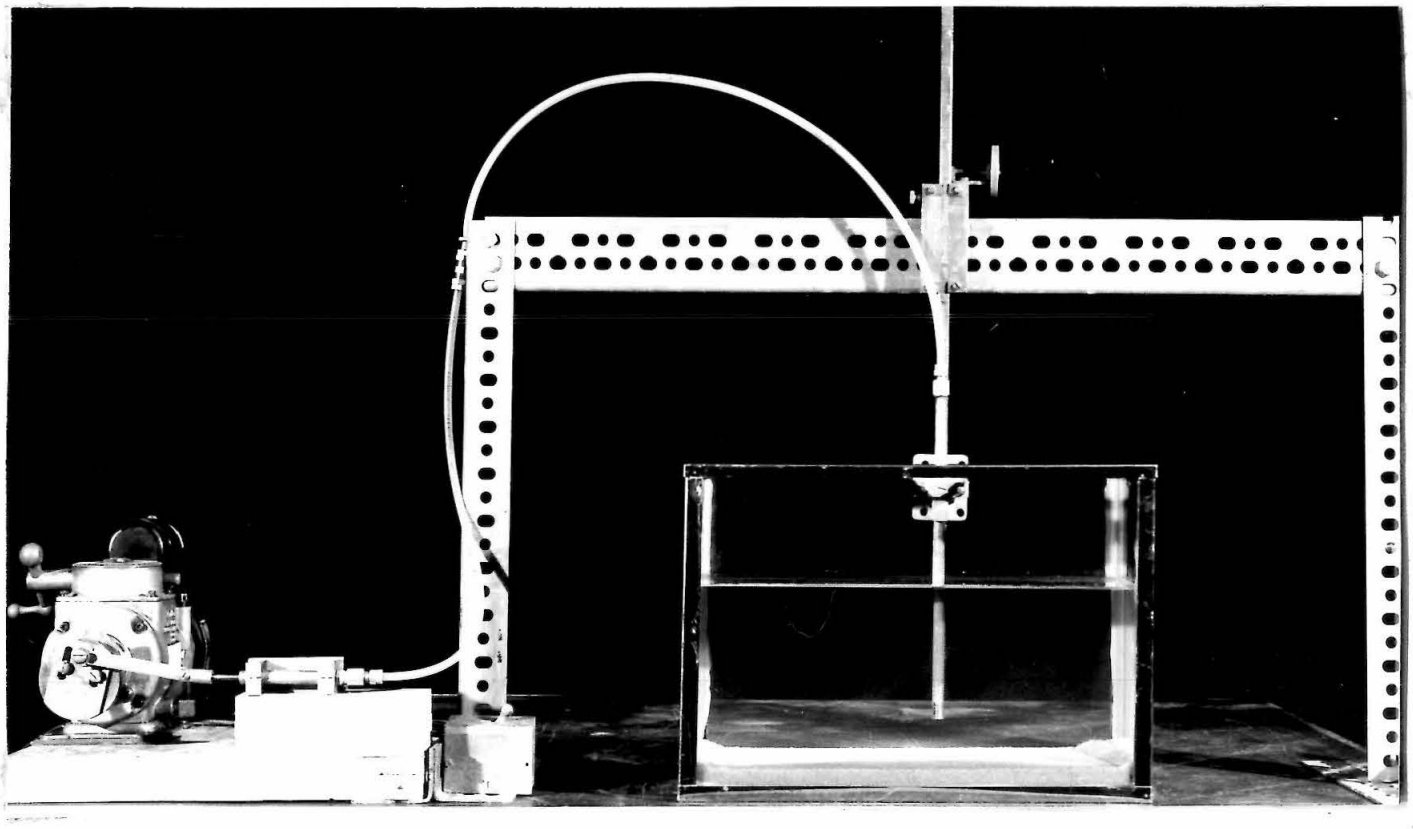

Fig. 3-1 Equipment used to produce the pulsating jet.
The dimensions of the glass tank are 14 in x 12 in x 8-1/2 in.

The pump was a brass cylinder with a $\frac{3}{8}$ in. diameter bore, inside of which a piston was moved. During the suction stroke, fluid was sucked into the cylinder, and on the exhaust stroke it was forced out as a pulse to be directed at the sand bed. It was necessary to calibrate the cylinder so that a relationship between stroke and volume of fluid ejected could be found. The calibration showed that the discharge at each stroke, was independent of frequency and varied linearly with amplitude. From these measurements, the bore of the cylinder was calculated to be 0.373 in.

A single phase, 1800 rpm motor connected directly to a variable speed reduction unit, was used to drive the pump. The speed reduction unit, a Graham Transmission model 15DM, allowed frequencies from 0 to 9 cycles/sec to be used. By means of a dial attached to this unit, the pumping frequency could be determined from a calibration curve. This curve, which was exactly linear throughout its range, determined the frequency to within 0.02 cycles/sec. At the lowest frequencies used, approximately 0.5 cycles/sec, this represents an error of 4% which is comparable with the limits of accuracy imposed upon the experiment by the eye of the observer. At higher frequencies the percentage error is much reduced.

Between the drive and the piston pump, was an adjustable stroke cam mechanism, shown in Figure 3-2. Strokes from 0 to $1\frac{1}{2}$ in. could be obtained. The stroke was adjusted by loosening the two locking screws, sliding the front portion of the cam to the desired setting and retightening the locking screws. The cam was adjusted for each experiment using a template to position its two portions, thus ensuring that the strokes were accurately set.

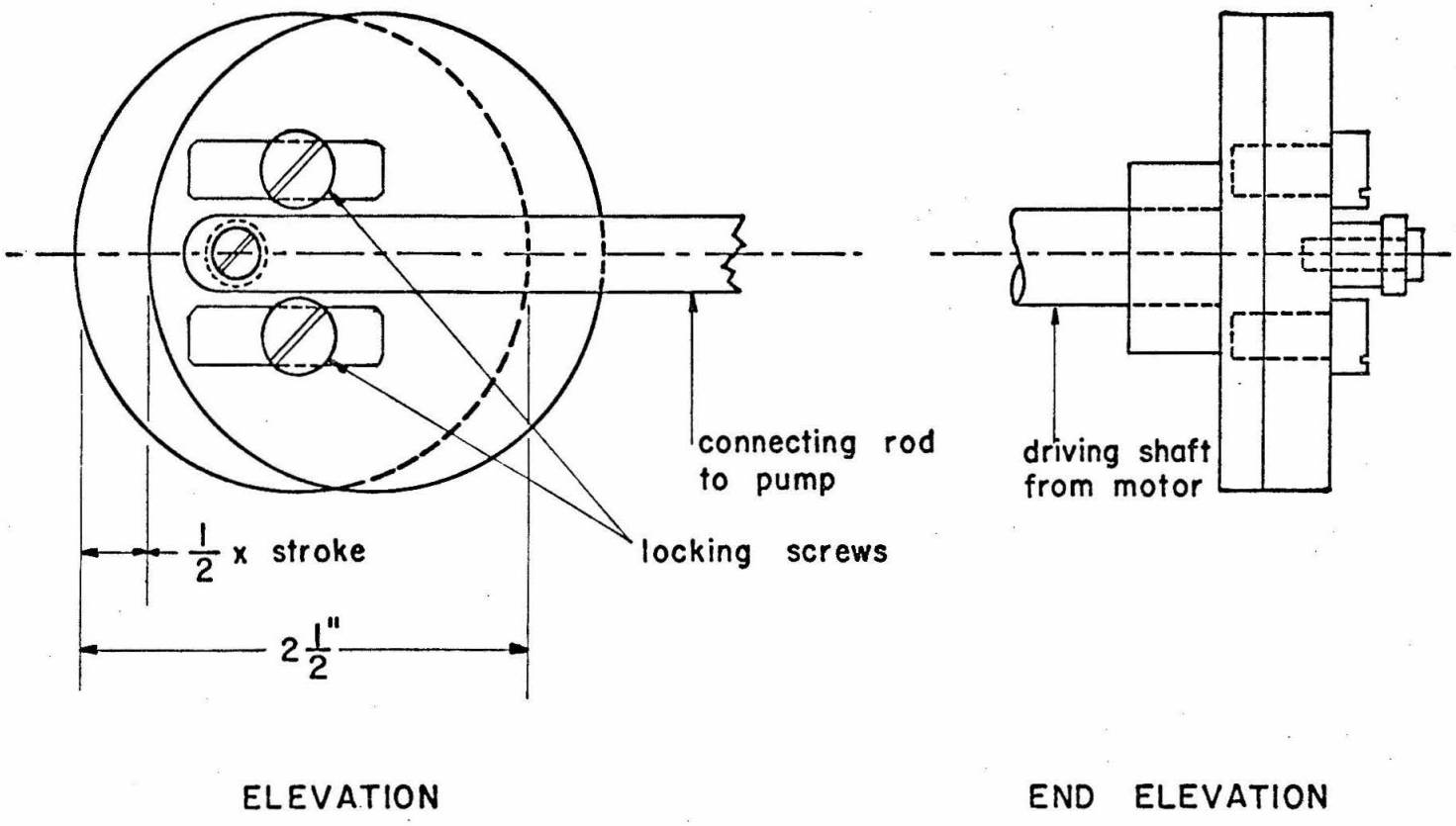

Fig. 3-2. Adjustable cam mechanism. Scale: Full size.

Three jet tubes of different diameters were used. They were clamped to an instrument holder which could be raised or lowered by means of a rack and pinion. The elevation of the tube above the sand bed could be determined to 0.001 ft by means of a vernier scale on the instrument holder. A framework, which straddled the tank, supported the holder and allowed movement of the tube to any position in the tank.

2. Hydrogen Bubble Equipment

A system for producing hydrogen bubbles in the flow field was used to obtain photographs of the motion of the pulse. By using a variable ratio transformer (Variac), and a rectifier, a D. C. voltage of approximately 40 volts was applied between two electrodes placed in the tank. The cathode, on which the hydrogen bubbles were formed, was a 0.002 in. diameter tungsten wire, stretched between two arms of a lucite stirrup which could be placed anywhere in the flow field. The anode consisted of a strip of copper placed at one corner of the tank. Figure 3-3 shows a block diagram of the circuit used.

When the bubbles were used to mark the flow field of a pulse, the wire was placed immediately beneath the end of the jet tube. The hydrogen bubbles formed on the wire and rose vertically to the surface. Those rising in line with the jet tube were caught up on the pulse and acted as flow tracers. An alternative system in which the jet tube acted as the cathode was sometimes used. In this case hydrogen bubbles formed on both the inside and outside of the tube. Those on the outside rose to the surface, while those on the inside were entrained by the pulse as it left the tube and travelled with it to the sediment bed.

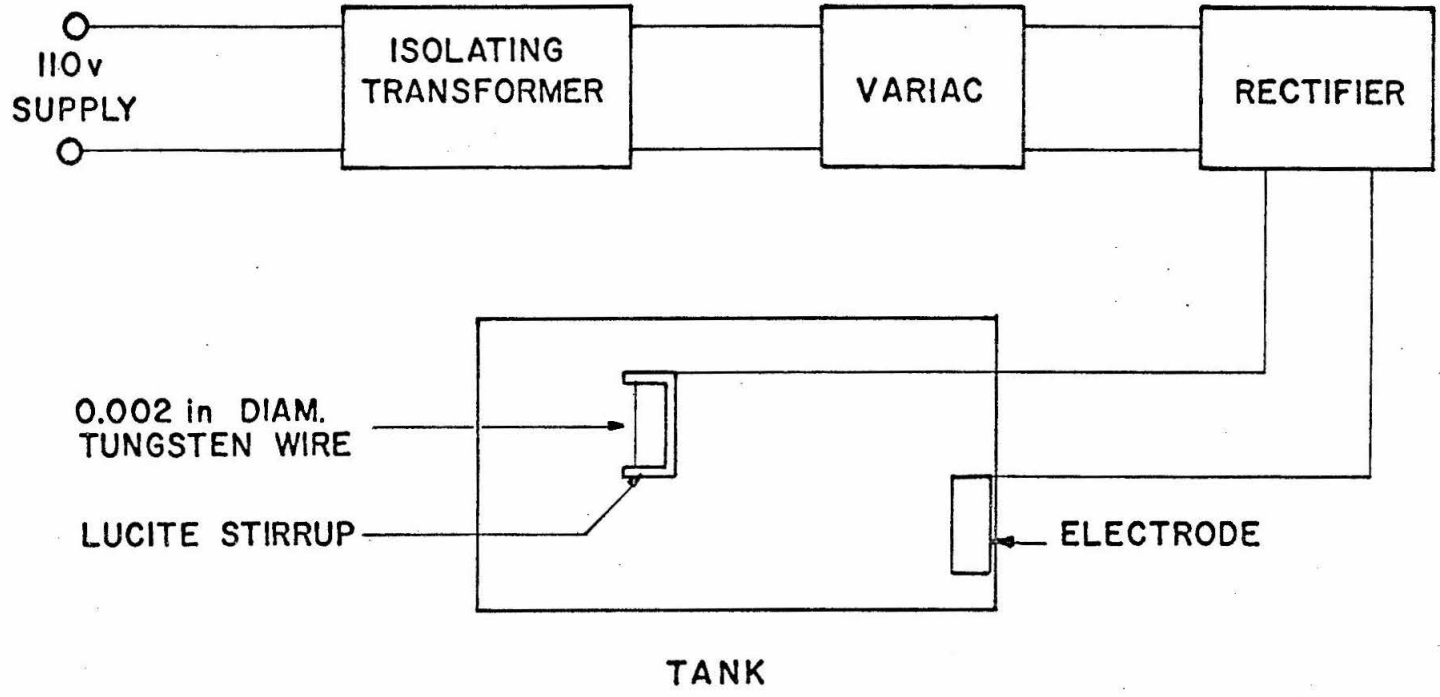

Fig. 3-3 Block diagram of circuit used to introduce hydrogen bubbles into the flow field of the pulsating jet.

3. Hot Film Equipment

To determine the velocities produced adjacent to a boundary by the pulsating jet, a hot film sensor was inserted into the flow field. A probe, with the sensor on the tip, was inserted through the base of a 6 in. x 6 in. lucite box, the sensing element being positioned adjacent to the upper surface of a lucite plate which served as a boundary. A photograph of the apparatus appears in Figure 3-4(a). The sensing element is a small glass cylinder coated with a platinum film which has a quartz layer sputtered over it. These coatings are each approximately 10^{-5} in. thick. The diameter of the element is 0.006 in. and its length is approximately 0.06 in. to 0.08 in. It is supported by two insulated needles which mesh into the main body of the probe. The hot film sensor was aligned with its longitudinal axis parallel to the boundary and perpendicular to a line drawn from the jet axis to the mid point of the cylinder, see Figure 3-4 (b).

By using the instrument holder described previously, the jet tube could be positioned accurately at any required distance from the boundary. In a horizontal plane the tube was positioned with the aid of a grid marked out on the lucite plate. This positioning was done first with the end of the tube adjacent to the lucite plate, and then the tube height was set by raising the tube.

The signal from the sensing element went first through a Shapiro Edwards model 60B hot film anemometer, and then through a Sanborn AC-DC preamplifier model 150-1000. The output from the preamplifier was recorded by a Sanborn single channel recorder.

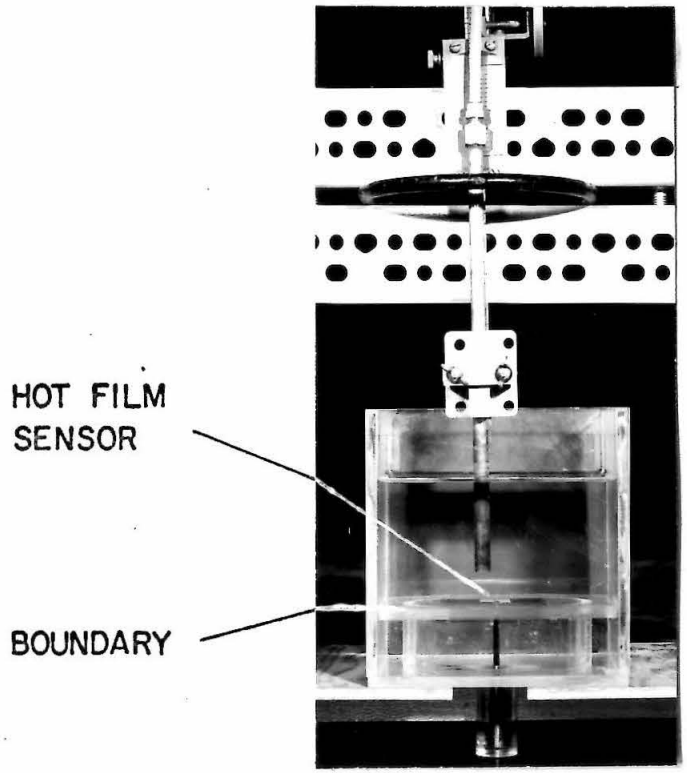

(a)

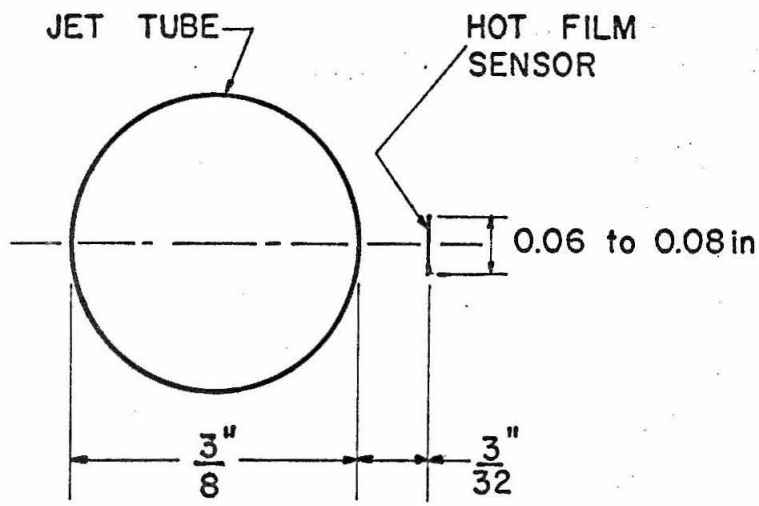

(b)

Fig. 3-4 (a) Equipment used with hot film sensor to measure fluid velocities produced adjacent to a boundary by the pulsating jet. Scale: 1/4 x full size.
(b) Plan view showing alignment of jet axis and hot film sensor. Scale: 4 x full size.

Hinze (32) page 78, derives the relation usually referred to as King's Law, that is used in hot wire anemometry. In his notation it reads $\frac{I^2R_w}{R_w-R_g} = A'+B'\sqrt{u}$. I is the current flowing in the wire, R_w is the total electrical resistance of the wire, R_g is the resistance of the wire at the temperature of the fluid, A' and B' are constants depending upon the physical properties of the wire and fluid and u is the velocity of the fluid over the wire. For a constant temperature anemometer R_w is constant and we can write, $I^2R^2_w = V^2 = \alpha + \beta\sqrt{u}$, where $\alpha = A'R_w(R_w-R_g)$ and $\beta = B'R_w(R_w-R_g)$ are both constants. V is the output voltage from the hot film sensor. To determine α and β, a calibration curve showing V^2 as a function of $\sqrt{u}$ is required. It should be linear.

Calibration of the system was done in a towing tank which was built and used by Townes (33). The towing speed was determined by timing the moving carriage,on which the probe was mounted, over a distance of 3 ft in the middle portion of its travel. From the output on the recorder paper and the measured probe velocity, a calibration curve was prepared. It is given in Figure 3-5.

4. Apparatus for Determination of Fluid Trajectories

In addition to the velocity adjacent to the sediment bed, it is of interest to determine the trajectory of the fluid elements in this portion of the flow field. An indication of these paths was obtained by photographing the motion of neutrally buoyant plastic beads under the action of a pulse.

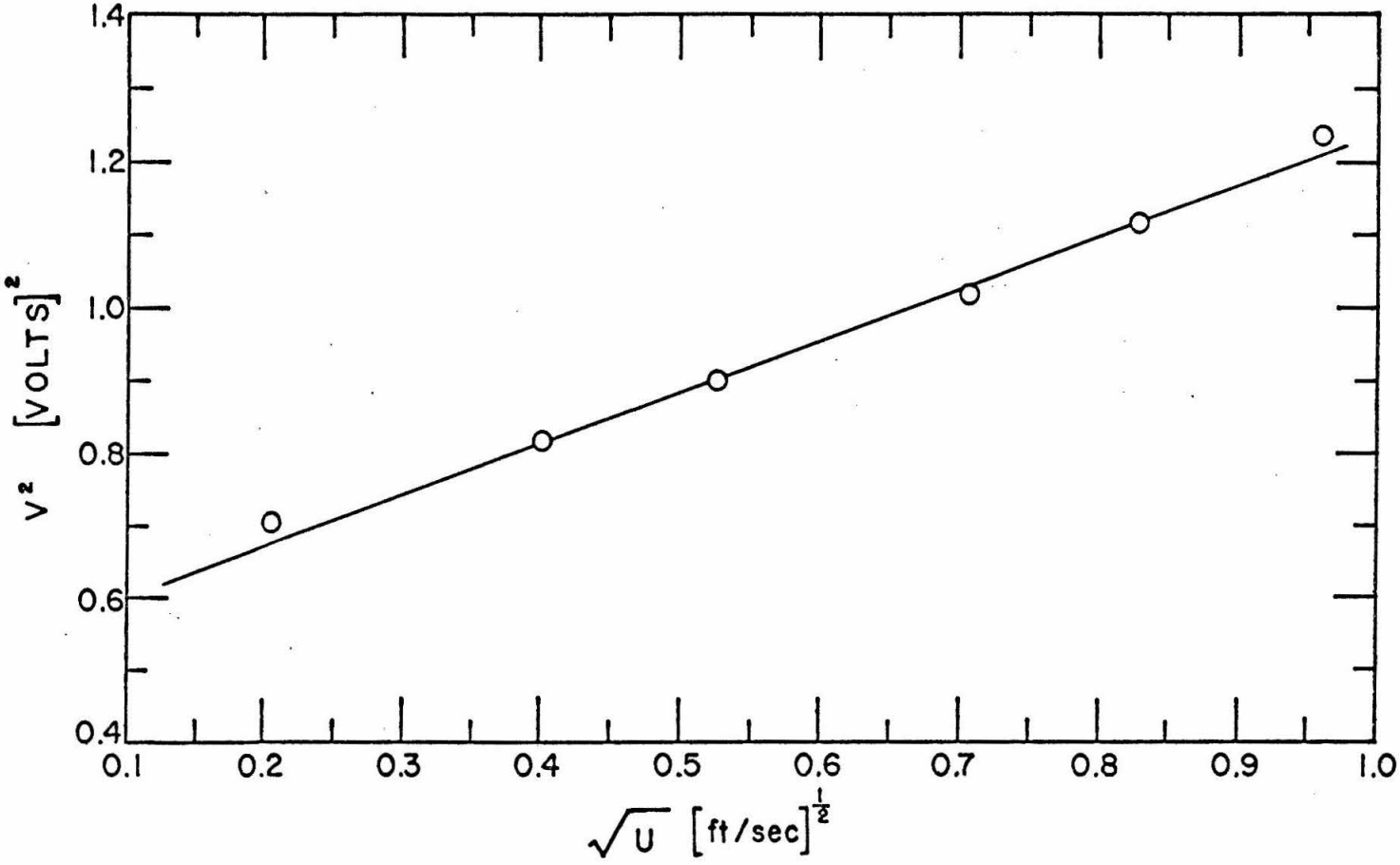

Fig. 3-5 Calibration curve for hot film sensor.

The beads used were approximately $\frac{1}{2}$ mm in diameter, with a specific gravity of 1.04. They were selected from Sediment No. 8, see Section B-2 below. A salt solution was prepared and adjusted by trial and error until the beads became nearly neutrally buoyant in it. Actually they were slightly heavier than the fluid, just sufficient to ensure that when placed on the base of a tank containing the salt solution, they would stay there. When placed in the main body of fluid, it was impossible to define a fall velocity because the beads showed no preference for any direction in which to move. They tended to follow convection currents or fluid movements caused by the introduction of the bead.

A photograph of the experimental apparatus is shown in Figure 3-6. A lucite box, 6 in. x 6 in. x 6 in., was placed between two synchronized flash lights. The jet tube, supported in the same way as in the experiments with sediment grains, was placed vertically in the center of the box. During the experiments, photographs were taken with a view camera using 4 in. x 5 in. black and white sheet film. It was placed close to the position from which the photograph in Figure 3-6 was taken. Two beads can be seen on the base of the tank. At the start of a run they were placed, with the aid of a grid, directly beneath the jet tube, one on each side of the jet axis and in a plane parallel to the film in the camera. The flash lights were powered by the laboratory high voltage supply. The flashing frequency was determined after each experiment by photographing the motion of a hand on a clock face. Measurement of the angle between the position of the hand at successive flashes, allowed the frequency of the flashes to be calculated. The duration of each flash was approximately 5 microseconds.

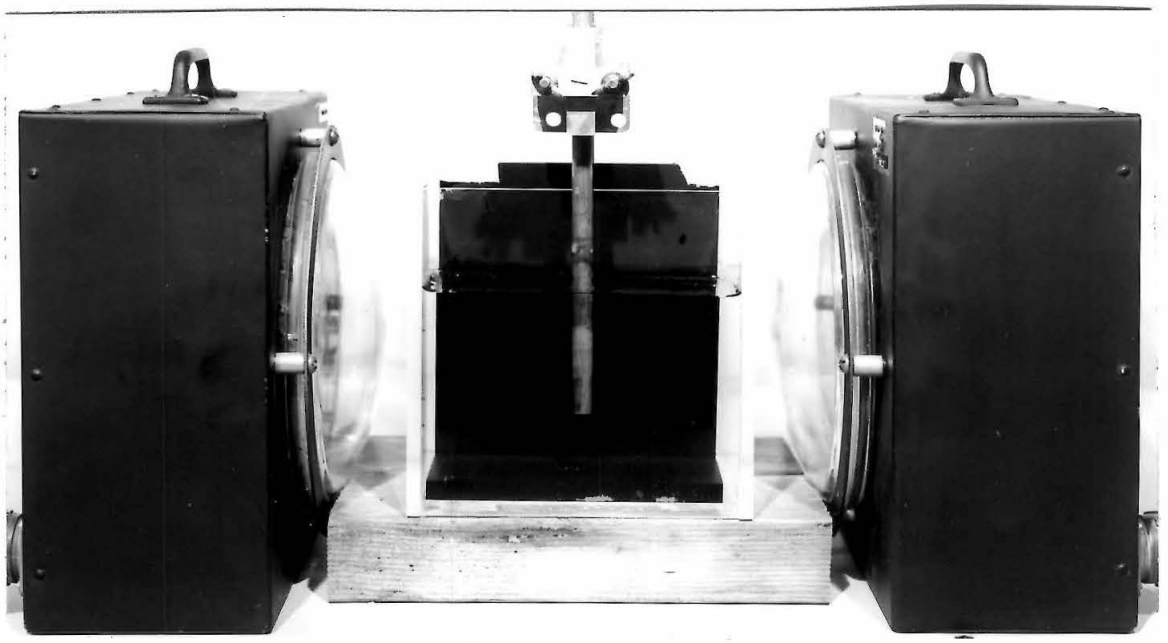

Fig. 3-6 Equipment used to determine trajectories of fluid elements in a pulse adjacent to a boundary. The lucite box has a 6 in. square base. Two plastic beads can be seen on the base beneath the jet tube.

In performing an experiment a pulse of known strength was generated, and the camera shutter held open during the subsequent motion of the beads. On the resultant picture each bead appeared as a series of circular images, each image recording the position of the bead at the particular instant that the lights flashed.

5. Flume

A series of experiments, reported in Chapter V, was performed in a laboratory flume. In Figure 3-7, a photograph of the flume and circulating system used, is presented. The 12 ft long working section has glass walls and a cross section 15 $\frac{3}{8}$ in. wide and 17 in. deep. Figure 3-8 shows a drawing of the cross section. The framework is steel, the member forming the floor being a 15 in. x 3 $\frac{1}{2}$ in. x $\frac{1}{2}$ in. channel section running the length of the working section. An instrument carriage, shown at the downstream end in Figure 3-7, can be moved to any position in the flume on two 1 in. diameter horizontal rails which are mounted on top of the flume walls. Depth measurements, using a vernier scale reading to 0.001 ft, were made with a point gage mounted on the instrument carriage. The bottom of the flume is made from $\frac{1}{2}$ in. lucite placed on specially machined stainless steel washers, which rested on the 15 in. channel section. The washers were spaced at 11 in. centers in two lines, each line being 2 in. from the nearest wall of the flume. To ensure that the finished face of the lucite lay in a horizontal plane, the required washer thickness at each position was determined with a point gage mounted on the instrument carriage. Thus the bottom of the flume was in a plane parallel to that of the rails.

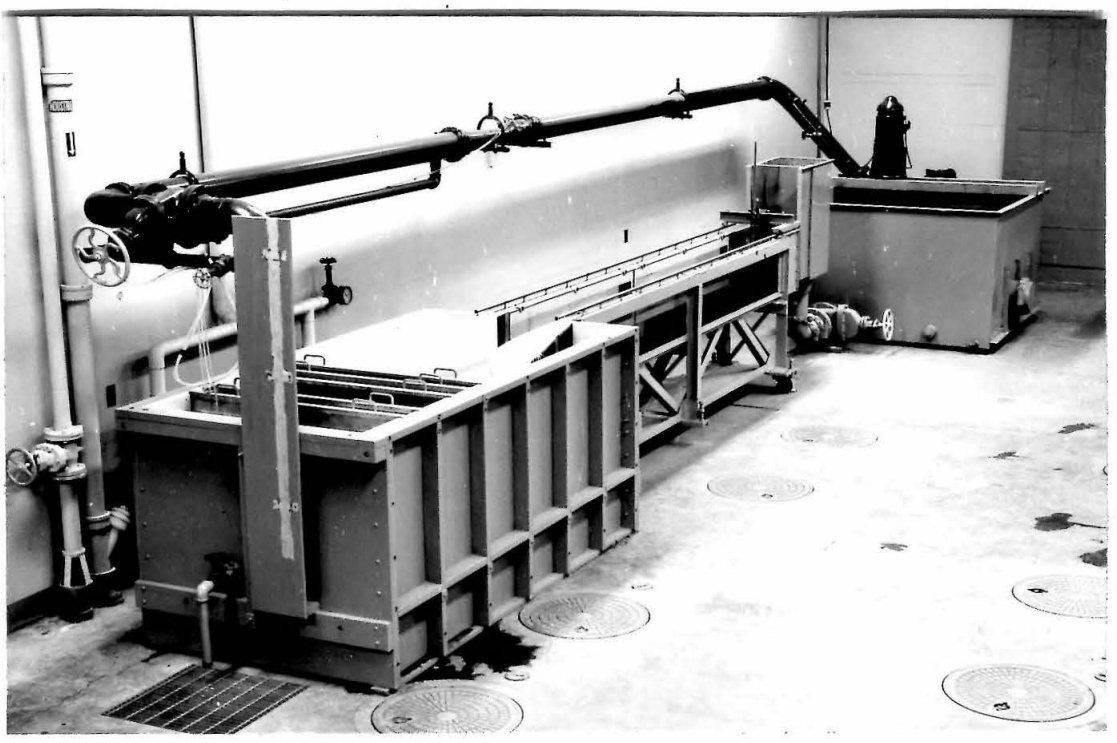

Fig. 3-7 Overall view of the flume used in the studies of grain motion under a turbulent boundary layer.

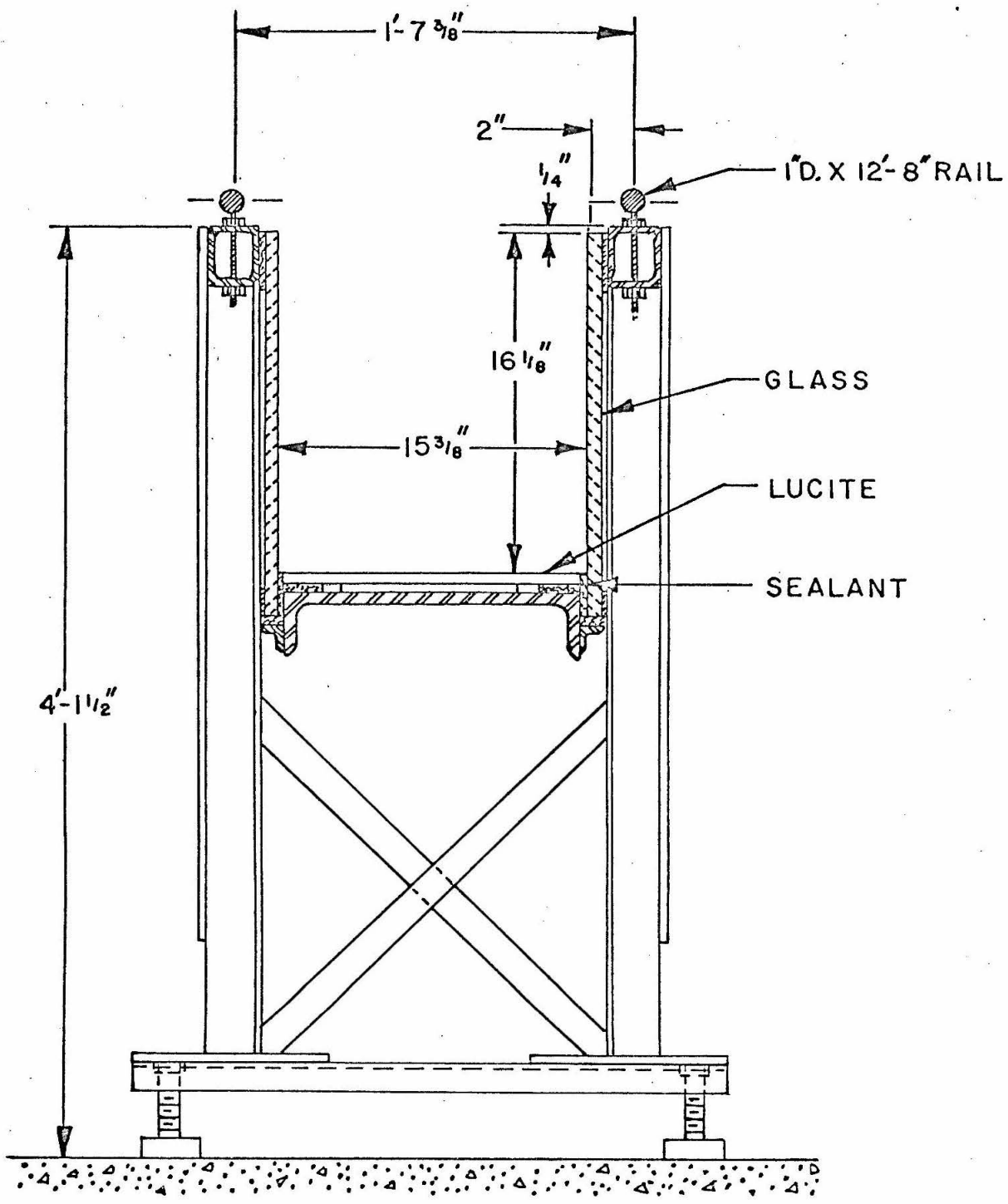

Fig. 3-8 Cross section of the flume.

A vertical pump circulates the water from a downstream reservoir through a 6 in. pipeline to an inlet tank. It then flows through the working section and back to the reservoir. A dimensioned plan view of the flow system is given in Figure 3-9. The flow enters the inlet tank through 312 holes in a manifold. Baffle plates of galvanized sheet metal, $\frac{1}{16}$ in. thick and perforated with $\frac{3}{16}$ in. diameter holes at $\frac{1}{4}$ in. centers, are fitted across the width of the tank immediately downstream of the manifold. Two plates spaced 6 in. apart were used. A 5 ft long transition section reduces the tank cross section of 3 ft 10 $\frac{1}{2}$ in. wide and 2 ft 9 in. deep, to the dimensions of the working section. It was designed to give a monotonically increasing velocity along any stream tube by a method proposed by Tsien (34).

Two gate valves are used to regulate the flow. The valve at the downstream end, an 8 in. gate valve, is used to regulate the flow depth in the working section. A 6 in. gate valve at the upstream end controls the discharge. An air-water manometer, reading to 0.001 ft of water, connected to a venturi meter in the 6 in. pipe, was used to determine the discharge. The meter was calibrated volumetrically in the Hydrodynamics Laboratory at the California Institute of Technology, to an accuracy of within 1 percent. The inlet and throat diameters were 6.109 in. and 3.437 in. respectively.

B. SEDIMENTS

Six different materials were used as sediments. Table 3-1 lists the sediments together with their physical properties.

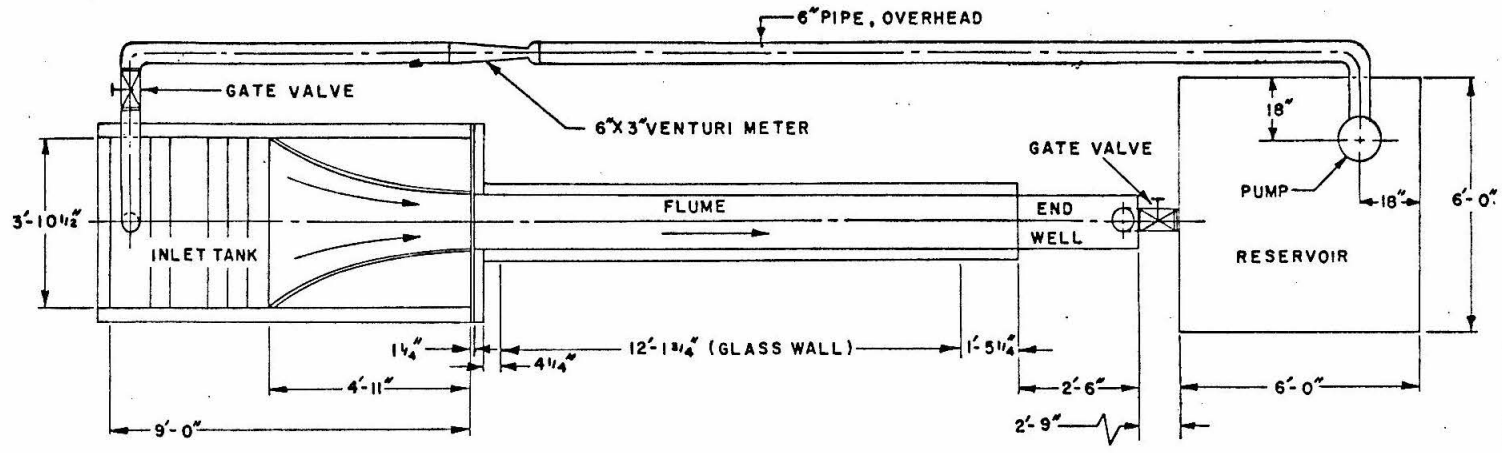

Fig. 3-9 Plan view of the flow system in the flume.

TABLE 3-1

Properties of Sediments Used in the Pulsating Jet Experiments.

Sediment No.	Material	Geom. mean size mm	Geom. Std. Deviation	Specific Gravity	Shape
1	sand	0.098	1.17	2.65	subrounded
2	sand	0.239	1.12	2.66	subrounded
3	sand	0.564	1.14	2.65	rounded
4	sand	0.825	1.14	2.66	rounded
5	glass	0.087	1.12	2.49	spherical
6	glass	0.214	1.07	2.49	spherical
7	glass	0.456	1.05	2.49	spherical
8	plastic	0.590	1.30	1.04	spherical
9	plastic	0.810	1.14	1.04	spherical
10	ilmenite	0.112	1.20	4.76	angular
11	ilmenite	0.271	1.23	4.15	angular
12	ilmenite	0.525	1.18	4.12	angular
13	coal	0.258	1.43	1.27	angular
14	coal	0.710	1.13	1.27	angular
15	coal	0.965	1.08	1.27	angular
16	saran	0.121	1.12	1.69	spherical
17	saran	0.170	1.12	1.69	spherical
18	saran	0.211	1.13	1.69	spherical

1. Analysis

The geometric mean size, d_s, and the geometric standard deviation, σ_g, were determined by means of a sieve analysis. A sample of each sediment, obtained by use of a Jones sample splitter, was sieved using a $\sqrt[4]{2}$ series of standard ten inch Tyler laboratory sieves which were shaken for ten minutes on a Tyler Rotap machine. The sediment retained on each sieve was then weighed on an analytical balance. Figures 3-10 through 3-14 show, for each of the sediments, the distributions of sieve sizes plotted on logarithmic probability paper. Those distributions which plot essentially as straight lines, have the logarithms of their sieve diameters distributed according to the normal error law. They are thus completely defined by the geometric mean size d_s and the geometric standard deviation $\sigma_g = \frac{d_{84.1}}{d_s}$, where d_s is the size for which 50% of the sediment by weight is finer, and $d_{84.1}$ is the size for which 84.1% of the sediment by weight is finer.

Those distributions which do not plot as straight lines are treated as though the distribution were straight, and passed through the points $d_{84.1}$ and $d_{15.9}$. For example Sediment No. 11, in Figure 3-12. This procedure, suggested by Otto (35), is the usual way of treating these almost logarithmic normal distributions.

The specific gravities of the sediments were determined by use of a pycnometer. This is a small glass bottle in which the weight of a volume sediment can be compared with the weight of the same volume of water. The procedure is to first determine the weight of the bottle when it is full of water, W_1, say. A known weight, W_2, of sediment is then placed in the bottle. Water is added until the bottle is full

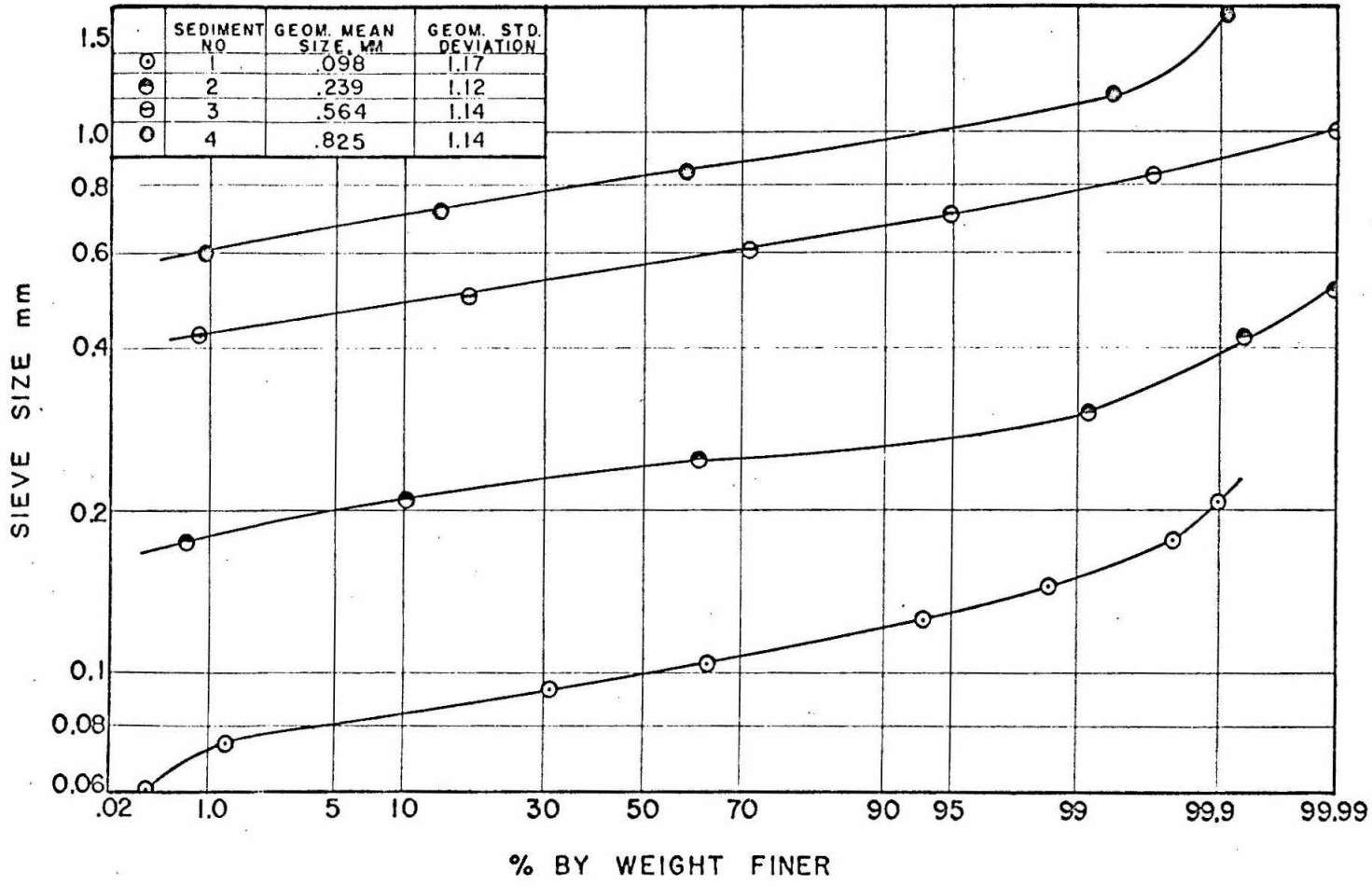

Fig. 3-10 Size-frequency distribution of Sediments No. 1, 2, 3, and 4.

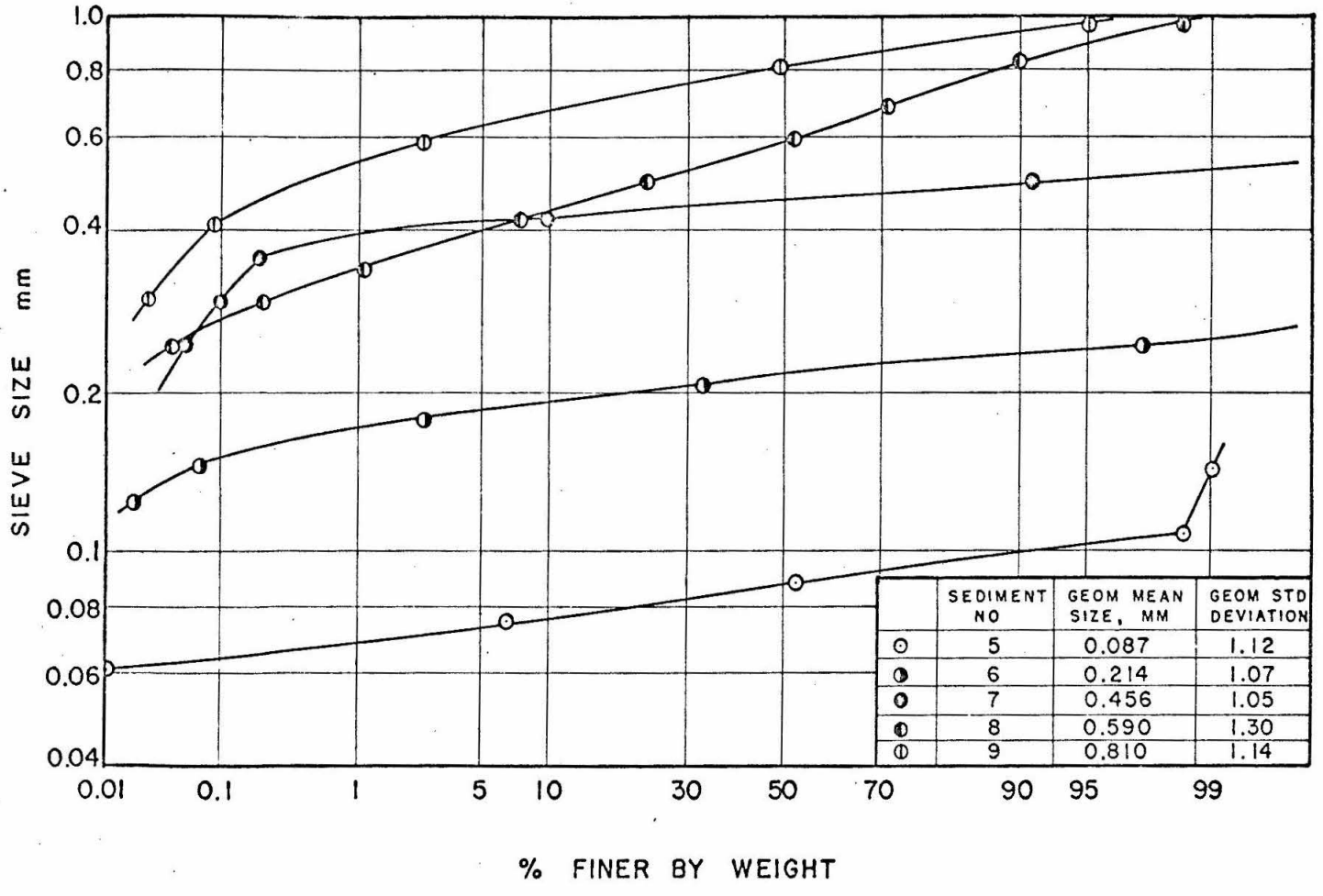

Fig. 3-11 Size-frequency distribution of Sediments No. 5, 6, 7, 8, and 9.

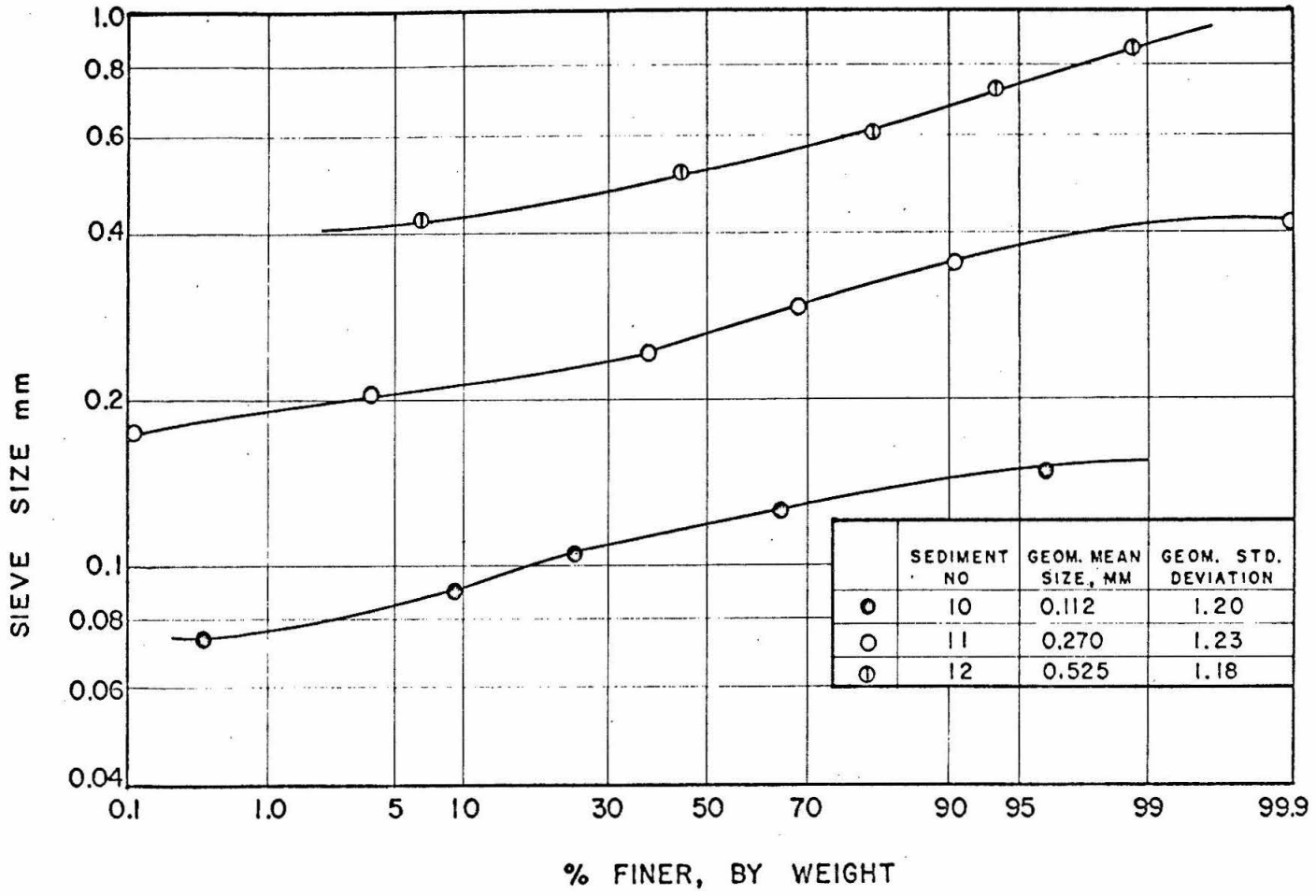

Fig. 3-12 Size-frequency distribution of Sediments No. 10, 11, and 12.

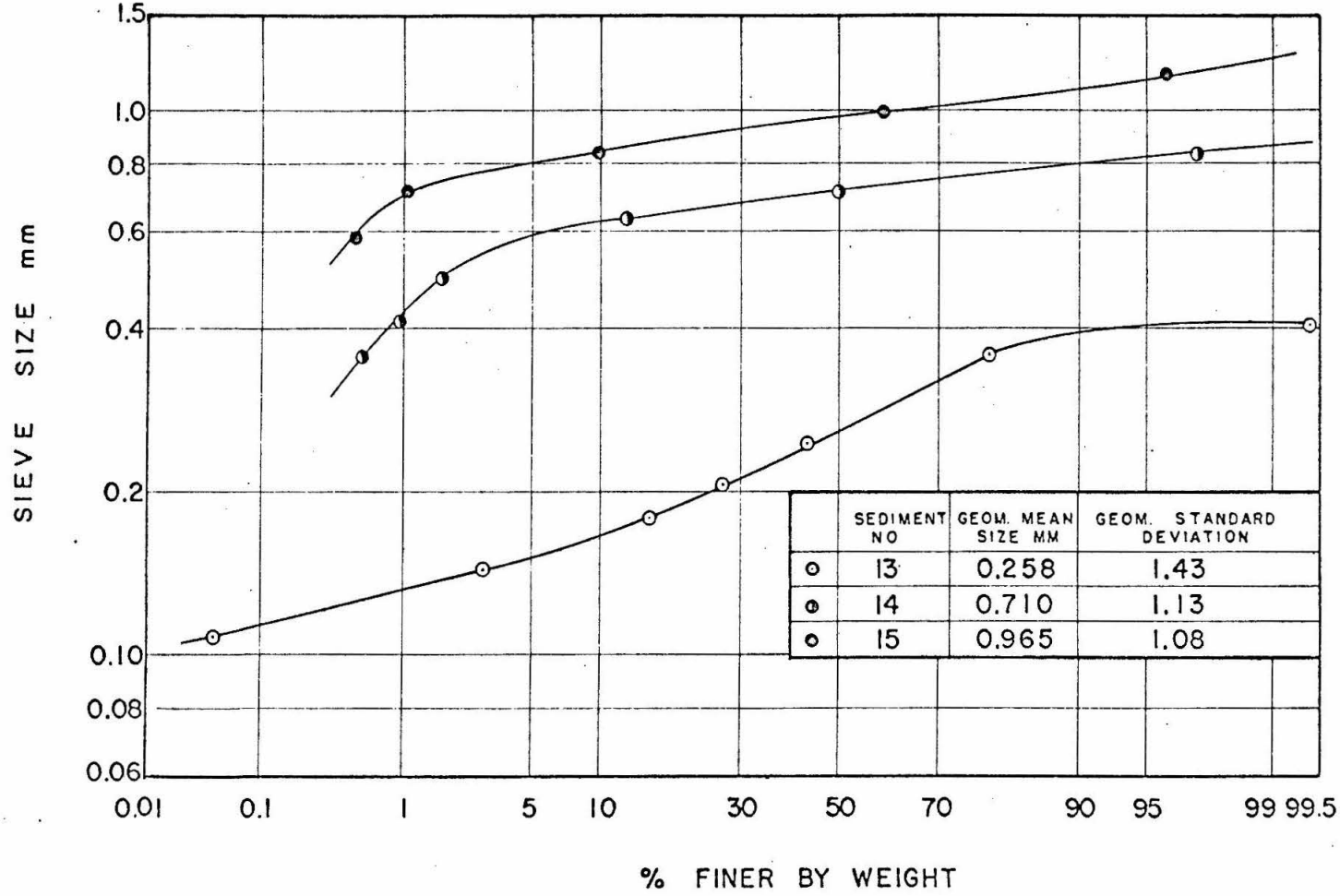

Fig. 3-13 Size-frequency distribution of Sediments No. 13, 14, and 15.

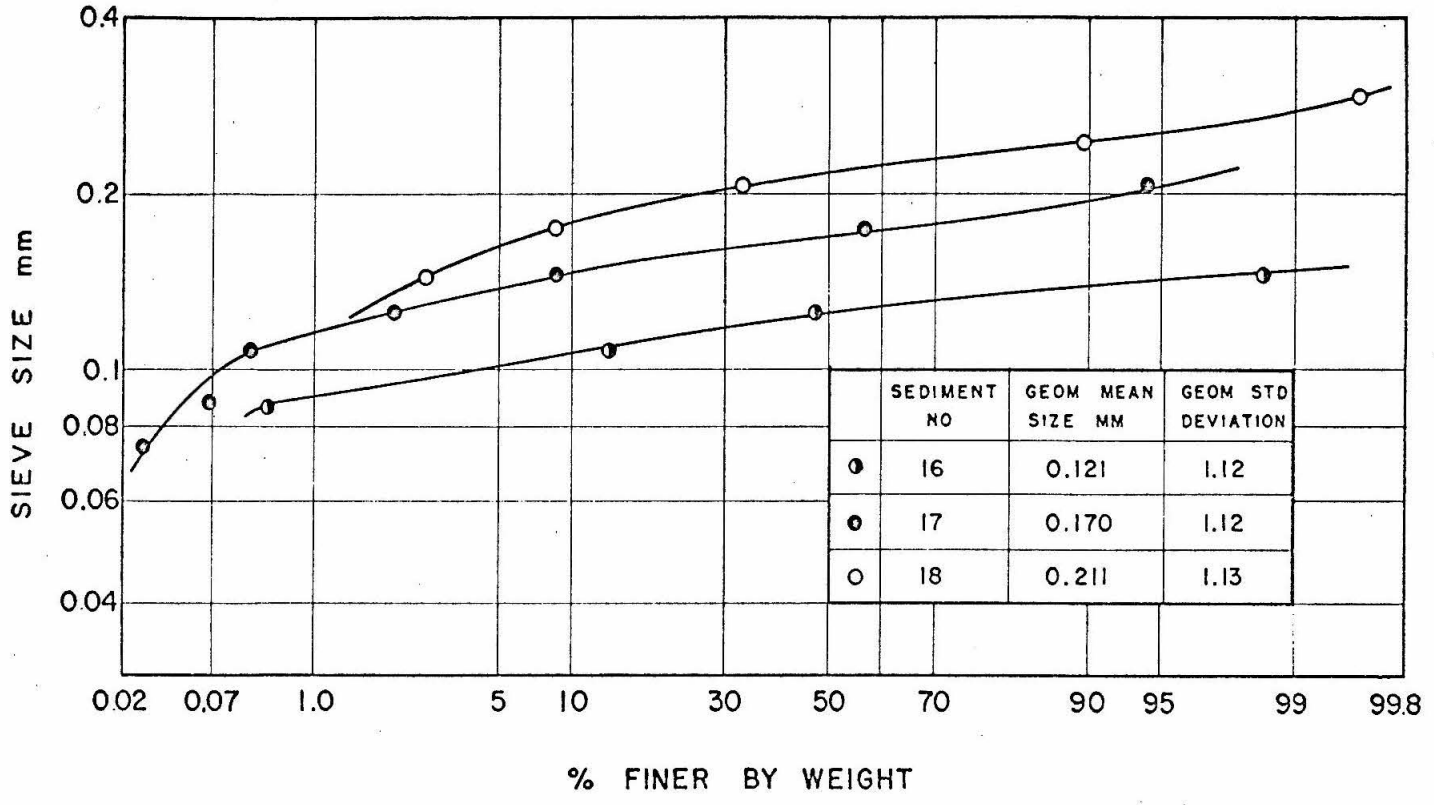

Fig. 3-14 Size-frequency distribution of Sediments No. 16, 17, and 18.

and its weight is determined. If W_3 is the weight of the bottle, sediment and water then the specific gravity of the sediment is given by

$$S.G. = \frac{W_2}{W_1 - (W_3 - W_2)}$$

Great care had to be taken with some of the sediments, notably plastic and coal, to ensure that no air remained trapped in the sample. A wetting agent was used to get the plastic beads into the water. After they were immersed the water was syphoned off and replaced with distilled water. This procedure was repeated four or five times until the contaminating effect of the wetting agent was removed. Once the sample was immersed, it was stirred vigorously to remove any air that may have been trapped between the grains. It was then transferred to the pycnometer without exposing it to the air.

The shape of the sediment was determined from examination of photomicrographs, some of which are shown in Figures 3-15 and 3-16. The magnification in each case is twenty times.

2. Source and Preparation

a. Sand: Sand samples were taken from the Keck Laboratory of Hydraulics and Water Resources Sediment Library. Sediment No. 1, sold under the name of 'Nevada 120', was obtained from a foundry supply company. It is a well sorted white silica sand. Sediment No. 2, known as a Gold Jacket sand, consists of quartz with an iron oxide coating. Sediment No. 3 was obtained from a foundry supply company and is marketed commercially as Ottawa sand. It is

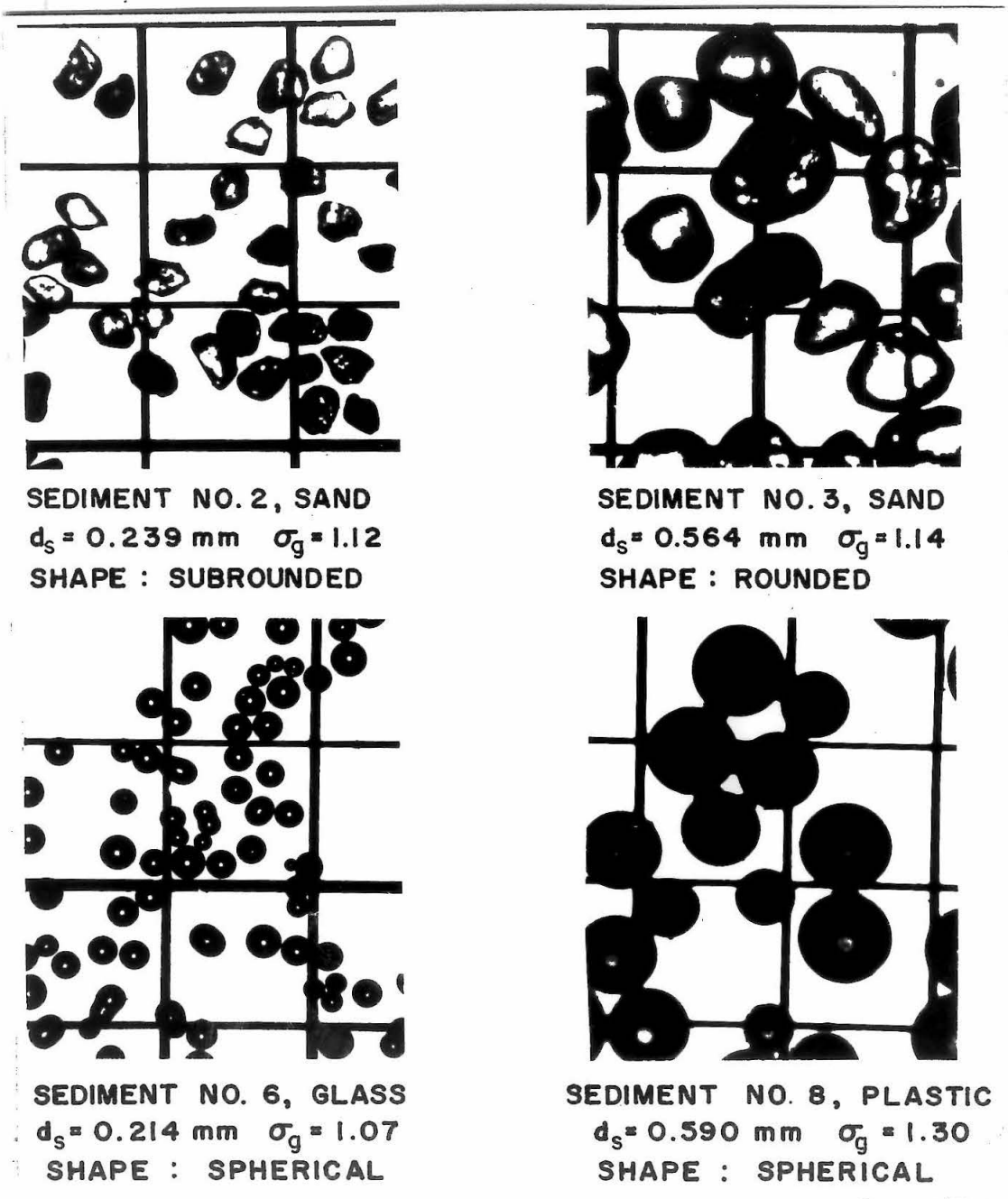

Fig. 3-15 Photomicrographs of Sediments No. 2, 3, 6, and 8. Magnification: 20 times.

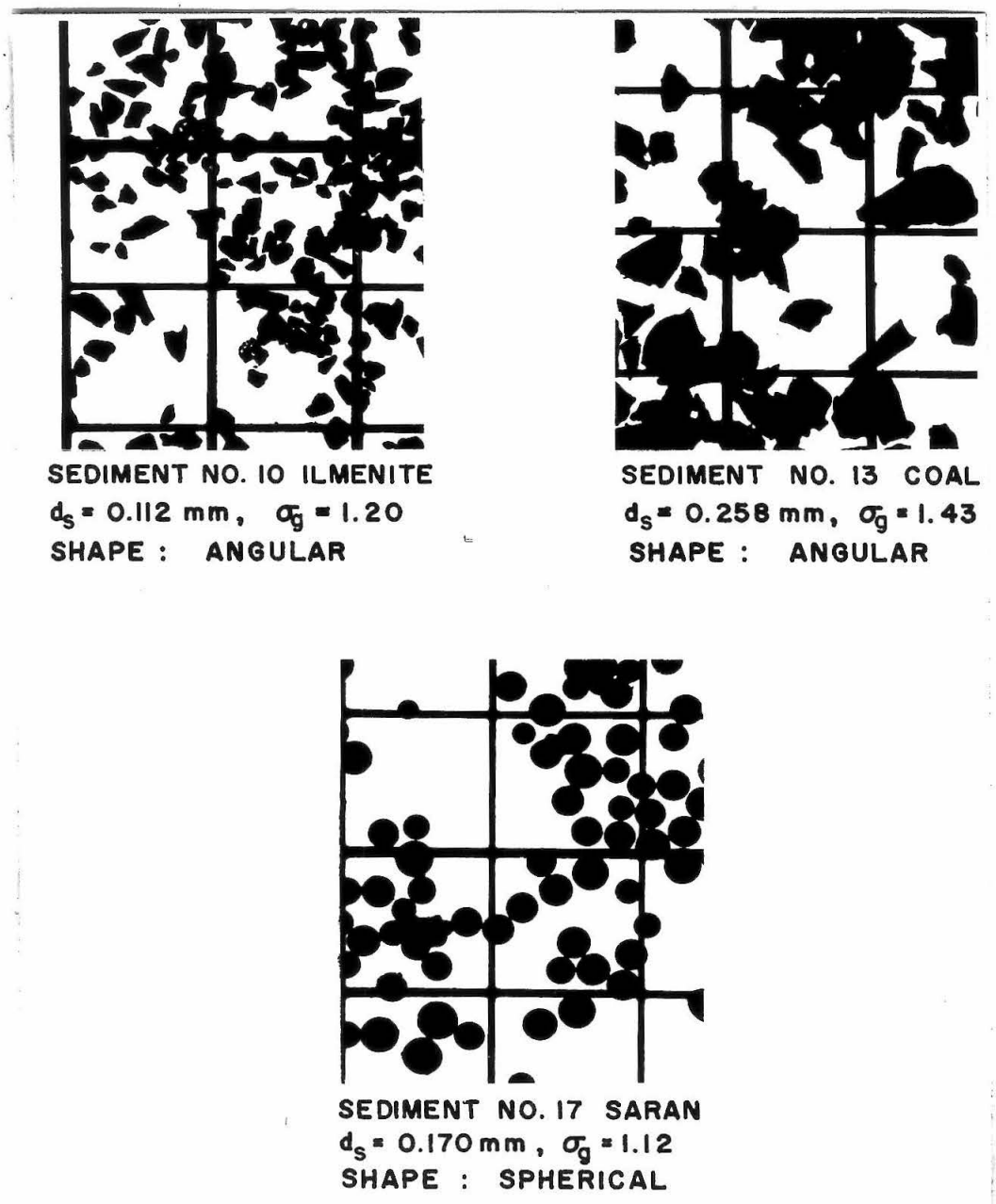

Fig. 3-16 Photomicrographs of Sediments No. 10, 13, and 17. Magnification: 20 times.

well rounded quartz sand. Sediment No. 4 was also a Gold Jacket sand, which was well rounded.

In preparation for the experiments a sample of sand was split with a Jones sample splitter, from the main stock. This was then washed and placed in the tank as a sediment bed. For analysis, a sample was split from the sand used in the experiments, after completion of the run.

b. Glass Beads: Glass beads from the laboratory sediment library were used as Sediments 5, 6 and 7. They were all obtained from the 3-M Company and were prepared for the experiments in the same manner as the sands.

c. Coal: A lump of coal was crushed, and three fractions of different sizes were separated from the crushed material. Each fraction was washed to remove the fine powder generated by the crushing, and then placed in the tank as a sediment bed. Care was required to ensure that all the air was expelled from the bed, because of a surface phenomenon which caused air to adhere strongly to the surface of the coal particles. A rotating propellor was placed in the tank to stir both the fluid and the grains. Bubbles of air caught on and between the grains were thus released. After the sediment was used in the experiments the sieve analysis was performed and the specific gravity determined.

d. Plastic Beads: Samples were taken from the laboratory sediment library, and two size fractions sieved out to form Sediments Nos. 8 and 9. As mentioned above, it was necessary to use a wetting agent before the beads could be made to sink in water. Even the

smallest amount of air adhering to the surface was sufficient to float a bead. The experiments were made in deaired water to ensure that the beads would remain submerged.

e. Ilmenite: Samples of a mineral sand were obtained from the Geology Department of the California Institute of Technology. They consisted of a black, lustrous sand with grains of ilmenite and pyroxene, together with a small percentage of magnetite. Ilmenite is an iron titanium oxide which has a specific gravity of 4.6 to 4.8. Pyroxene is an iron magnesium silicate with a specific gravity of 3.5. The magnetite has a specific gravity of close to 5.0. For the purposes of identification the sediment will be referred to as ilmenite.

The specific gravity of the sediment will depend upon the percentage of each constituent present, which in turn depends upon the mean grain size. Three fractions were sieved from a large supply of sand. The specific gravity of each was determined, and the results are given in Table 3-1. It is seen that the finer fraction has a high percentage of ilmenite, while the two coarser fractions have more pyroxene.

f. Saran: A sample of saran was obtained from the Dow Chemical Company. It is a thermoplastic with the chemical name of Vinylidene Chloride. The Handbook of Chemistry and Physics, 38th Edition, gives a complete list of its properties on page 1473. Of main interest are the following: water absorption $< 0.1\%$ in 24 hours at $25^{\circ}C$ and effect of cold water - none. The specific gravity is listed as 1.6 to 1.8. By measurement it was found to be 1.685 for the sample used.

Three size fractions were split from the main sample and washed to remove any dust. Experiments were performed with each fraction and then a sample taken from each for analysis. No difficulty was encountered in placing the grains under water.

C. OBSERVATIONS OF GRAIN MOVEMENT.

Throughout this section, and the remainder of this report, the term frequency of pulse or jet is used. In some ways this is a misnomer because frequency gives the impression of a repeating phenomenon. As outlined below, the observations made were of the movement induced by one pulse and not a series of pulses. The frequency of this pulse is actually one half the reciprocal of the time taken for the pulse to leave the tube. The pulse amplitude, A, is defined to be the volume of fluid ejected in the pulse, divided by the cross sectional area of the tube. It is related to the stroke of the piston by the equation $A = r \frac{d^2}{a^2}$, where d is the diameter of the piston, a is the diameter of the jet tube, and r is the stroke of the piston.

For a fixed pulse amplitude, the sequence of events at the sand bed parallels that described in connection with the turbulence jar, when the frequency is increased. With increasing frequency, a point is reached at which the grains directly under the tube are first disturbed. The motion is merely a slight agitation of some of the grains. These are the ones that have been left in an unstable position by the levelling process; in all probability they project slightly above the mean bed level. By increasing the frequency slightly, these grains can be made to roll across the bed along radial lines emanating from the jet axis.

After two or three pulses at this frequency all movement ceases. The unstable grains have been rolled to a position outside the influence of the jet, and the remaining ones are not affected by it. The bed at this stage still appears undisturbed. With further increase in frequency many grains are set in motion, moving outward from a center as indicated in Figure 3-17. There is a small region in the center which remains undisturbed. If this frequency is maintained, grain movement continues with each burst until a definite scour hole or annular shape appears. Eventually an equilibrium stage is reached, at which time no further erosion takes place; this occurs only after a considerable number of pulses, and a scour hole is always left.

It is convenient, at this point, to introduce a definition of the first critical frequency as follows: The first critical frequency, ω_1, is that frequency which is just sufficient to cause motion of a significant number of grains with each pulse. This implies that the frequency causing the unstable grains to move, is disregarded.

Increasing the frequency further, results in more violent motion and subsequent increase in the erosion of the bed. A second critical frequency is reached when the type of grain motion changes from rolling to leaping. The height of the leap, which depends upon the pulse strength, can be up to $\frac{1}{2}$ in., approximately 30 or 40 grain diameters off the bed. The second critical frequency, ω_2, is thus defined as that frequency which is just sufficient to cause grains to leave a level bed with each pulse. The final phrase is necessary because of the presence of unstable grains, and a level bed is stipulated because the presence of a scour hole, or other irregularity, is an aid to 'grain

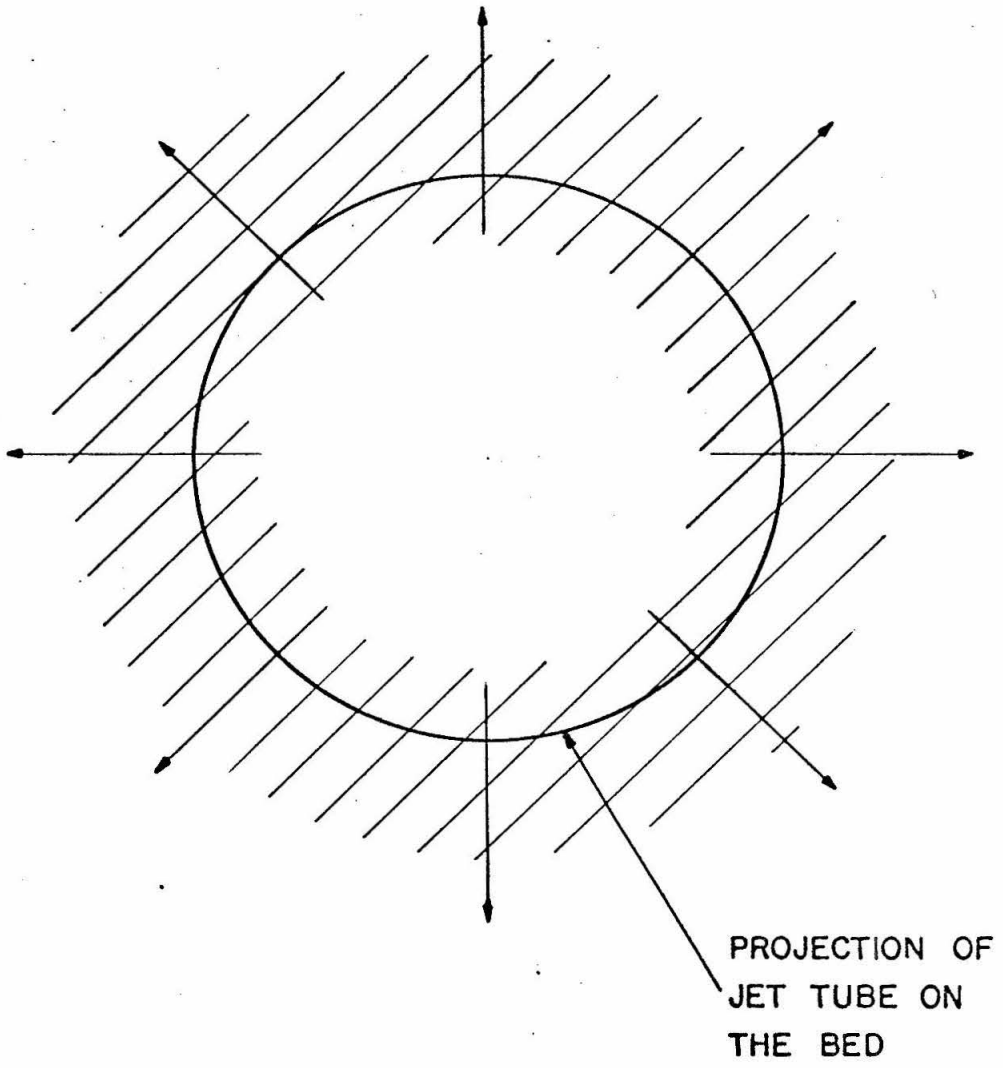

Fig. 3-17 Plan view of grain motion caused by a pulsating jet at critical conditions for moving. Motion takes place from the shaded area in the direction of the arrows.

leap off'. It is conceivable that a grain which is rolled up the side of a scour hole, could be launched away from the bed by a ski-jump action rather than as a result of the pulse alone.

At still higher frequencies very violent scouring takes place, causing the formation of a large crater. Thus, the majority of the grains must be thrown outwards from the center, and not in a vertical path from which they would settle back into the hole and tend to fill it. A sweeping action by the jet can be inferred.

D. EXPERIMENTAL PROGRAM.

1. Scope

The experimental program consisted of determining the values of the two critical frequencies, ω_1 and ω_2, corresponding to a given pulse amplitude under a wide range of conditions. Observations were made using each of the six sediments described in Section III-B-2. At least two different grain sizes of each sediment were investigated, using three tube diameters and three different tube heights. The tube height is defined as the distance from the end of the jet tube to the sediment bed. Eight runs were made with water-glycerine mixtures, four with a 24% glycerine solution and four with a 59% glycerine solution. The kinematic viscosity of these solutions was determined using a Canon-Fenske viscometer, by following the procedure given in ASTM Standards, Part 5, 1955, page 192.

The experiments were divided into a series of runs. Each run was made up of sufficient observations to determine the relationship between amplitude and frequency at critical conditions, for fixed

sediment and fluid properties, tube diameter and tube height. The run number has two parts, e.g. Run No. 1-1. The first part indicates a particular combination of sediment and fluid. It is referred to as the series number. The second part differentiates between different combinations of tube diameter and tube height for the particular series. Table 3-2, lists the conditions under which each series of runs was made. Within each series, different combinations of tube height and diameter were used. Table 4-1, at the beginning of Chapter IV lists these in detail.

To obtain a qualitative picture of the flow field, experiments were made using both hydrogen bubbles and a dye solution as flow markers. They are reported in Sections IV-D-1 and 2. Measurements of the velocity produced adjacent to the sediment bed were made using the hot film equipment and are reported in Section IV-D-3.

2. Procedure

The procedure used in making a run was as follows. Values of tube diameter and tube height were selected and kept constant, as were the sediment and fluid, throughout the run. The bed was carefully levelled, and checked by noting its elevation at various points. This was done using the jet tube, in conjunction with the scale on the instrument carriage, as a point gage. Adjustments were made to the leveller until the reading became constant. The required distance from bed to jet was then set. A cam setting, and thus the pulse amplitude, was selected and the corresponding values of the two critical frequencies, ω_1 and ω_2 were determined. This was done using the following steps:

TABLE 3-2

Properties of the Sediments and Fluids used in each Series of Runs.

Series No.	Sediment No.	Geom. Mean size mm	Fluid Density slugs/cu ft	Fluid Kinematic Viscosity $ft^2/sec \times 10^5$	$\frac{\gamma_s - \gamma}{\gamma}$ *
1	1	0.098	1.94	1.05	1.65
2	3	0.564	1.94	1.05	1.65
3	4	0.825	1.94	1.05	1.66
4	2	0.239	1.94	1.05	1.66
5	3	0.564	2.05	2.06	1.52
6	1	0.098	2.05	2.06	1.52
7	3	0.564	2.22	8.86	1.33
8	1	0.098	2.22	8.86	1.33
9	6	0.214	1.94	1.05	1.49
10	7	0.456	1.94	1.05	1.49
11	11	0.271	1.94	1.05	3.15
12	12	0.525	1.94	1.05	3.12
13	10	0.112	1.94	1.05	3.76
14	9	0.810	1.94	1.05	0.04
15	8	0.590	1.94	1.05	0.04
16	15	0.965	1.94	1.05	0.27
17	14	0.710	1.94	1.05	0.27
18	13	0.258	1.94	1.05	0.27
19	17	0.170	1.94	1.05	0.69
20	18	0.211	1.94	1.05	0.69
21	16	0.121	1.94	1.05	0.69
22	5	0.087	1.94	1.05	1.49

*γ_s is the specific weight of the sediment.
γ is the specific weight of the fluid.

i) increase the frequency continuously until the grains appear just about to move. This gives an approximate value for ω_1.

ii) shift to a new, undisturbed position on the sand bed and note the effect of the first few pulses.

iii) adjust the frequency as indicated by the results of (ii) and observe the effect of the first few pulses at a new, undisturbed position on the bed.

iv) continue in this way until the frequency which just moves grains at each pulse is found. This is ω_1.

v) increase the frequency continuously until grains start to jump from the bed.

vi) select a new position and note the effect of the first pulse.

vii) continue until the frequency is found which just causes grains to jump with each pulse, from a level bed. This is then ω_2.

viii) change the pulse amplitude and repeat steps (i) through (viii).

In each run approximately ten different values of pulse amplitude were investigated. At each setting both critical frequencies were well defined, and could be reproduced in any subsequent run. Each run was done at least twice, and some three times if the scatter of the data was considered to be too great.

Determination of ω_2 required a little more judgement than was necessary for ω_1. The reason is that the first pulse will always disturb some grains, (it has a frequency greater than ω_1), and some of them may jump. In so doing they leave a small crater on the surface of the bed, which could aid jumping on the next pulse. Now if the grains

which jumped at the first pulse were only those in unstable positions, then the value read as w_2 will be slightly low. Care is thus required in judging the results of the first pulse, and then deciding if the crater formed was significant in assisting jumping at the next pulse. Different observers may well have varying ideas about the value for w_2, but if one observer makes all the readings, as in this case, a consistent method or criterion can be established. After the first one or two runs the writer felt that his observations were consistent, and would not differ greatly from any that might be made by independent observers.

CHAPTER IV

PRESENTATION AND DISCUSSION OF RESULTS FROM THE PULSATING JET EXPERIMENTS

Table 4-1 gives a complete list of the results from all the experiments with the pulsating jet. The dashes correspond to quantities which were not determined. In the table, a convention which will be used throughout the remainder of the thesis has been introduced. Variables subscripted with the figure 1, refer to critical conditions for moving, and those subscripted with the figure 2 refer to critical conditions for jumping. The number of runs in each series with the exception of series 10, decreases sharply after the first two series. Series 1, 2 and 10 served to determine the effects of both tube diameter and tube height upon the results. As reported more fully below, changing the tube diameter while keeping the pulse amplitude constant did not affect either of the critical frequencies. The remaining series of runs were thus all made with the same tube diameter. Only two values of tube height were used in each of these series.

A. AMPLITUDE-FREQUENCY RELATIONS.

In each run, corresponding values of critical frequency and amplitude were determined for both types of grain motion, i.e. moving and jumping. When plotted on logarithmic paper, these variables were found to define a straight line of negative slope, indicating that a relationship of the form $\frac{A}{\omega^s}$ = constant exists for each run. Here A is the pulse amplitude, ω is the corresponding frequency and s is the slope of

TABLE 4-1

Summary of Results Obtained in the Pulsating Jet Experiments

Run No.	Geom. Mean Sediment Size d_s mm	Fluid Density ρ Slug/cu ft	Kinematic Viscosity ν ft^2/sec $\times 10^5$	Difference in Spec. Wgts. of Sed. & Fluid $\gamma_s - \gamma$ lb/cu ft	Tube Height h ft	Tube Diam. a in.	Jet Strength K_1 cin	Jet Strength K_2 cin	Slope of 'move' line s_1	Slope of 'jump' line s_2	Bed Velocity U_{o1} ft/sec	Bed Velocity U_{o2} ft/sec	$\beta \left[\frac{\gamma_s - \gamma}{\rho} \frac{d_s^3}{\nu^2}\right]^{1/2}$
1-1	0.098	1.94	1.05	103.8	0.1	.305	1.01	1.69	-0.61	-0.67	.308	.800	3.82
1-2	0.098	1.94	1.05	103.8	0.3	.305	1.40	2.27	-0.68	-0.74	-	-	3.82
1-3	0.098	1.94	1.05	103.8	0.2	.305	1.21	1.95	-0.53	-0.60	.315	.802	3.82
1-4	0.098	1.94	1.05	103.8	0.1	.244	1.04	1.74	-0.64	-0.70	-	-	3.82
1-5	0.098	1.94	1.05	103.8	0.3	.244	1.45	2.56	-0.69	-0.66	-	-	3.82
1-6	0.098	1.94	1.05	103.8	0.2	.244	1.22	2.04	-0.63	-0.71	-	-	3.82
1-7	0.098	1.94	1.05	103.8	0.1	.182	0.80	1.49	-0.64	-0.75	-	-	3.82
1-8	0.098	1.94	1.05	103.8	0.2	.182	1.26	2.26	-0.76	-0.85	-	-	3.82
2-1	0.564	1.94	1.05	103.8	0.1	.244	1.40	1.91	-0.70	-0.72	-	-	52.8
2-2	0.564	1.94	1.05	103.8	0.15	.244	1.47	2.06	-0.68	-0.71	-	-	52.8
2-3	0.564	1.94	1.05	103.8	0.2	.244	1.62	2.25	-0.67	-0.71	-	-	52.8
2-4	0.564	1.94	1.05	103.8	0.25	.244	1.70	2.42	-0.62	-0.62	-	-	52.8
2-5	0.564	1.94	1.05	103.8	0.1	.305	1.42	1.95	-0.68	-0.71	.570	1.03	52.8
2-6	0.564	1.94	1.05	103.8	0.15	.305	1.52	2.02	-0.65	-0.67	-	-	52.8
2-7	0.564	1.94	1.05	103.8	0.25	.305	1.66	2.40	-0.60	-0.60	-	-	52.8
2-8	0.564	1.94	1.05	103.8	0.2	.305	1.61	2.20	-0.62	-0.62	.557	1.02	52.8
2-9	0.564	1.94	1.05	103.8	0.1	.182	1.40	1.96	-0.74	-0.75	-	-	52.8
2-10	0.564	1.94	1.05	103.8	0.15	.182	1.64	2.15	-0.68	-0.69	-		52.8
2-11	0.564	1.94	1.05	103.8	0.2	.182	1.70	2.24	-0.74	-	-	-	52.8
3-1	0.825	1.94	1.05	103.8	0.1	.305	1.64	2.06	-0.66	-0.68	.745	1.15	93.9
3-2	0.825	1.94	1.05	103.8	0.2	.305	1.84	2.29	-0.66	-0.64	.726	1.11	93.9
3-3	0.825	1.94	1.05	103.8	0.1	.244	1.62	2.01	-0.65	-0.66	-	-	93.9
3-4	0.825	1.94	1.05	103.8	0.2	.244	1.85	2.31	-0.70	-0.70	-	-	93.9
4-1	0.239	1.94	1.05	103.8	0.1	.305	1.16	1.78	-0.71	-0.69	.403	.880	14.56
4-2	0.239	1.94	1.05	103.8	0.2	.305	1.35	2.07	-0.65	-0.67	.400	.902	14.56
4-3	0.239	1.94	1.05	103.8	0.25	.305	1.52	2.07	-0.66	-0.62	-	-	14.56
5-1	0.564	2.05	2.06	100.2	0.2	.305	1.48	2.14	-0.67	-0.68	-	-	27.0
5-2	0.564	2.05	2.06	100.2	0.1	.305	1.25	1.87	-0.68	-0.69	-	-	27.0
6-1	0.098	2.05	2.06	100.2	0.2	.305	1.10	1.80	-0.60	-0.64	-	-	1.96
6-2	0.098	2.05	2.06	100.2	0.1	.305	0.89	1.67	-0.60	-0.67	-	-	1.96
7-1	0.564	2.22	8.86	94.6	0.2	.305	1.58	2.46	-0.63	-0.63	-	-	5.86
7-2	0.564	2.22	8.86	94.6	0.1	.305	1.26	2.08	-0.68	-0.67	-	-	5.86

TABLE 4-1 (continued)

Run No.	Geom. Mean Sediment Size d_s mm	Fluid Density ρ Slug/cu ft	Kinematic Viscosity ν ft^2/sec x 10^5	Difference in Spec. Wgts. of Sed. & Fluid $\gamma_s-\gamma$ lb/cu ft	Tube Height h ft	Tube Diam. a in.	Jet Strength K_1 cin	Jet Strength K_2 cin	Slope of 'move' line s_1	Slope of 'jump' line s_2	Bed Velocity U_{o1} ft/sec	Bed Velocity U_{o2} ft/sec	$\beta \left[\frac{\gamma_s-\gamma}{\rho}\frac{d_s^3}{\nu^2}\right]^{1/2}$
8-1	0.098	2.22	8.86	94.6	0.2	.305	1.30	2.50	-0.74	-0.68	-	-	0.43
8-2	0.098	2.22	8.86	94.6	0.1	.305	1.02	2.15	-0.71	-0.71	-	-	0.43
9-1	0.214	1.94	1.05	93.4	0.1	.305	0.98	1.73	-0.67	-0.74	.300	.834	11.15
9-2	0.214	1.94	1.05	93.4	0.2	.305	1.15	1.99	-0.66	-0.70	.295	.837	11.15
10-1	0.456	1.94	1.05	93.4	0.1	.305	1.17	1.77	-0.73	-0.75	.410	.870	37.3
10-2	0.456	1.94	1.05	93.4	0.2	.305	1.36	2.06	-0.67	-0.69	.404	.890	37.3
10-3	0.456	1.94	1.05	93.4	0.084	.305	1.15	1.89	-0.75	-0.74	-	-	37.3
10-4	0.456	1.94	1.05	93.4	0.168	.305	1.45	2.10	-0.66	-0.66	-	-	37.3
10-5	0.456	1.94	1.05	93.4	0.216	.305	1.49	2.10	-0.63	-0.68	-	-	37.3
10-6	0.456	1.94	1.05	93.4	0.084	.244	1.11	1.71	-0.75	-0.75	-	-	37.3
10-7	0.456	1.94	1.05	93.4	0.168	.244	1.30	1.91	-0.72	-0.70	-	-	37.3
10-8	0.456	1.94	1.05	93.4	0.216	.244	1.47	2.27	-0.68	-0.75	-	-	37.3
11-1	0.271	1.94	1.05	196	0.1	.305	1.30	1.97	-0.74	-0.75	.493	1.05	24.5
11-2	0.271	1.94	1.05	196	0.2	.305	1.45	2.28	-0.75	-0.75	.459	1.09	24.5
12-1	0.525	1.94	1.05	195	0.1	.305	1.56	2.11	-0.75	-0.75	.690	1.17	63.5
12-2	0.525	1.94	1.05	195	0.2	.305	1.70	2.30	-0.63	-0.65	.623	1.10	63.5
13-1	0.112	1.94	1.05	234	0.1	.305	1.14	1.92	-0.70	-0.69	.387	1.00	6.98
13-2	0.112	1.94	1.05	234	0.2	.305	1.34	2.24	-0.66	-0.73	.390	1.02	6.98
14-1	0.810	1.94	1.05	2.496	0.1	.305	0.61	0.84	-0.61	-0.61	.129	.220	14.13
14-2	0.810	1.94	1.05	2.496	0.2	.305	0.66	0.885	-0.70	-0.73	.105	.180	14.13
15-1	0.590	1.94	1.05	2.496	0.1	.305	0.53	0.81	-0.65	-0.60	.098	.210	8.64
15-2	0.590	1.94	1.05	2.496	0.2	.305	0.63	0.85	-0.67	-0.74	.092	.164	8.64
16-1	0.965	1.94	1.05	16.8	0.1	.305	1.00	1.33	-0.65	-0.67	.308	.520	47.8
16-2	0.965	1.94	1.05	16.8	0.2	.305	1.16	1.38	-0.63	-0.64	.302	.420	47.8
17-1	0.710	1.94	1.05	16.8	0.1	.305	0.87	1.19	-0.64	-0.68	.240	.420	29.6
17-2	0.710	1.94	1.05	16.8	0.2	.305	1.04	1.27	-0.60	-0.60	.243	.361	29.6
18-1	0.258	1.94	1.05	16.8	0.1	.305	0.575	0.97	-0.62	-0.66	.113	.290	6.61
18-2	0.258	1.94	1.05	16.8	0.2	.305	0.757	1.05	-0.60	-0.67	.124	.250	6.61
19-1	0.170	1.94	1.05	42.7	0.1	.305	0.708	1.40	-0.63	-0.67	.165	.570	5.99
19-2	0.170	1.94	1.05	42.7	0.2	.305	0.875	1.60	-0.61	-0.61	.166	.551	5.99
20-1	0.211	1.94	1.05	42.7	0.1	.305	0.738	1.42	-0.60	-0.67	.176	.580	7.75
20-2	0.211	1.94	1.05	42.7	0.2	.305	0.925	1.63	-0.61	-0.67	.187	.574	7.75
21-1	0.121	1.94	1.05	42.7	0.1	.305	0.665	1.38	-0.60	-0.64	.148	.560	3.58
21-2	0.121	1.94	1.05	42.7	0.2	.305	0.841	1.57	-0.60	-0.61	.161	.540	3.58
22-1	0.087	1.94	1.05	93.4	0.1	.305	0.885	1.67	-0.64	-0.73	.246	.800	3.01
22-2	0.087	1.94	1.05	93.4	0.2	.305	1.03	2.04	-0.67	-0.73	.236	.870	3.01

the line through the data points. Two examples of these plots are given in Figures 4-1 and 4-2. The upper line on each plot corresponds to the critical conditions for grain jumping and will be referred to as the 'jump' curve; the lower corresponds to the critical conditions for grain motion and is termed the 'move' curve. Values quoted for h and a refer to the tube height and tube diameter respectively. The runs chosen are typical of the whole set of results. Run 2-5, Figure 4-1, is one of the runs exhibiting small scatter between repeated measurements. Run 1-6, Figure 4-2, is one of those which, by inspection, appeared to show most scatter and gives an idea of the reproducibility of the experiments. Points from three runs, 1-6-a, 1-6-b and 1-6-c are shown. In spite of the scattering, a line can be drawn through the data, which will define the frequency-amplitude relation.

The slopes of the lines in all the experiments, with a very few exceptions which will be discussed, varied from -0.60 to -0.75. In view of the inevitable scattering of the data, the line drawn through each set of results is actually a line of best fit as determined by eye. Values given for the slopes of these lines are therefore subject to small errors. In some instances, for example Run 1-6, Figure 4-2, this error may be as large as 0.05. This amounts to one third of the difference between the extreme values of the actual slopes, viz.-0.60 and -0.75. Hence any dependence of slope of the lines upon tube diameter,tube height or sand size, which, if it exists must necessarily be small, will not be revealed by the results. Table 4-1 shows that the absolute value of the slope of the 'move' curves, $|s_1|$, is in general less than $|s_2|$, the absolute value of the slope of the 'jump' curves. This is borne out

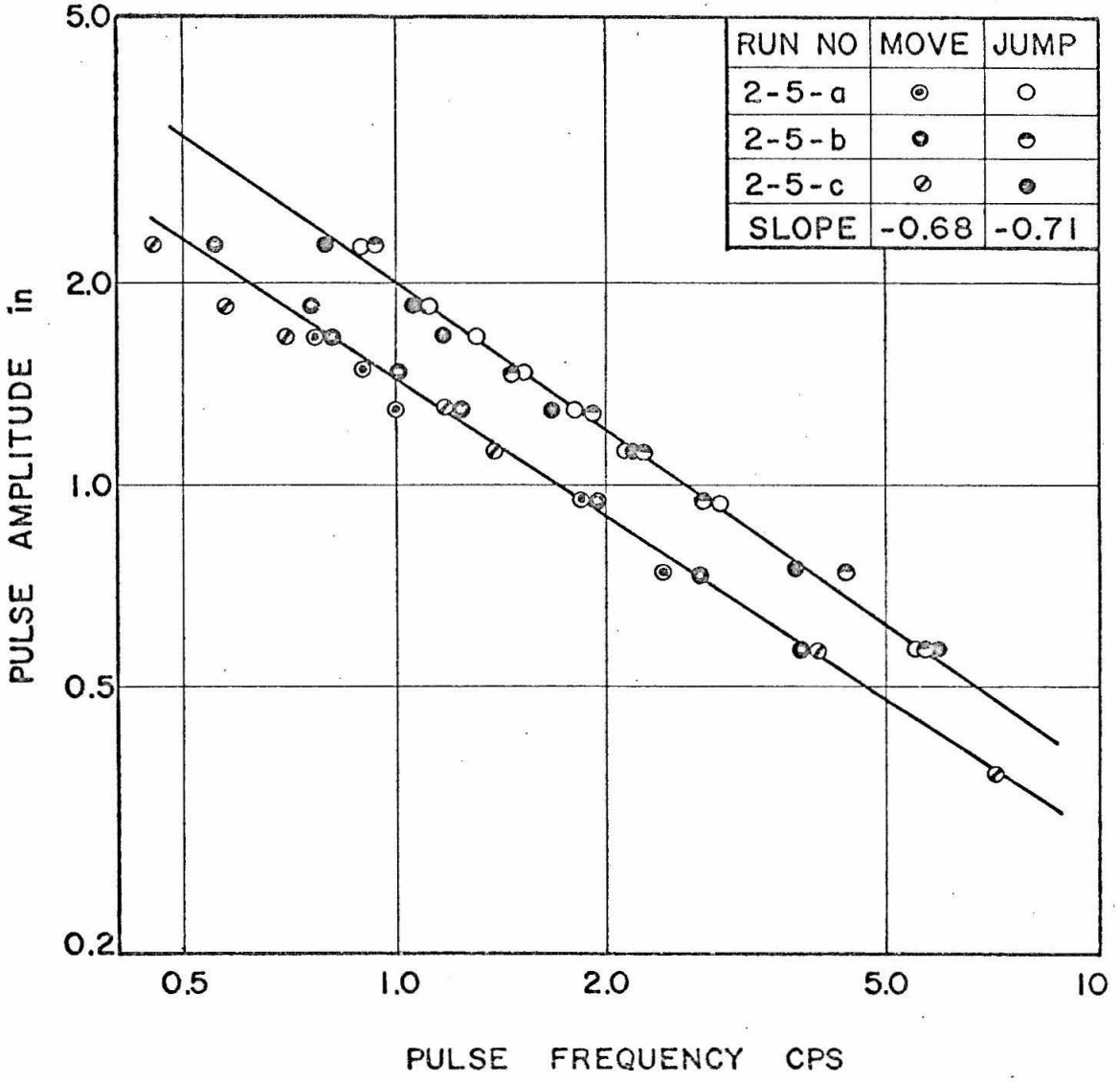

Fig. 4-1 Amplitude-frequency relations for critical conditions of move and jump in Run No. 2-5. Sand grains, d_s = 0.564 mm, in water with h = 0.1 ft and a_s = 0.305 in.

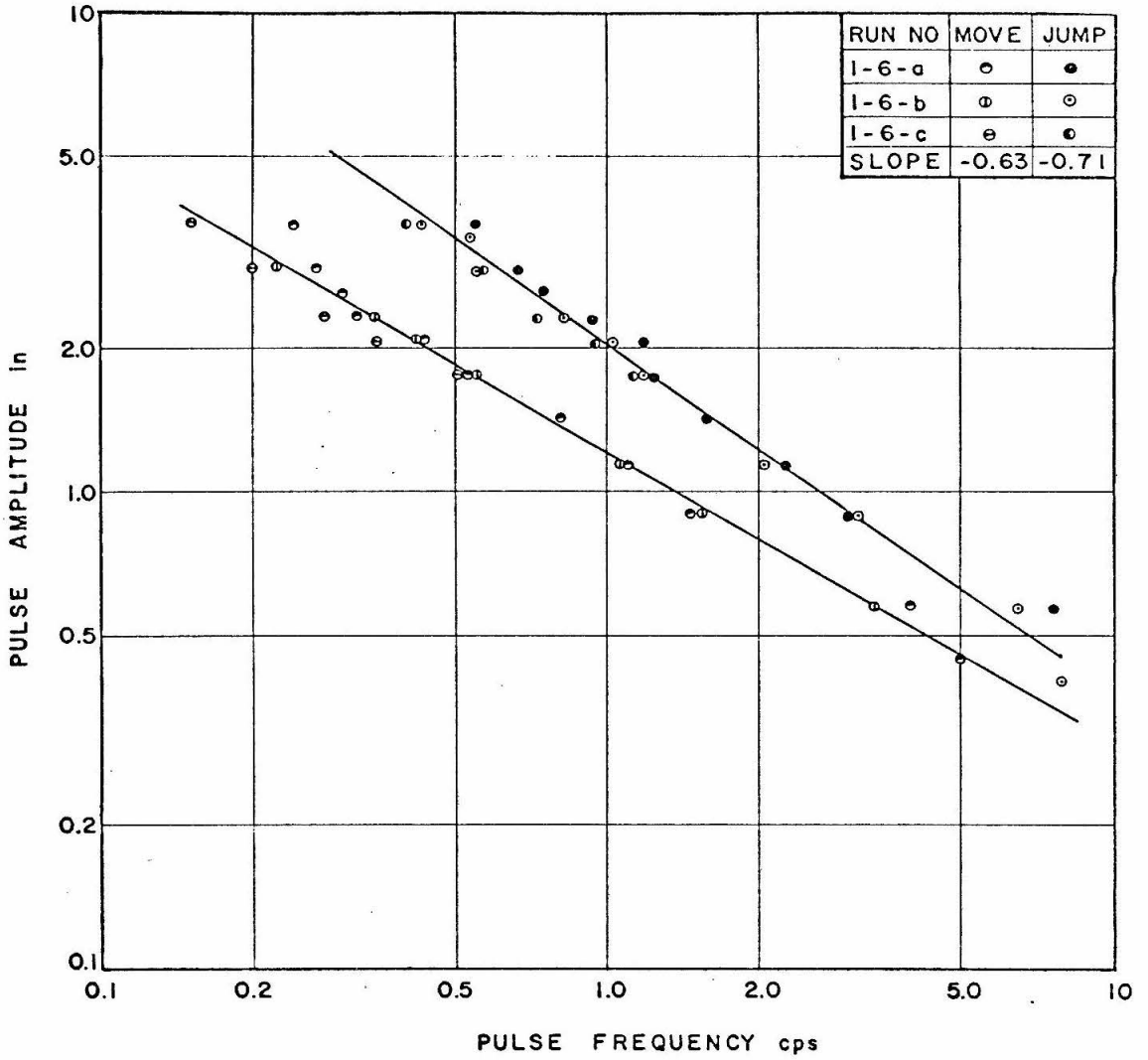

Fig. 4-2 Amplitude-frequency relations for critical conditions of move and jump in Run No. 1-6. Sand grains, d_s = 0.098 mm, in water with h = 0.2 ft and a^s = 0.244 in.

by taking an arithmetic mean $\overline{s}_1$ of all the s_1 values, and comparing it with $\overline{s}_2$, the mean of the s_2 values. The results are $\overline{s}_1 = -0.672$ and $\overline{s}_2 = -0.685$, a difference of only 2%.

Data from a few runs did not plot as single straight lines, but had amplitude frequency curves which displayed two straight sections of different slopes. One of these runs is Run 2-11, the data from which are plotted in Figure 4-3. The change in slope is from -0.74 to about -1.1. Other runs which exhibit these breaks do not have such an abrupt change of slope as seen in Figure 4-4 which presents data from Run 3-4, which has the most pronounced break in Series 3. Table 4-2 lists those runs with breaks and notes the type of break in each case. 'Definite' implies a break similar to that in Figure 4-3. 'Weak' implies a break similar to that in Figure 4-4.

TABLE 4-2

Runs in which the Amplitude-frequency curves consisted of two straight sections.

RUN NO.	TYPE OF BREAK
2-3	weak, jump curve only
2-4	definite
2-9	definite, jump curve only
2-10	definite
2-11	definite
3-2	weak, jump curve only
3-3	weak, jump curve only
3-4	weak
12-2	weak, jump curve only

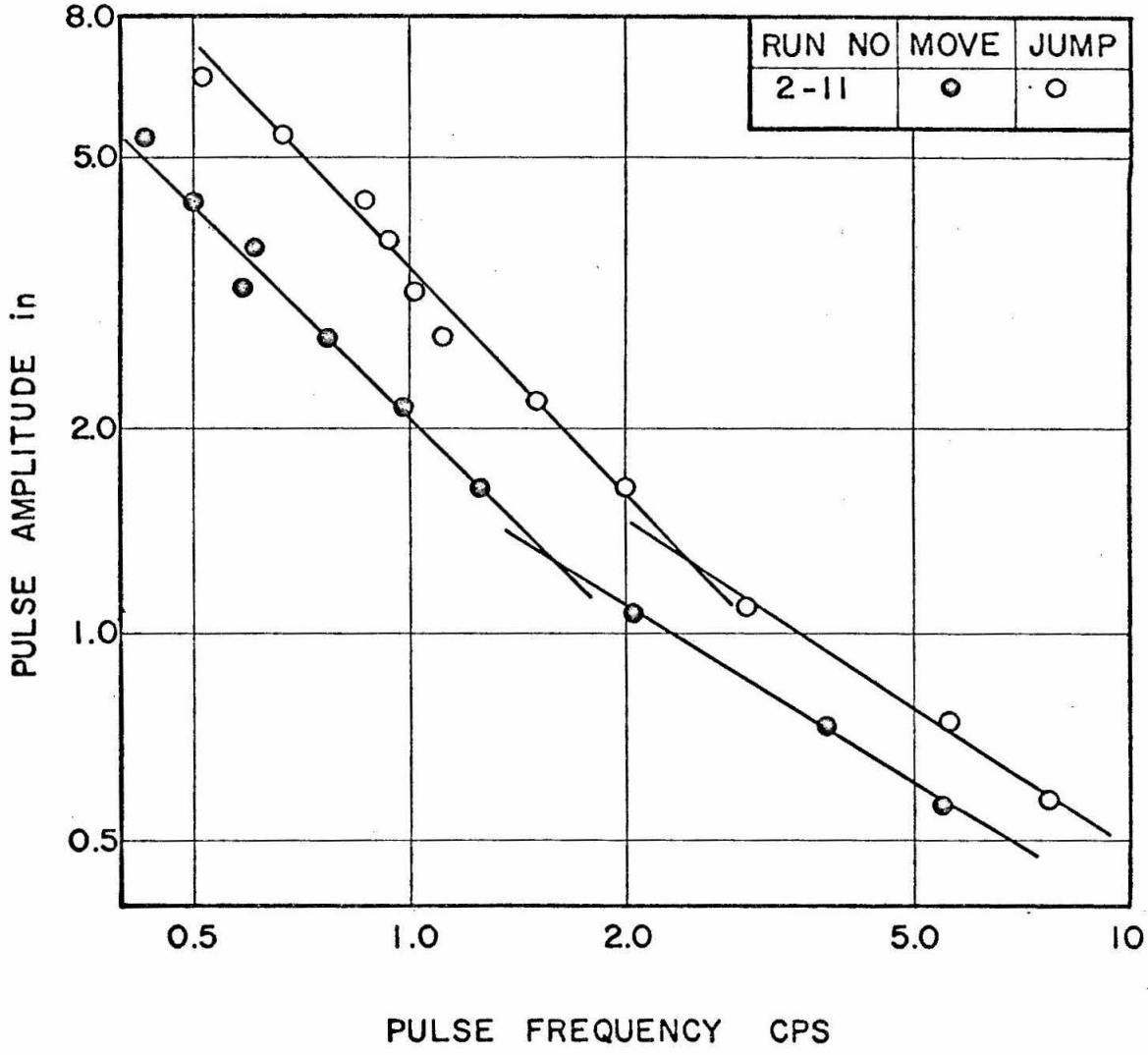

Fig. 4-3 Amplitude-frequency relations for critical conditions of move and jump in Run No. 2-11. Sand grains, d_s = 0.564 mm, in water with h = 0.2 ft and a^s = 0.182 in.

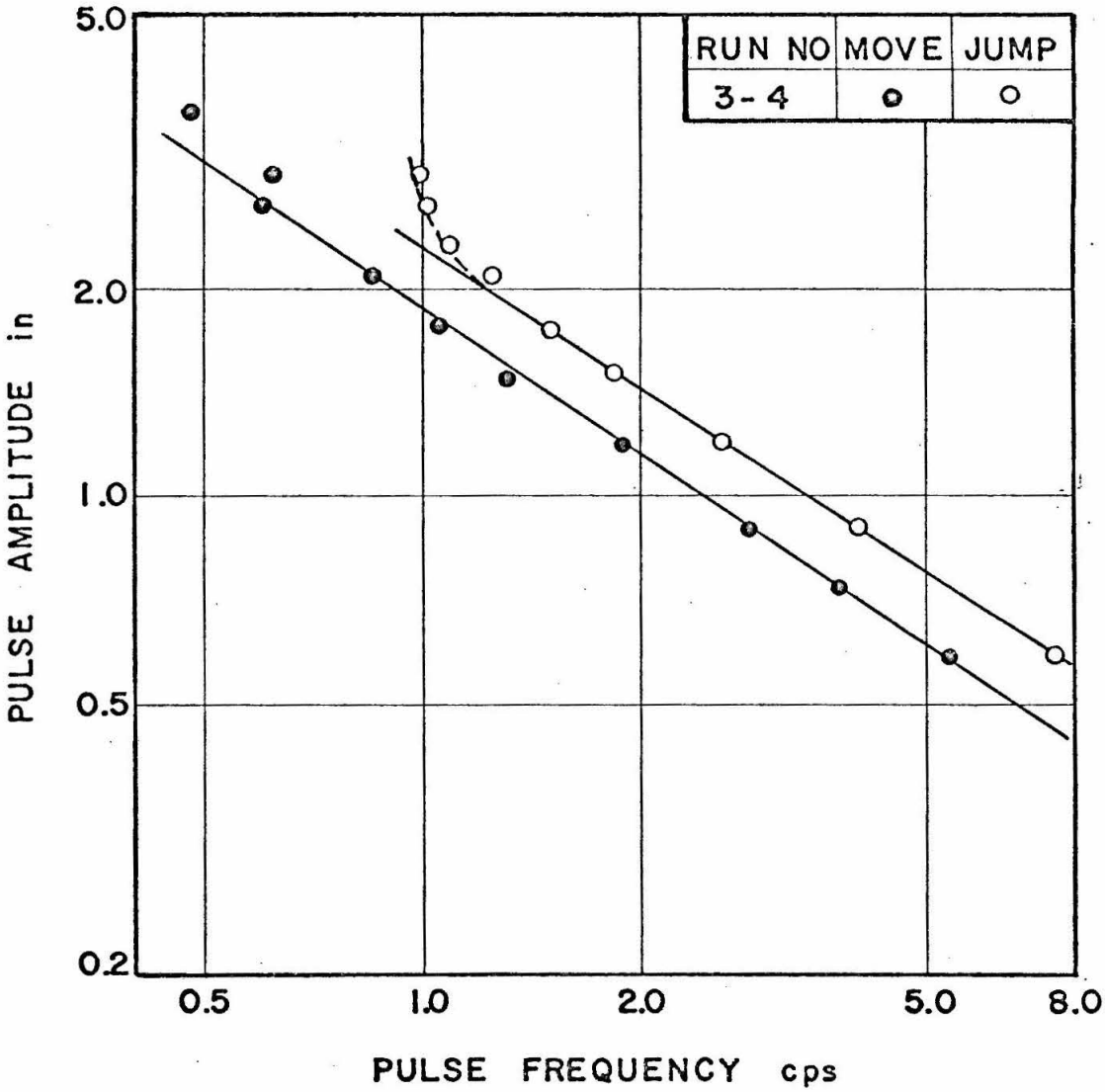

Fig. 4-4 Amplitude-frequency relations for critical conditions of move and jump in Run No. 3-4. Sand grains, d_s = 0.825 mm, in water with h = 0.2 ft and a = 0.244 in.

Runs 2-3, 2-9, 3-3 and 12-2, have breaks only on the 'jump' curve. In Section IV-D-2 this effect is considered in greater detail and an explanation offered for it.

B. DEPENDENCE OF CRITICAL JET STRENGTH ON THE EXPERIMENTAL VARIABLES.

1. Definition of Jet Strength.

As a measure of jet strength necessary to cause grain motion, it is proposed to take that quantity which remains constant along the line of critical amplitude and frequency, for the conditions of interest. The basis for this lies in the fact that a grain's resistance to motion remains fixed, independent of the changes in pulse frequency or amplitude. Under conditions just sufficient to cause motion, or to cause jumping, the forces applied to the grain must be equal to the resistance offered by it. The applied force must then be the same at all points on the curve defining critical conditions.

Since $\frac{A}{\omega^s}$ = constant = K, say on each line the jet strength is defined as:

$$\text{jet strength} = K = \frac{A}{\omega^s} . \qquad (3)$$

The jet strength required to move grains will be K_1 and that to cause jumping will be K_2. The units of jet strength are $\left[\text{length } (\text{time})^s\right]$. This unit will be denoted by the letters, cin when the amplitude is measured in inches and the frequency in cycles/second.

The mean exit velocity, U, of the pulse from the tube is given by $U = 2A\omega$. By substitution, the jet strength can be written in terms of this velocity. The result is $K = \frac{1}{2} \frac{U}{s+1}$. Now s is approximately equal to $-\frac{2}{3}$, see Section IV-A, so $K = A\omega^{2/3}$ or $K = \frac{1}{2} U\omega^{-1/3}$. A convenient method of determining K is to note that regardless of the value of s, K is numerically equal to the pulse amplitude corresponding to 1 cycle/sec. This can be read directly from the amplitude frequency curve as determined by the experiments.

2. Effect of Tube Diameter.

It can be seen from Table 4-1 that the effect of tube diameter, in most cases, is small. The exceptions are those runs which have a break in their amplitude-frequency curves. This suggests plotting the results for fixed tube height, sediment and fluid on the same graph. Figure 4-5 is such a plot in which the data corresponding to three different tube diameters define a single line with values of K_1 and K_2 very close to those given in Table 4-1 for each individual run.

Curves obtained in this way depend upon both sediment and fluid properties as well as upon the tube height. Because the slopes of all the lines are essentially the same it is possible to collapse them all into one curve by plotting in the dimensionless coordinates $\frac{A}{A_o}$ and $\frac{\omega}{\omega_o}$. Here A_o is the amplitude corresponding to ω_o where ω_o is defined to be 1 cycle/second. The result on logarithmic paper, must be a line of slope $-\frac{2}{3}$, through the point (1, 1). By doing one experiment at 1 cycle per second to determine A_o, for the sediment and fluid of interest, the critical frequency corresponding to any pulse amplitude can then be

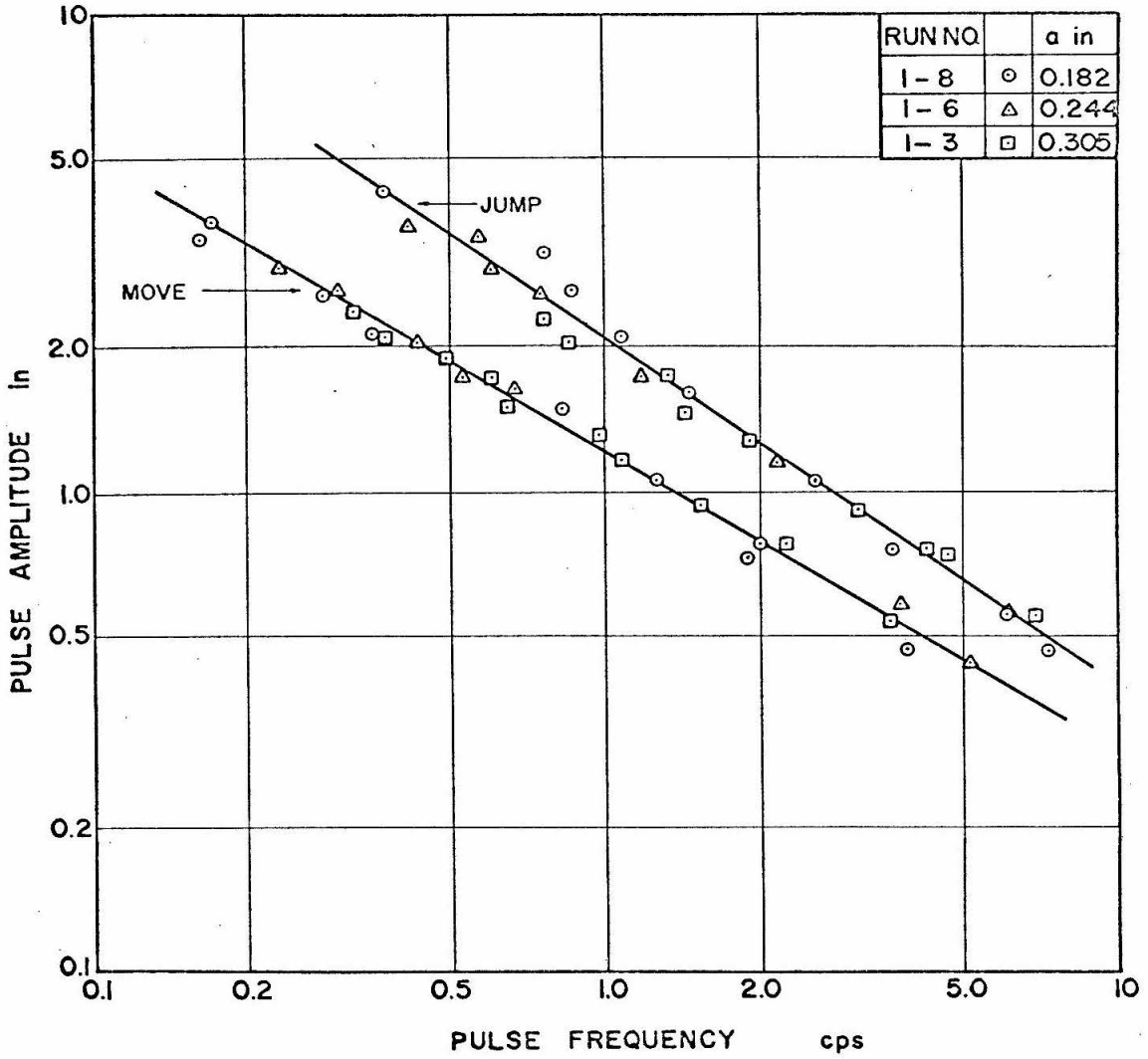

Fig. 4-5 Amplitude-frequency relations for critical conditions of move and jump in Runs No. 1-8, 1-6 and 1-3. Sand grains, d_s = 0.098 mm, in water with h = 0.2 ft.

found. In Section IV-C a better method of determining critical conditions is presented, one which does not require any experiments.

3. Effect of Tube Height.

Increasing the distance from the end of the jet tube to the sand bed, reduces the effectiveness of a given pulse. This is the result of the increased viscous dissipation that occurs with the greater distance that the pulse travels. Clearly there is a minimum jet strength which a pulse can have, at each tube height, and still be able to reach the sediment bed. Figure 4-6 shows that the jet strength required for grain motion does increase with tube height for each of the sediment sizes shown. The relation appears to be linear and the slope of each line to be the same, independent of sediment size.

Now consider the jet strength to be made up of two parts, the strength required to overcome the resistance offered by the fluid, and the strength required to cause grain motion. The former, K_h, will depend upon the fluid, the distance to the bed and possibly the jet strength K. The latter, K_s, is a function of the properties of the fluid and sediment. K_s may be considered to be the critical jet strength required for a zero tube height. It is also the strength of the pulse measured at the bed after it has travelled through the fluid from the end of the jet tube. If the sediment size is increased, and all other variables held constant, the increase in critical jet strength comes mostly from the K_s component. Thus for all values of h, the increase in jet strength caused by a given increase in sediment size will be the same. In other words, lines of constant sediment size on a plot of tube height

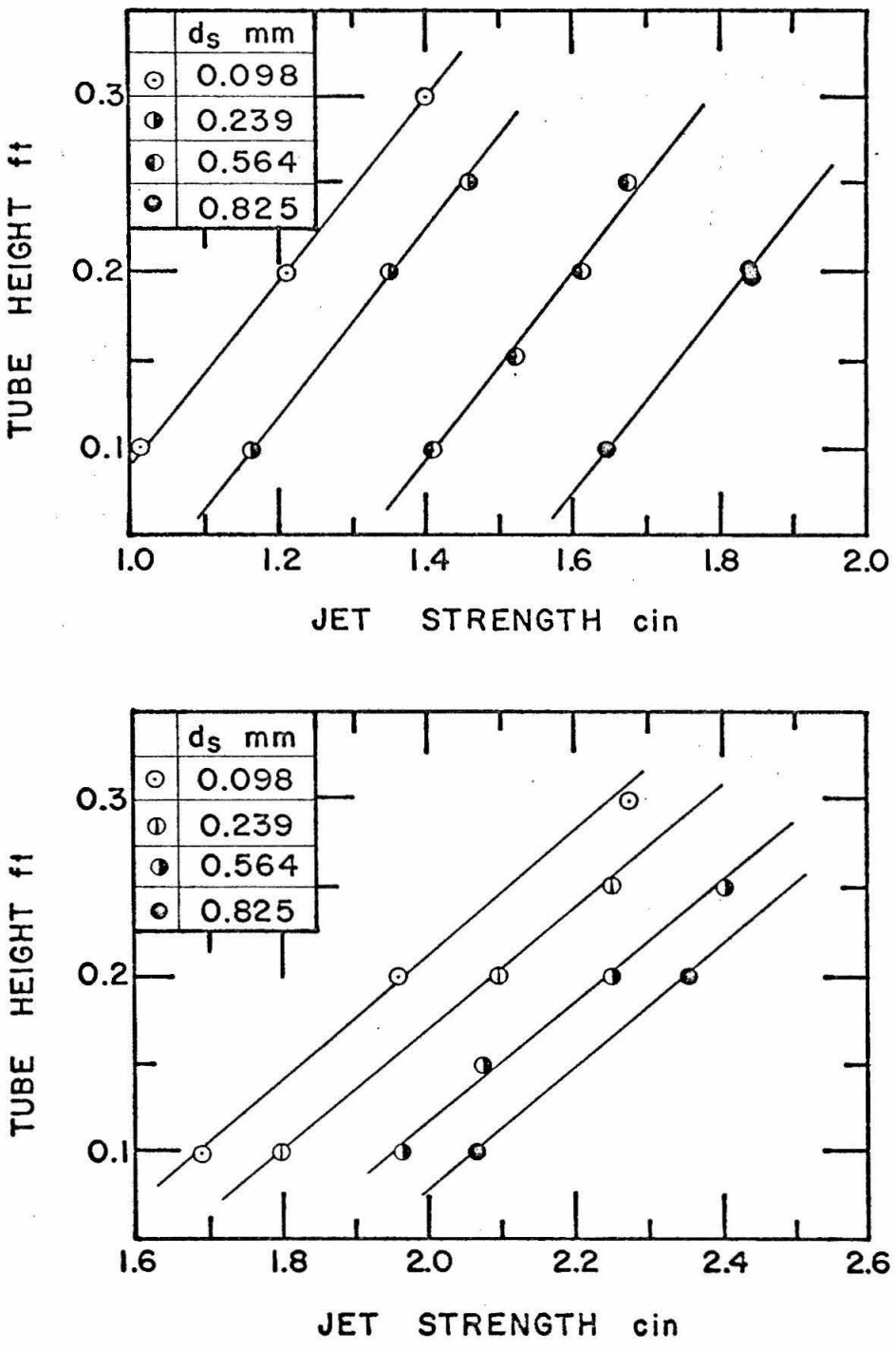

Fig. 4-6 The effect of tube height, for four different sand sizes, d_s, on the jet strength required to cause sand grain movement (upper) and jumping (lower) in water. Tube diameter a = 0.305 in.

against jet strength will be parallel. Figure 4-6 shows this to be the case.

In the lower graph of Figure 4-6, the slope of the lines is less than in the upper graph. It is suggested that a reason for this is the dependence of K_h upon the jet strength K. At higher values of K, the fluid motion inside the pulse must be more intense which would result in the pulse experiencing more viscous dissipation. Consequently the reduction in jet strength over a given distance will be increased. Since the jet strengths are larger in the jump case, the necessary increase in K to compensate for a given increase in tube height, will be larger, implying that the slope of the jump lines will be less.

4. Effect of Viscosity.

Changing the viscosity of the fluid will affect the critical jet strength in two opposing ways. First, in a more viscous fluid the pulse will encounter more resistance before reaching the bed, thus losing some of its effectiveness. Secondly, at the bed the mechanism by which grains are moved will be affected. The action of the pulse is to exert a drag force upon the grain, which causes it to move. If the viscosity is increased, the drag coefficient of the grain increases. Hence, if two otherwise identical pulses act on a grain, the one made up of the more viscous fluid will exert the greater drag force. By increasing the viscosity one can thus increase the effectiveness of a pulse acting on a grain.

Figure 4-7 presents the effect upon the jet strength of changing the viscosity. All the points correspond to a sand size of 0.098 mm.

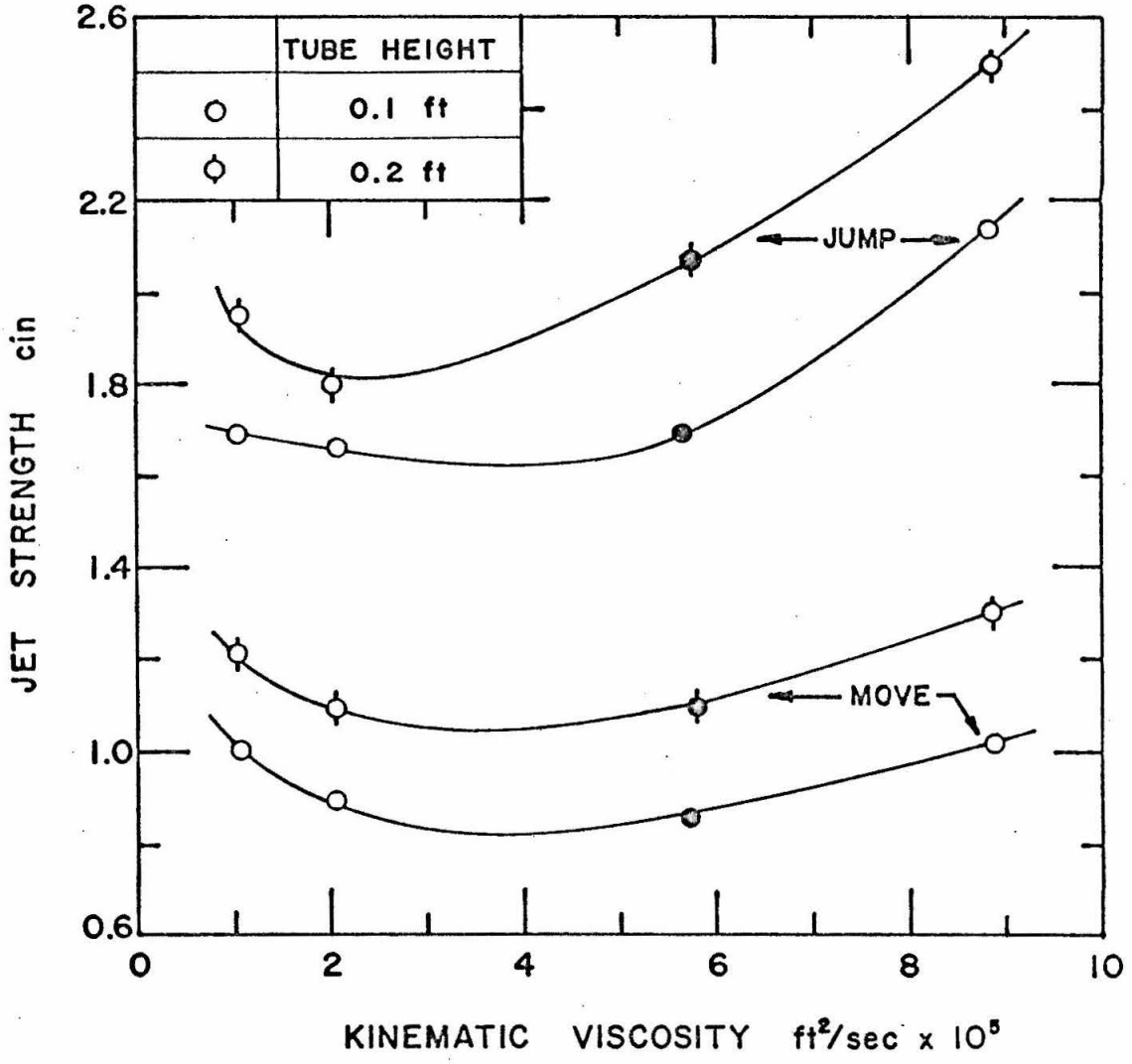

Fig. 4-7 Jet strength required to cause sand grains to move or jump as a function of kinematic viscosity. Hollow points are experimental, solid points are calculated. Values of $\frac{\gamma_s - \gamma}{\gamma}$ range from 1.65, at the left, to 1.33 at the right of the horizontal axis; d_s = 0.098 mm, a = 0.305 in.

The hollow symbols are actual experimental points and the solid ones are calculated values of jet strength. They were calculated by a method presented in Section IV-C below. Before discussing the possible interplay of the two effects mentioned above it should be noted that in the experiments the relative density of the sediment and fluid was not held constant as the viscosity was increased. The glycerol solutions both had specific gravities in excess of that of water, namely 1.058 and 1.146. By decreasing the relative density of sediment and fluid grain motion is aided and one would expect to measure lower values of both K_1 and K_2.

With this in mind it appears that an increase in kinematic viscosity, to approximately two or three times that of water makes it easier for the pulse to cause grain motion. The second effect discussed above, must be the dominant one in these conditions. For larger increases in viscosity the required jet strength increases sharply, particularly in the jump cases. This implies that the greater dissipative effect of the increased viscosity is of more importance than the increase in drag coefficient. The greater increase in the jump case is in keeping with the suggestion, put forward in the preceding section, that the stronger pulses are more susceptible to the viscous resistance offered by the fluid.

5. Effect of Sediment Size.

As the sediment size is increased the jet strength required for movement must increase. Figure 4-8 shows three runs with the same values of tube height and tube diameter. With increasing sediment size

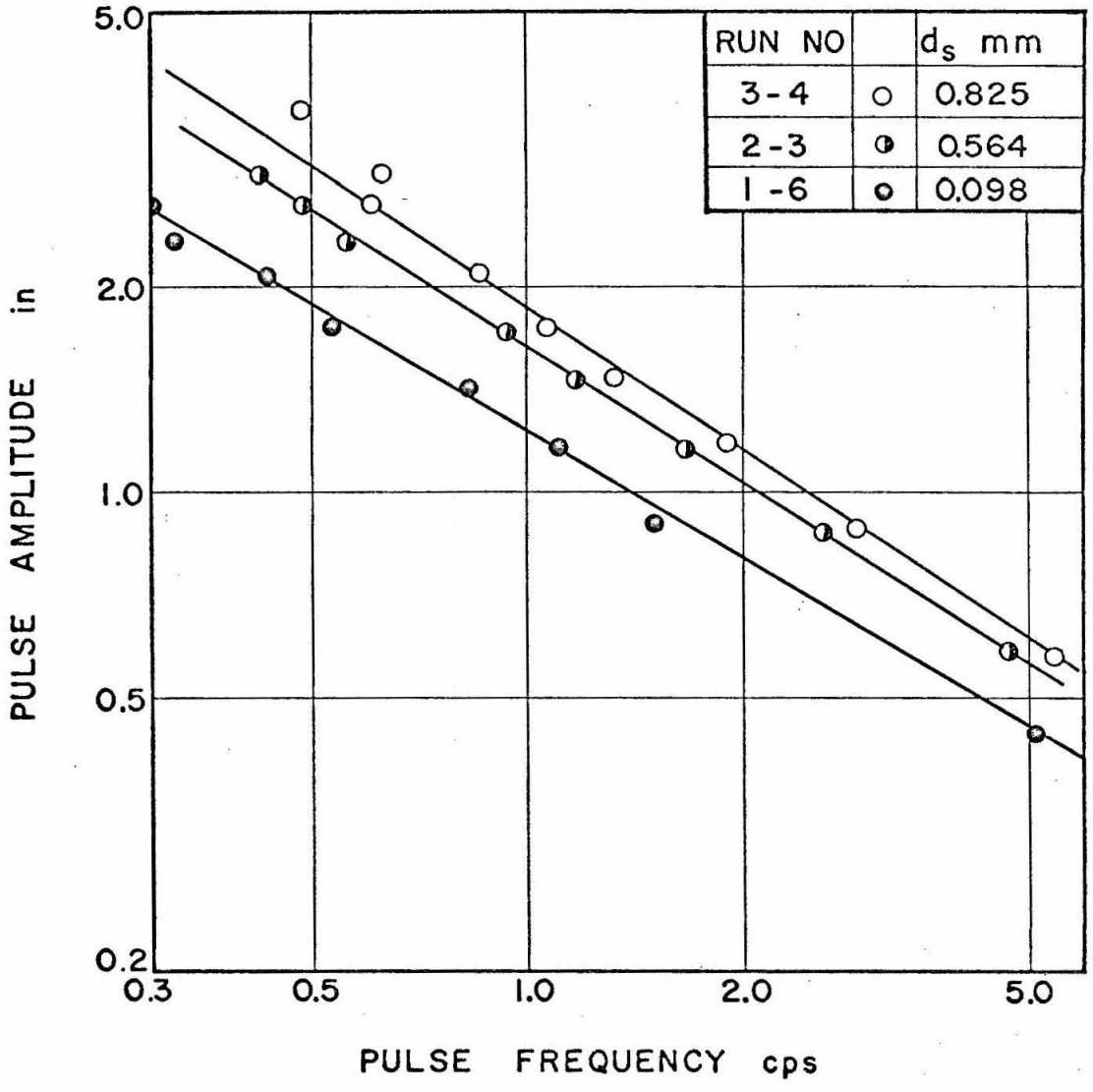

Fig. 4-8 Amplitude-frequency relations for critical conditions of sand grain movement in water, h = 0.2 ft, a = 0.244 in.

the curves are displaced away from the origin while remaining essentially parallel. To examine the effect of sediment size upon jet strength, Figure 4-9 has been prepared. All the data on the plot are from experiments with sand grains in water. Those points which correspond to the same tube height have been joined. The line marked $h = 0$ was determined from Figure 4-6, by assuming that the lines in that figure can be extended with the same slope to $h = 0$. The values of jet strength for zero tube height can then be found. This is a reasonable assumption in view of the suggested breakdown of jet strength into two parts K_h and K_s, discussed in the section on tube height.

Since the effect produced at the bed is the same along lines of constant sediment size, the difference in jet strengths, between the lines of constant tube height, must represent the increase in jet strength required for the pulse to travel the extra distance to the bed. It has been suggested that the stronger pulses will have a greater dissipation in moving a given distance. This would imply that the lines of constant tube height in Figure 4-9 should diverge with increasing jet strength, and that the lines should be spaced farther apart in the jump plot than in the move plot. Both these effects are present in Figure 4-9.

From experiments with the other sediments, the dependence of jet strength on the sediment size can be derived for a range of values of $\frac{\gamma_s - \gamma}{\gamma}$. Here γ_s is the specific weight of the sediment and γ is the specific weight of the fluid. Figures 4-10 and 4-11 show the 'move' and 'jump' results respectively for a tube height of 0.1 ft in water at a fixed temperature. The sediment and the corresponding values of $\frac{\gamma_s - \gamma}{\gamma}$ are given on the plot adjacent to each curve. Results with

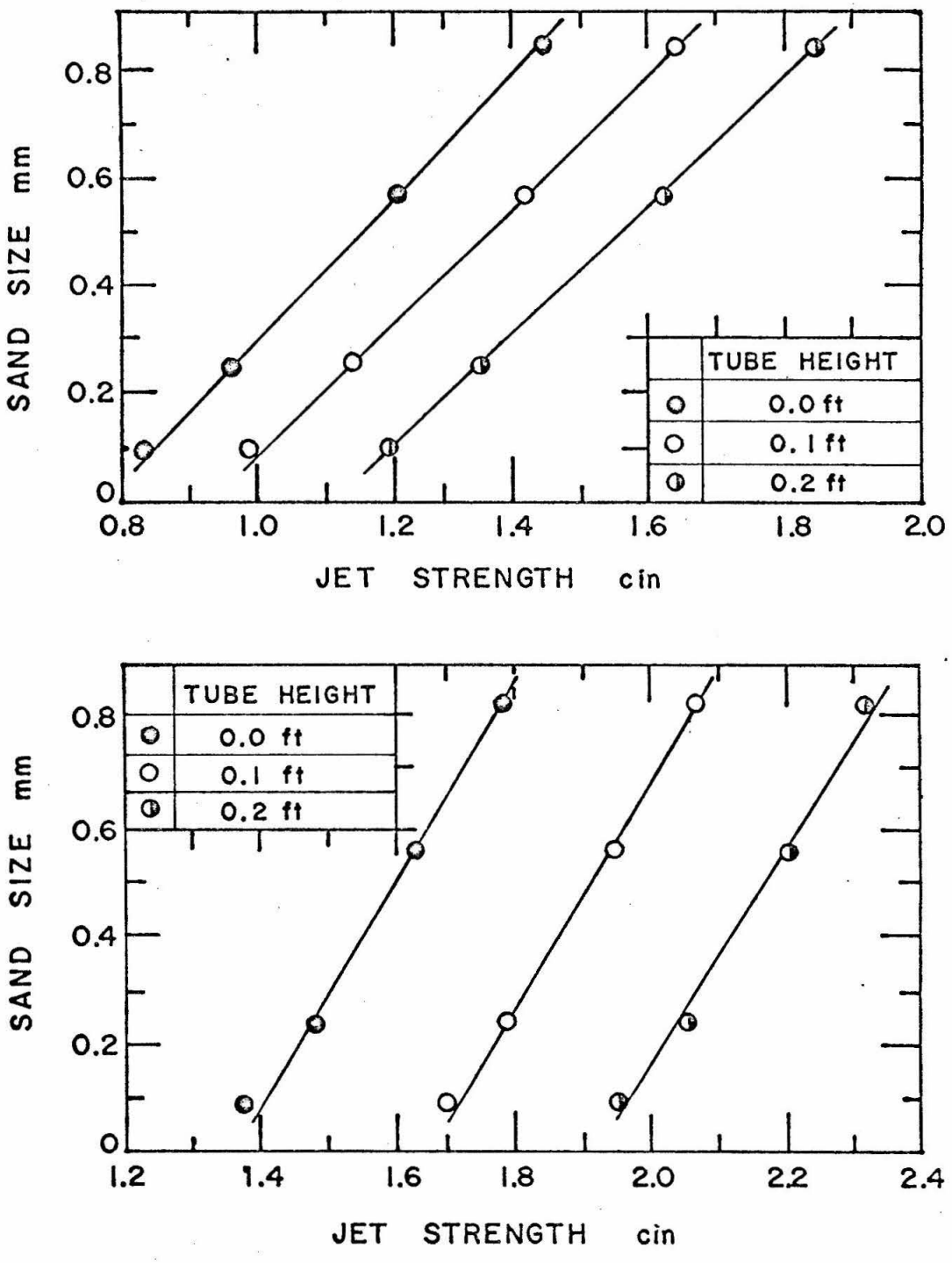

Fig. 4-9 The effect of sand size, at three different tube heights, on the jet strength required to cause grain movement (upper) and jumping (lower) in water. Tube diameter a = 0.305 in.

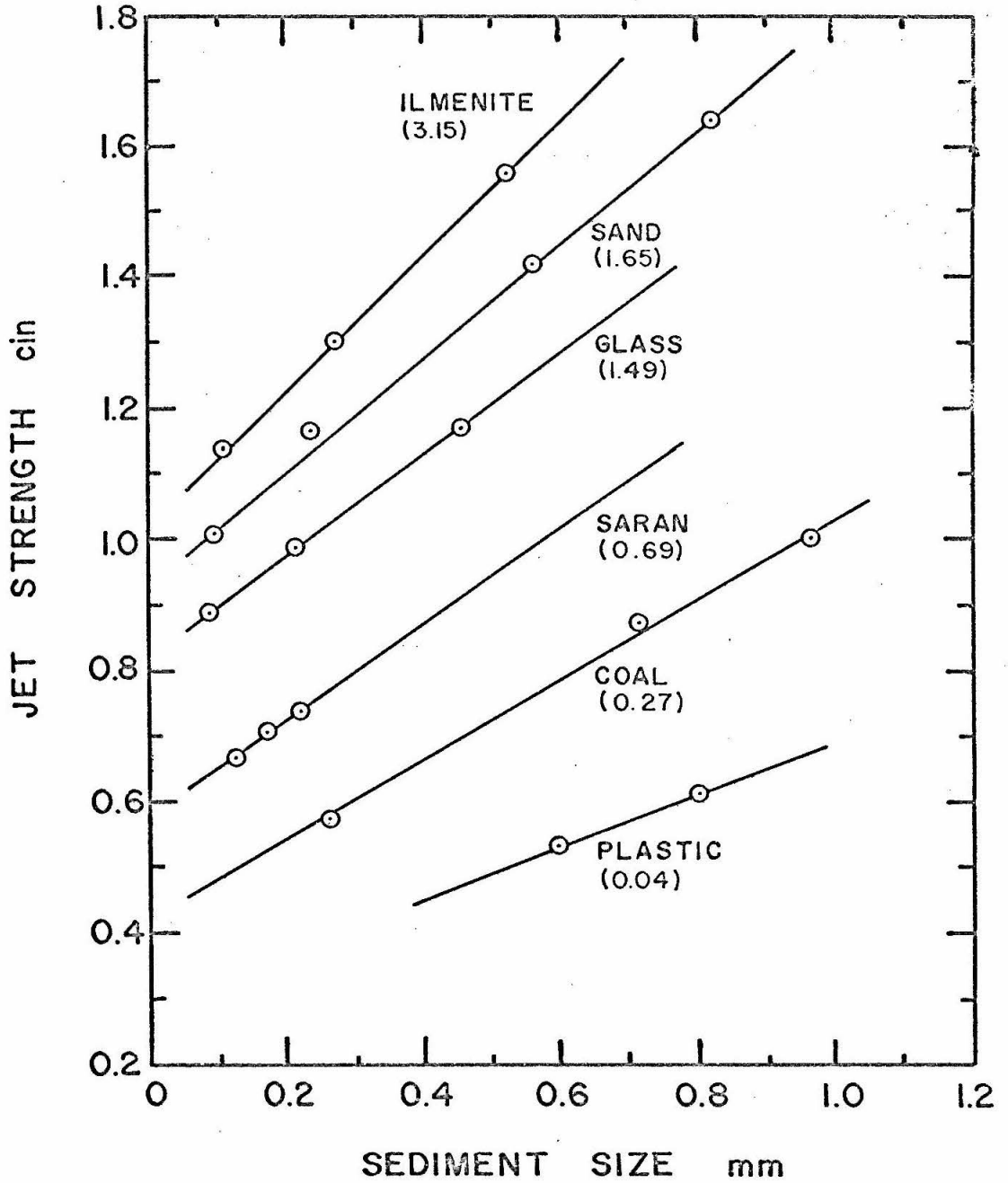

Fig. 4-10 Jet Strength required to move sediment grains in water as a function of sediment size. Tube height, h = 0.1 ft. Numbers in parentheses are values of $\frac{\gamma_s - \gamma}{\gamma}$ for each sediment.

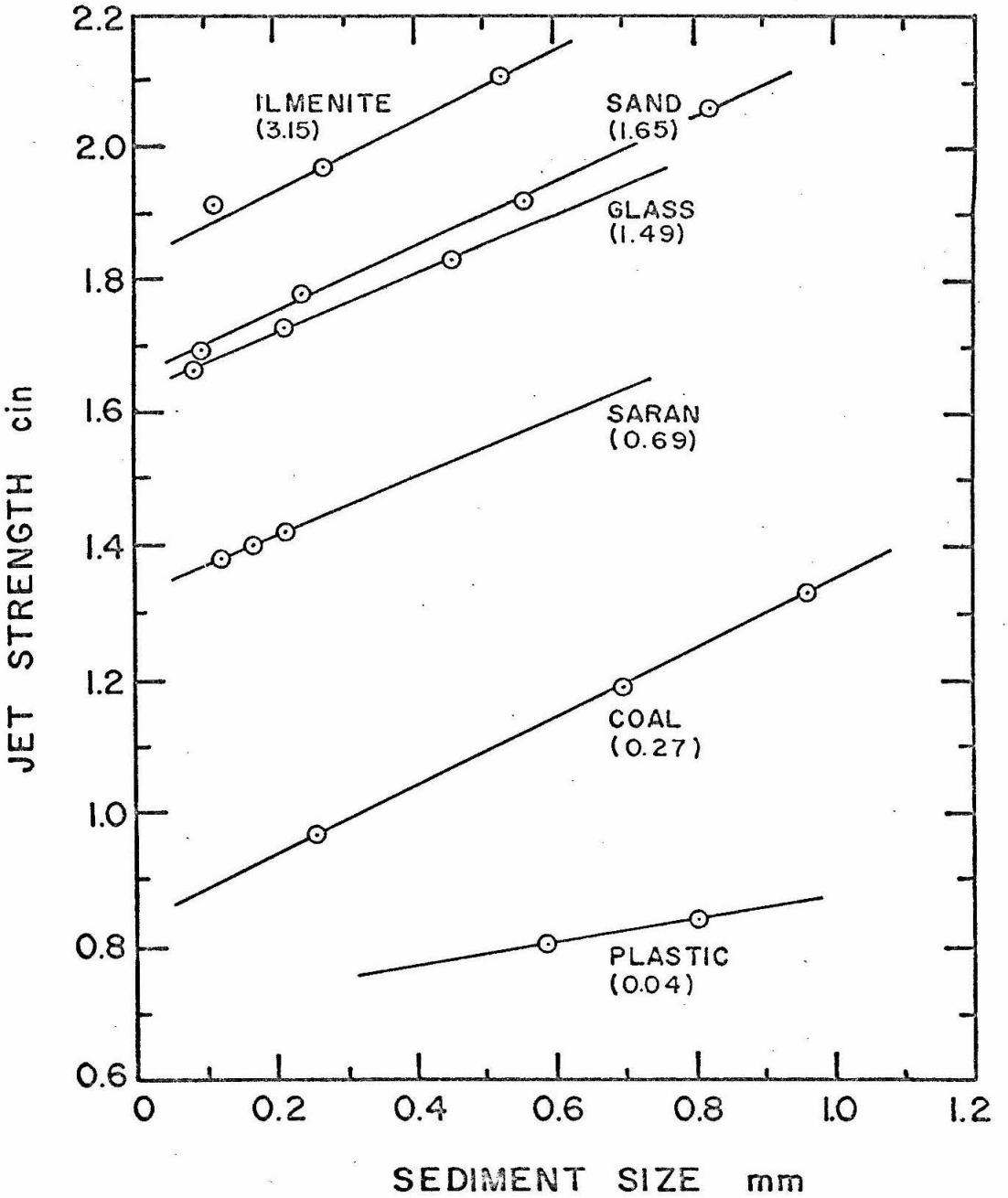

Fig. 4-11 Jet strength required to cause grain jumping in water as a function of sediment size. Tube height, h = 0.1 ft. Numbers in parentheses are values of $\frac{\gamma_s - \gamma}{\gamma}$ for each sediment.

h = 0.2 ft are similar and are not presented in graphical form. They can be obtained from Table 4-1. On the basis of the linearity of the results obtained with sand, it has been assumed that the data for each sediment lie on a straight line. The two data points for plastic beads have been joined and extended linearly. For the remainder of the data, the best straight line through the points has been drawn. Deviations from these lines are very small, indicating that the assumption of linearity is justified. The data for ilmenite require some explanation. Reference to Table 3-1 will show that the two larger sizes have almost equal specific gravities, but that for the smaller size the specific gravity is much larger, 4.76 as opposed to 4.15. For this reason the lines through the data corresponding to ilmenite in Figures 4-10 and 4-11 have been drawn through the two points corresponding to the larger sizes. In all cases this line passed below the third point.

The results can be summarized by saying that the jet strength and sediment size are related by an expression of the form $K = G_1 d_s + G_2$. Where G_1 and G_2 are functions of the fluid, the tube height and the difference in specific weights of the sediment and fluid. For the particular conditions of Figure 4-10, where the fluid and tube height are constant, $G_1 = 0.8 \left(\frac{\gamma_s - \gamma}{\gamma}\right)^{0.22}$ and no simple analytical expression could be found for G_2. This analysis is not pursued further since a more complete approach is given in Section IV-C.

6. Effect of the Parameter $\frac{\gamma_s - \gamma}{\gamma}$.

The parameter $\frac{\gamma_s - \gamma}{\gamma}$ is a measure of the relative inertial effects. It is one that has received very little attention in the past, except to note that it is responsible for differences in the observed behavior of sediment in air and in water. In wind blown sand, values of $\frac{\gamma_s - \gamma}{\gamma}$ are approximately 2000, while for sand in water, the value is 1.65. This great difference gives rise to different types of motion in the two cases, e.g. saltation is a major transport mechanism in air but a negligible one in water. The reason for this lack of attention is not hard to find. Virtually all the sedimentation problems encountered by hydraulic engineers and research workers in the normal course of their work, are concerned with sand grains in water. This situation is reflected very strongly in the published literature on sedimentation. Notable exceptions are papers by Shields (6), who experimented with sediments having a wide range of specific gravities, and Bagnold (39) who worked with neutrally buoyant particles in connection with his studies on the suspension of sediment. At the other end of the spectrum geologists and agronomists, e.g. Bagnold (40) and Chepil (16) have made extensive studies of sand transport by wind. Thus under only two very different conditions has transport been well documented, leaving a large gap in the range of possible values of $\frac{\gamma_s - \gamma}{\gamma}$.

Using the pulsating jet, a range of values of $\frac{\gamma_s - \gamma}{\gamma}$ can be investigated. This has been done for values ranging from 0.04 to 4.0, a range which straddles the sand in water value of 1.65. In doing this, the other variables in the system e.g. viscosity, jet geometry and sediment size, must be kept constant. The first two are easily controlled, but

the third one is much more difficult, if not impossible. It is necessary to use the known relationship between jet strength and sediment size presented in Figure 4-10. By reading the intersections of lines of constant sediment size and constant $\frac{\gamma_s - \gamma}{\gamma}$, the required values of jet strength as a function of $\frac{\gamma_s - \gamma}{\gamma}$ can be found for each sediment size.

Three sediment sizes, d_s = 0.2, 0.6, and 0.8 mm were selected for computation and the results are shown in Figures 4-12 and 4-13. Only data for a tube height of h = 0.1 ft have been plotted. Data for h = 0.2 ft, which define curves of the same type, can be found in Table 4-1. All the data were taken from experiments in water because the kinematic viscosity of the fluid was required to be constant.

In Figure 4-12 two points in each sediment size are shown below the curve. One of them is derived from experiments using glass beads and the other from experiments with saran. Reference to Figures 3-15 and 3-16, which are photomicrographs of these sediments, shows that they both have extremely rounded grains. A shape effect is thus indicated. Because of their roundness the resistance offered to the grains' motion, as a result of grain interference, will be less than that offered to more angular particles. The critical jet strength will thus be reduced. Figure 4-13 shows that in the case of grain jumping all the data lie on the curve. In jumping, a grain does not encounter as much interference as does one which rolls across the surface of the sediment bed. The shape effect is thus minimized and the data are no longer affected by it. Other investigators have noticed this shape effect. White (7) made allowance for it by introducing the angle of repose into his analysis. However, when his experimental results are plotted on a Shield's

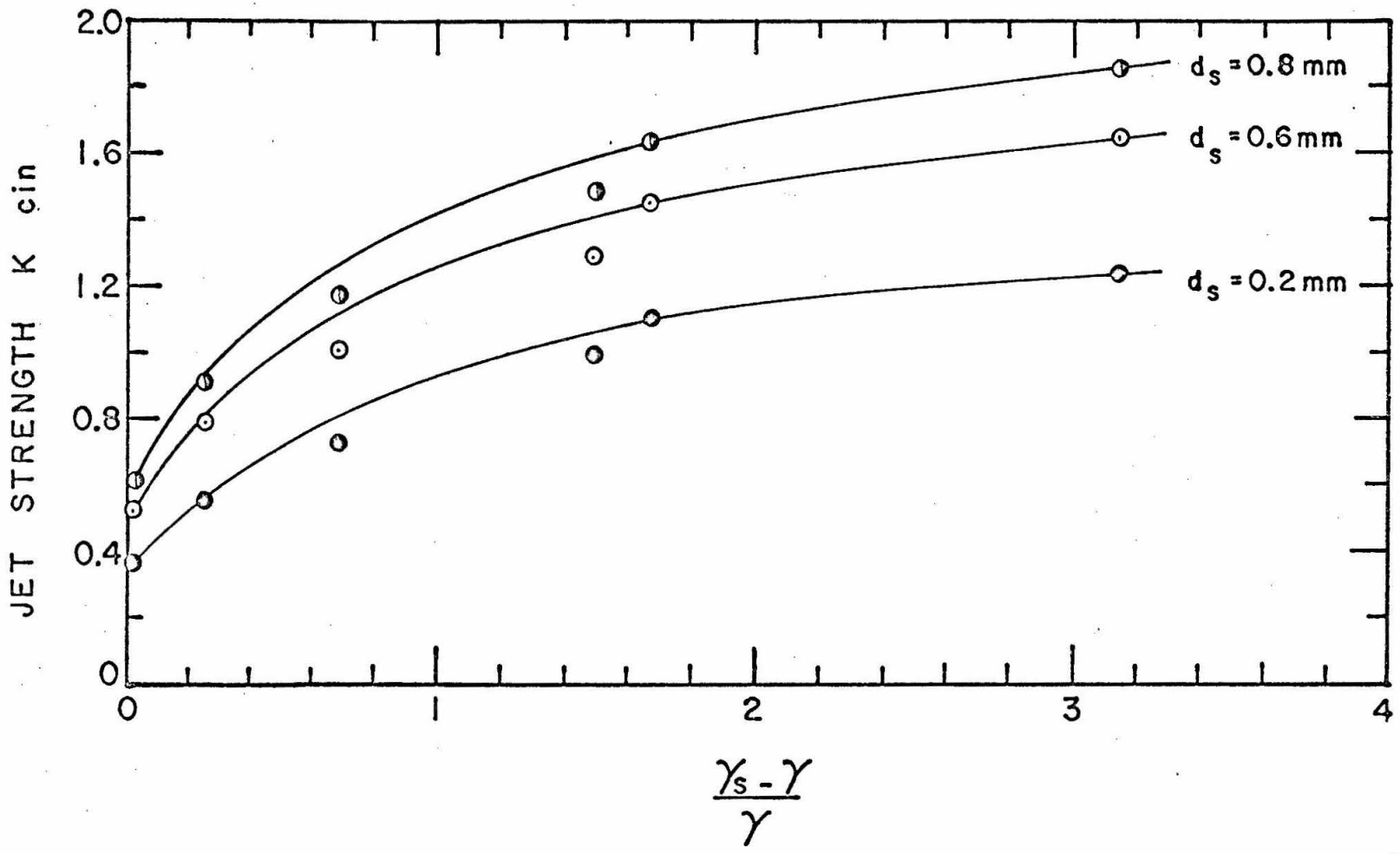

Fig. 4-12 Jet strength required to cause grain movement as a function of $\frac{\gamma_s - \gamma}{\gamma}$. Tube height, h = 0.1 ft in water.

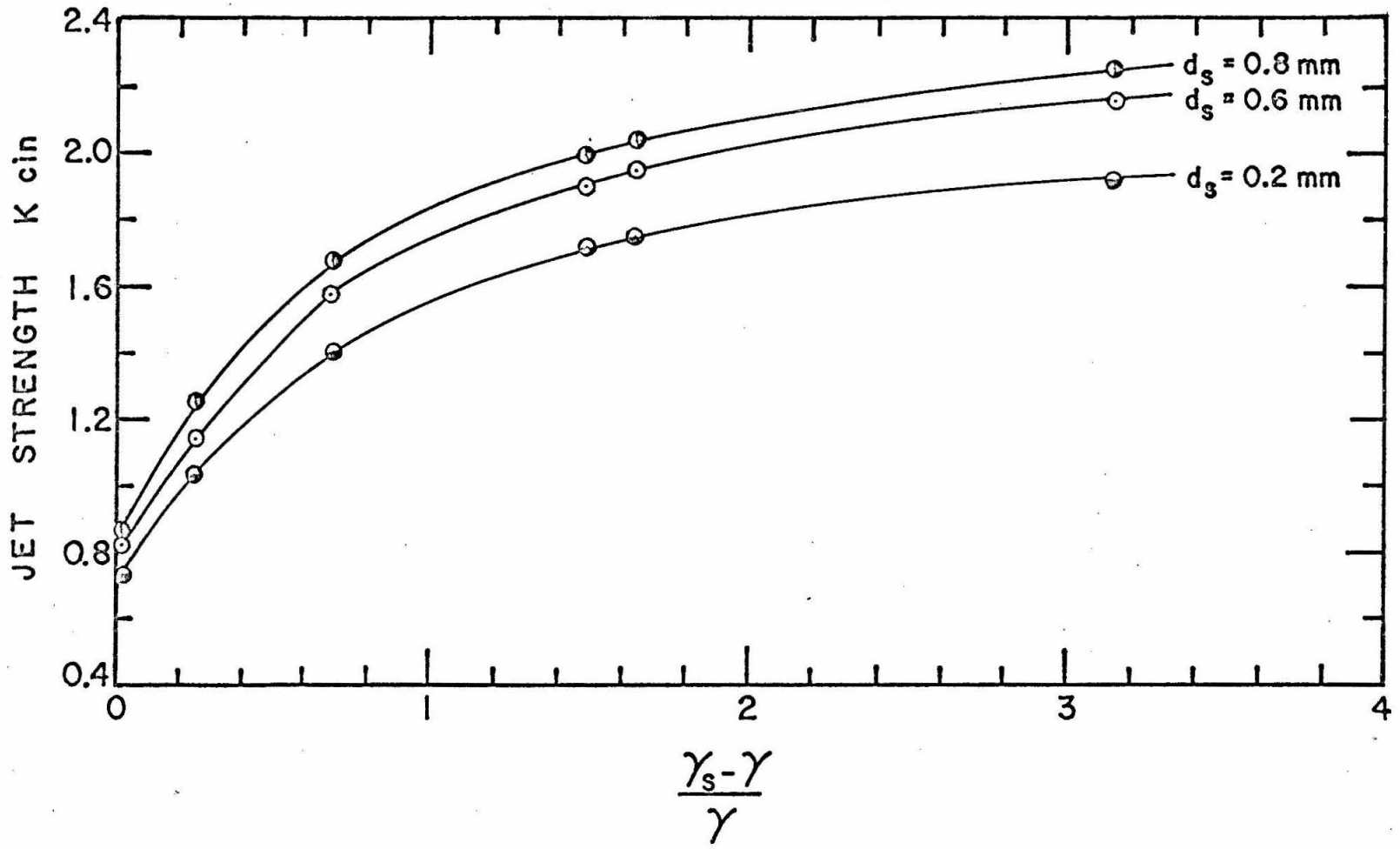

Fig. 4-13 Jet strength required to cause grain jumping as a function of $\frac{\gamma_s - \gamma}{\gamma}$. Tube height, h = 0.1 ft in water.

diagram it is found that data for steel shot, a rounded sediment, plot at appreciably lower values of Shield's parameter, $\frac{\tau_o}{(\gamma_s - \gamma)d_s}$, than do data from experiments with sand in both air and water. Vanoni (24) found similar results with glass beads in water in his experiments on the entrainment of sediments.

The plastic beads used in the experiments were also very rounded, and it might be expected that data derived from them would plot below the curves for the move conditions. However another factor became important in the case of plastic beads, namely, the difficulty of working with particles having a specific gravity close to that of water. In this range, specific gravity approximately 1.05, an error of $\frac{1}{2}$% in determining the specific gravity results in an error of approximately 10% in $(\frac{\gamma_s - \gamma}{\gamma})$. In spite of all the precautions taken in this determination, see Section III-B-1, the possibility of air being present in the pycnometer during weighing means that the value obtained, 1.04, is actually a lower bound for the specific gravity. The true position for the data from plastic beads is probably a little to the right of the plotted position, and thus under the curve.

All the curves in Figures 4-12 and 4-13 indicate a tendency for the jet strength to be less dependent upon $\frac{\gamma_s - \gamma}{\gamma}$ as this parameter is increased. By plotting the data on logarithmic paper it can be shown that the jet strength for a fixed sediment size varies as the one fourth power, approximately, of $\frac{\gamma_s - \gamma}{\gamma}$. The jet strength corresponding to plastic beads did not fit this relation and was higher than predicted by it. A power law variation cannot be expected to hold for small values of K because a finite jet strength, K_h, is required for the pulse to

reach the bed. The curves cannot therefore pass through the origin, but should converge to a value of $K = K_h$ as $\frac{\gamma_s - \gamma}{\gamma}$ tends to zero. The difficulty of determining K_h for each value of K precludes the use of $K-K_h$, which is certainly a more appropriate variable at small values of K. At larger values of K, we have $K >> K_h$ and the power law relation, as given above, appears to be adequate. The sediment size determines the value of the proportionality constant in each case. In the next section these relationships are explored more fully.

7. The Effect of the Parameter $(\gamma_s - \gamma)\, d_s$.

The product of the difference in specific weights of sediment and fluid, and the sediment size $(\gamma_s - \gamma)d_s$ arises frequently in sediment transport work. For example it is used to form the dimensionless shear stress in Shield's (6) analysis and occurs in White's (7) expression for critical shear stress. It is essentially a measure of the resistance of a particle to drag forces as a result of its immersed weight.

The parameter arises in a natural way from an analysis of the forces which act on a grain in a sediment bed. Drag forces arising from the action of the fluid may be written as

$$F = \tau_o \alpha_1 d_s^2$$

where τ_o is the shear stress acting on the grains and α_1 is a numerical coefficient. The resistance offered to motion by the sediment grain depends upon its immersed weight, and can be written

$$R = \alpha_2 (\gamma_s - \gamma) d_s^3$$

where α_2 is a numerical coefficient depending upon the grain shape and packing. Under critical conditions for motion R = F and we have

$$\tau_c \alpha_1 d_s^2 = \alpha_2 (\gamma_s - \gamma) d_s^3$$

$$\therefore \quad \tau_c = \left(\frac{\alpha_2}{\alpha_1}\right) (\gamma_s - \gamma) d_s$$

where τ_c is the critical value of τ_o and the ratio α_1 / α_2 is a function of the parameter $U_* d_s / \nu$ where $U_* = \sqrt{\tau_c / \rho}$.

In view of the apparent usefulness of the parameter $(\gamma_s - \gamma) d_s$ one would expect a well defined relationship between it and critical jet strength to exist. The jet strength required to move sediment is related to $\frac{\gamma_s - \gamma}{\gamma}$ by a power law, with the proportionality constant depending upon the sediment size. Multiplying $(\gamma_s - \gamma)$ by d_s will not change the slope of the lines on a logarithmic plot of jet strength, K against $(\gamma_s - \gamma)$. It will however shift their location. Figures 4-14 and 4-15 show that the multiplication by d_s actually collapses all the data so that it defines a single line. Figure 4-14 refers to a tube height of h = 0.1 ft, and Figure 4-15 to h = 0.2 ft. Again, data at the smaller values of jet strength tend to plot above the line. Both of these figures refer to critical conditions for grain movement.

From these plots we deduce that for the mechanism by which the pulsating jet moves sediment, the following relations hold

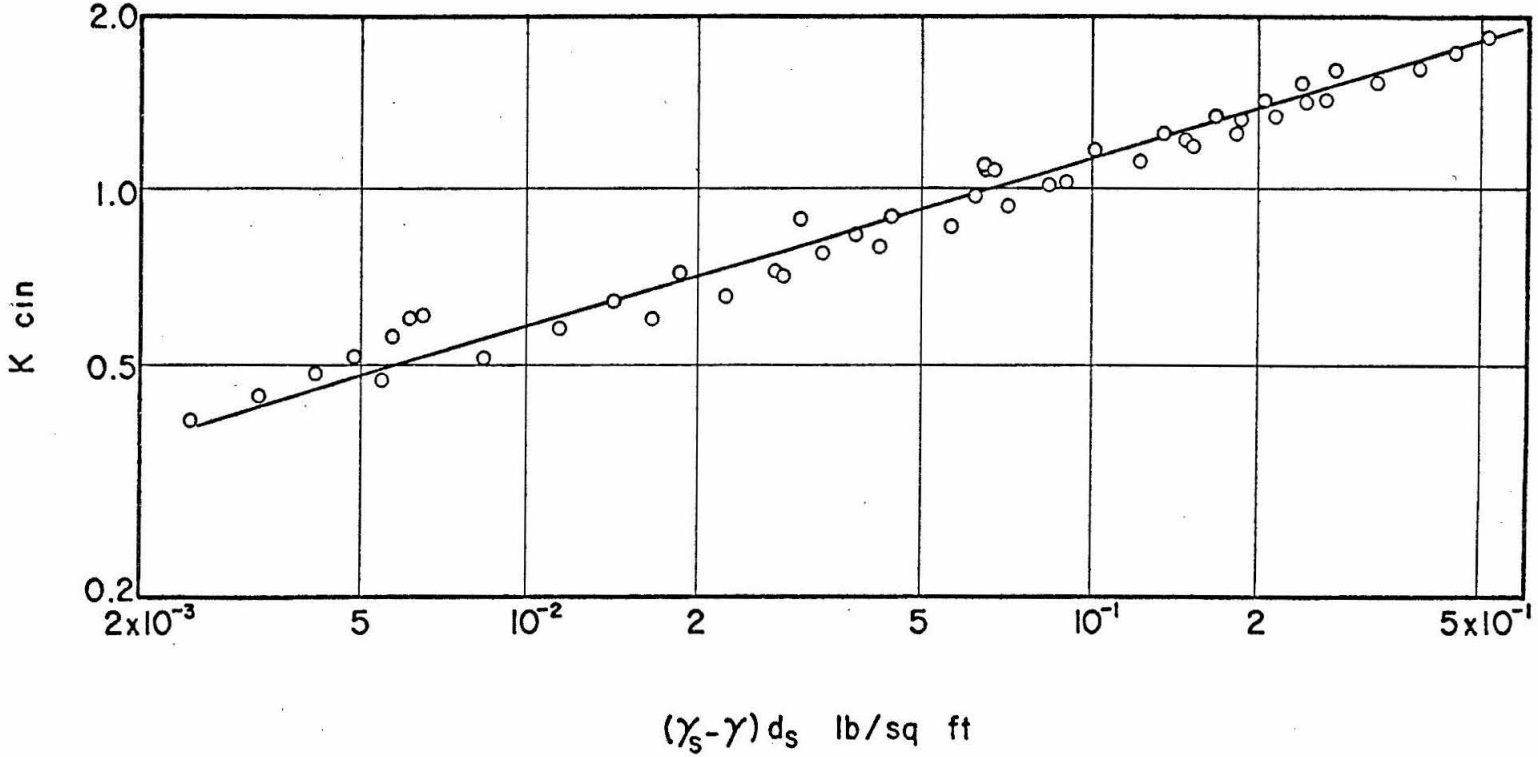

Fig. 4-14 Jet strength required to cause grain movement as a function of $(\gamma_s - \gamma)d_s$. Tube height, h = 0.1 ft in water.

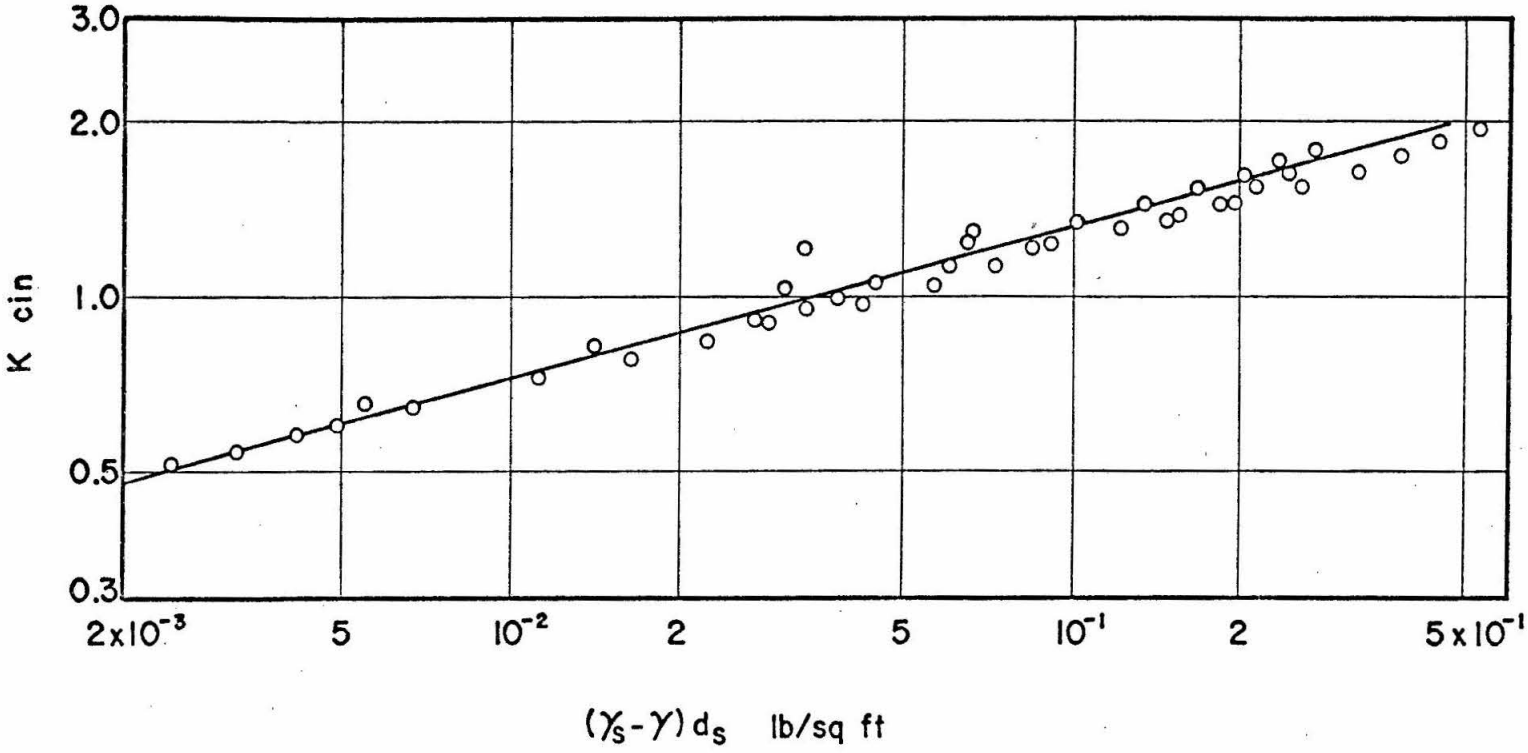

Fig. 4-15 Jet strength required to cause grain movement as a function of $(\gamma_s - \gamma)d_s$. Tube height, h = 0.2 ft in water.

$$K_1 = 2.21 \left[(\gamma_s - \gamma)d_s\right]^{0.286} \text{ for } h = 0.1 \text{ ft} \quad (4)$$

and

$$K_1 = 2.39 \left[(\gamma_s - \gamma)d_s\right]^{0.263} \text{ for } h = 0.2 \text{ ft} . \quad (5)$$

When $\gamma_s - \gamma$ is in lb/cu ft, and d_s is in ft the jet strength is given by the above in cin. It is recalled that the fluid viscosity, tube height and jet geometry are all fixed, Values of $\gamma_s - \gamma$ range from 2 lb/cu ft to 200 lb/cu ft, and d_s from 0.1 mm to 0.8 mm.

That the same parameter, $(\gamma_s - \gamma)d_s$, which correlates data from many different sediments in flume experiments, see Shields (6) and White (7), also correlates data from the pulsating jet, is an indication that the mechanism of fluid grain interaction is the same in the two cases.

C. DIMENSIONAL ANALYSIS OF THE PROBLEM.

The system has eight independent variables; two geometric parameters, two pulse generation variables, two fluid properties and two sediment parameters. They can be listed as

h = distance from jet tube to sand bed (tube height)

a = diameter of jet tube

A = amplitude of pulse

U = exit velocity of pulse

ρ = fluid density

ν = fluid kinematic viscosity

d_s = sediment size

$\gamma_s - \gamma$ = difference in sediment and fluid specific weights.

The burst frequency does not appear. This is because it is directly related to the amplitude and exit velocity of the pulse, viz $U = 2A\omega$. It is thus not an independent variable. The choice of $\gamma_s - \gamma$ may appear unusual, but there are two reasons why it was chosen. A physical reason for its inclusion is that gravity enters the problem only in the submerged weight of the particle, which is proportional to $(\gamma_s - \gamma)$. Use of $(\gamma_s - \gamma)$ results in a reduction in the number of independent variables in the problem. If it were omitted it would be necessary to include the sediment density ρ_s, and fall velocity w, in the list, making nine variables in all. In this case gravity enters in with the fall velocity. However by replacing ρ_s with $\gamma_s - \gamma$, one of the variables becomes dependent by virtue of the relation

$$w = f(\rho, \ (\gamma_s - \gamma), \ \nu, d_s).$$

The fall velocity will thus be omitted, leaving the eight variables listed above.

With such a large number of variables the dimensional analysis can be done in many different ways. It is certainly not clear a priori which choice of dimensionless parameters is most useful. Proceeding in the usual way three reference quantities are chosen. For a reference length the choice is wide; for a reference mass the fluid density would seem to be appropriate, while the reference time must come from either the exit velocity or the fluid viscosity.

Choosing the reference quantities as d_s, ρ, ν the following equation is obtained

$$f\left\{\frac{Ud_s}{\nu}, \frac{A}{d_s}, \frac{h}{d_s}, \frac{a}{d_s}, \frac{\gamma_s-\gamma}{\rho}\frac{d_s^3}{\nu^2}\right\} = 0.$$

By combining the A/d_s with h/d_s, an alternative and more useful expression is obtained

$$f\left\{\frac{Ud_s}{\nu}, \frac{A}{h}, \frac{h}{d_s}, \frac{a}{d_s}, \frac{\gamma_s-\gamma}{\rho}\frac{d_s^3}{\nu^2}\right\} = 0. \qquad (6)$$

For a particular combination of variables to be significant in such a relation, it should be capable of a physical interpretation. For example $\frac{Ud_s}{\nu}$ has the form of a Reynolds number. It may be called a system Reynolds number, in the sense that it links the pulse generation with both the sediment and fluid properties. As a measure of the damping effect exerted by the fluid on the pulse, the parameter A/h may be a satisfactory one. Together $\frac{h}{d_s}$ and $\frac{a}{d_s}$, which are geometrical parameters, define the experimental configuration.

The relative mass of sediment and fluid $\frac{\rho_s}{\rho}$, where ρ_s and ρ are respectively the sediment and fluid densities, does not appear in this analysis. Since ρ_s was not included in the list of eight independent variables, $\frac{\rho_s}{\rho}$ cannot appear in the parameters that were derived. The appearance of $(\frac{\rho_s}{\rho} - 1)$ rather than $\frac{\rho_s}{\rho}$ in the parameter $\frac{\gamma_s-\gamma}{\rho}\frac{d_s^3}{\nu^2}$, which can be written as $(\frac{\rho_s}{\rho} - 1)\frac{gd_s^3}{\nu^2}$, emphasizes the fact that the important quantity is not the density ratio but rather the ratio $\frac{\Delta\rho}{\rho}$ where $\Delta\rho$ is the

density difference between the sediment and the fluid. Although the density difference does not appear explicitly in the work of Shields (6), it is present in the Shields parameter viz, $\frac{\tau_o}{(\gamma_s - \gamma)d_s}$ which can be written as $\frac{U_*^2}{(\frac{\rho_s}{\rho} - 1)gd_s}$. A similar comment applies to the work of White (7) whose main result can be written as $U_*^2 = 0.18\,(\frac{\rho_s}{\rho} - 1)\,gd_s$.

As noted previously, the tube size a exerts very little effect upon the results and can in fact be neglected. This leaves four parameters in the problem as formulated by equation (6). To obtain an insight into their relationship, Figures 4-16 and 4-17 have been prepared. They show $\frac{A}{h}$ as a function of $\frac{Ud_s}{\nu}$. Figure 4-16 is derived from data obtained from the conditions which make grains move. The abscissa is thus $\phi = \frac{U_1 d_s}{\nu}$, where U_1 is the mean exit velocity of the pulse which just causes grain motion. Figure 4-17 corresponds to 'jump' conditions and the abscissa is thus $\psi = \frac{U_2 d_s}{\nu}$ where U_2 is the mean exit velocity of the pulse which just causes grains to jump. The most obvious characteristic of these graphs is the separation of the data into groups, in each of which the fluid and sediment properties are constant. Each group includes points with different tube heights and tube diameters. A different symbol has been used to denote the data from each series of experimental runs, see the table in each figure. It can be seen that each group of data points is derived from one series. Runs which exhibited strong breaks in the amplitude frequency curves contribute to the scatter of points from Series 1, 2 and 3.

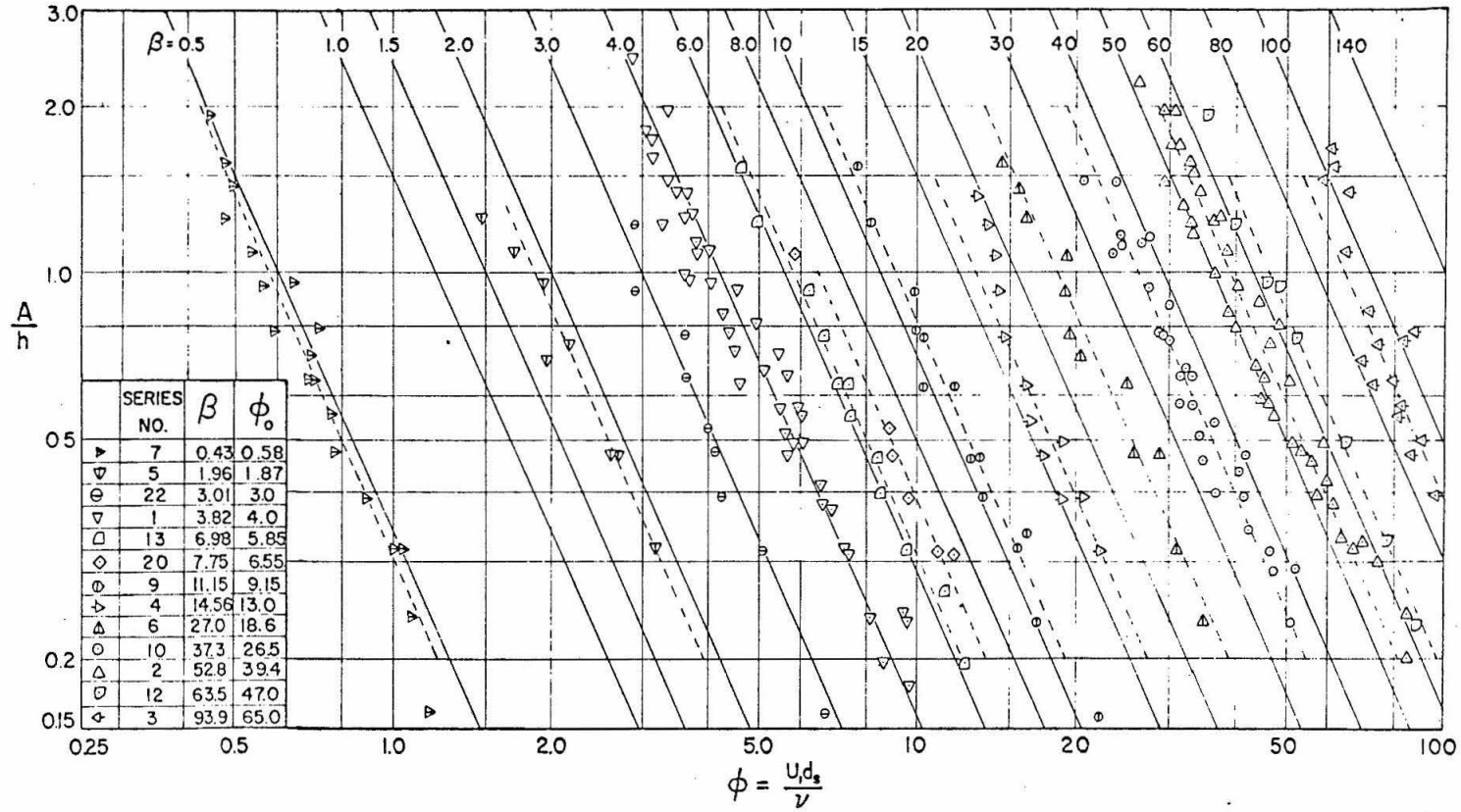

Fig. 4-16 The ratio A/h as a function of the parameter $\phi = \frac{U_1 d_s}{\nu}$. Data refer to critical conditions for grain movement.

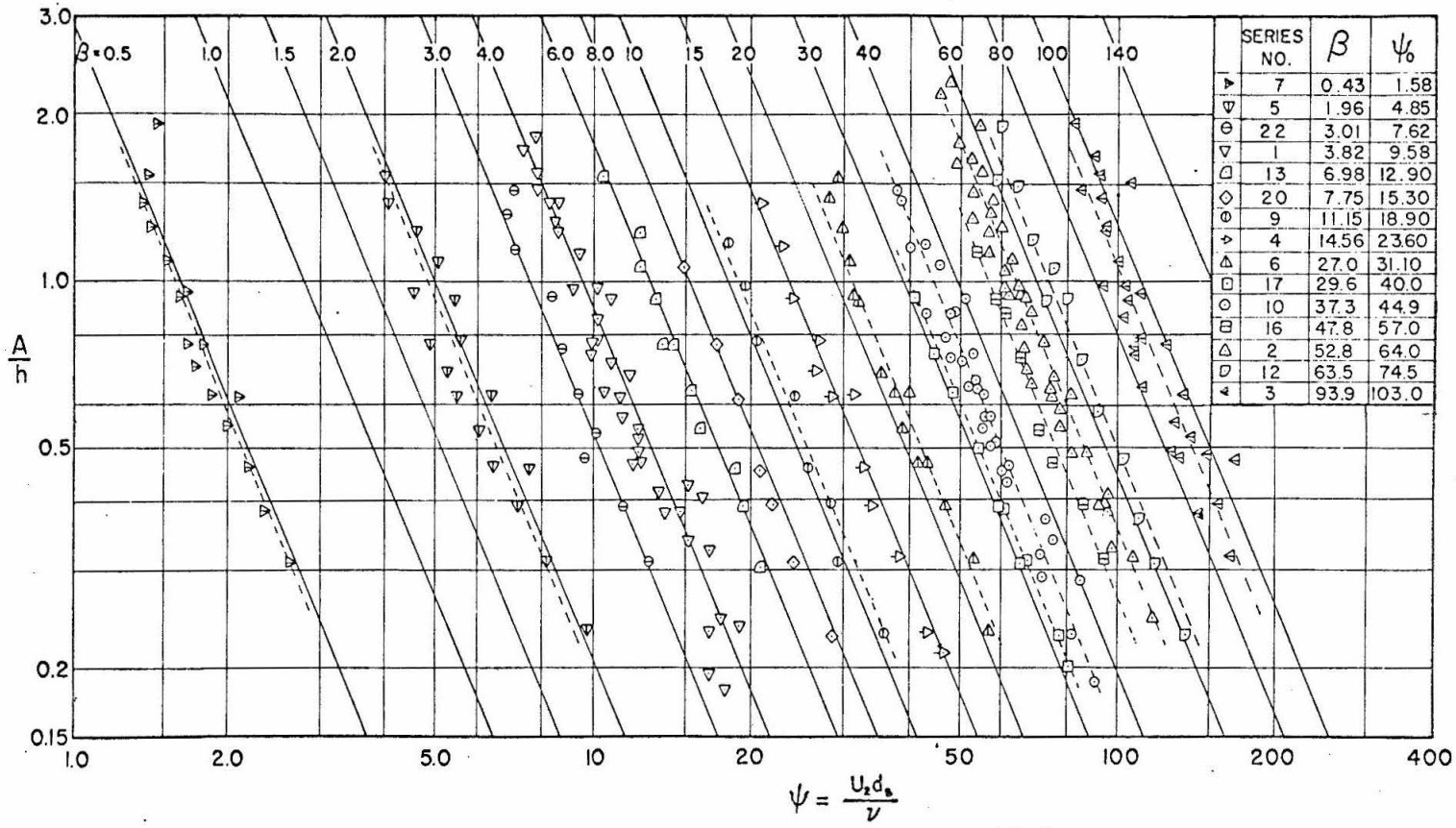

Fig. 4-17 The ratio A/h as a function of the parameter $\psi = \frac{U_2 d_s}{\nu}$. Data refer to critical conditions for grain jumping.

The parameter $\frac{h}{d_s}$ does not differentiate between the groups and in fact is not constant within a group. The other parameter in the function derived by dimensional analysis, $\frac{\gamma_s - \gamma}{\rho} \frac{d_s^3}{\nu^2} = \beta^2$ say, is constant in each group and increases from left to right from group to group. The fact that all the groups arrange themselves according to the value of β is an indication that β is one of the important parameters of the problem.

As such, β should be capable of a wider interpretation than that of a parameter that happened to turn up in a dimensional analysis. This can be found by introducing the shear stress, τ_o, which existed at the bed at the time of grain motion. Now

$$\beta = \left[\frac{\gamma_s - \gamma}{\rho} \frac{d_s^3}{\nu^2}\right]^{\frac{1}{2}} = \left[\frac{(\gamma_s - \gamma) d_s}{\tau_o}\right]^{\frac{1}{2}} \left[\frac{\tau_o}{\rho} \frac{d_s^2}{\nu^2}\right]^{\frac{1}{2}}$$

$$= \frac{R_{e*}}{S^{1/2}}$$

where S is Shields parameter and R_{e*} is a Reynolds number based on shear velocity, $U_* = \sqrt{\tau_o/\rho}$. These two parameters are the ones that Shields (6) used as coordinates to define his curve of critical grain motion. Here the ratio of the parameters defines the curve on which the data must lie. Another interpretation of β can be found by considering the expression for the fall velocity w, of a particle in free fall, $w^2 = \frac{4}{3} \frac{g d_s}{C_D} \frac{\gamma_s - \gamma}{\gamma}$ where C_D is the drag coefficient and g is the gravitational acceleration. Rewriting this expression we have

$$w^2 = \frac{4}{3C_D}\beta^2\frac{\nu^2}{d_s^2} \quad \therefore \quad \beta^2 = \frac{3}{4}C_D R_e^2$$

where $R_e = \frac{wd_s}{\nu}$ is the Reynolds number of a particle in free fall. Now C_D is a function of R_e. For $R_e < 1.0$, the Stokes Range, $C_D = {}^{24}/R_e$ and thus

$$\beta^2 = 18R_e$$

For higher values of R_e, C_D cannot be expressed analytically as a function of R_e but has been well defined experimentally. The parameter β can thus be considered as a function of the particle Reynolds number based on the fall velocity. As such it would seem an appropriate parameter to describe the critical conditions for grain jumping.

By defining new variables ϕ_o and ψ_o, as the values of ϕ and ψ which correspond to ${}^{A}/h = 1$, and plotting them as functions of β, the dependence of group position on β can be determined. The table in Figure 4-16 lists corresponding values of β and ϕ_o. Corresponding values of β and ψ_o are listed in the table in Figure 4-17. Using the plots of ϕ_o and ψ_o vs β, lines of constant β can be drawn in on the ${}^{A}/h - \phi$ diagram and the ${}^{A}/h - \psi$ diagram. This has been done, and Figures 4-16 and 4-17 show an auxiliary scale of β along the top. It is assumed in doing this that all the data define lines which have the same slope; that this condition is met can be seen from the Figures.

The result of plotting ϕ_o and ψ_o as functions of β is shown in Figures 4-18 and 4-19. For values of β greater than about 6, there is a linear relation with both ϕ_o and ψ_o. For small values of β, (see the

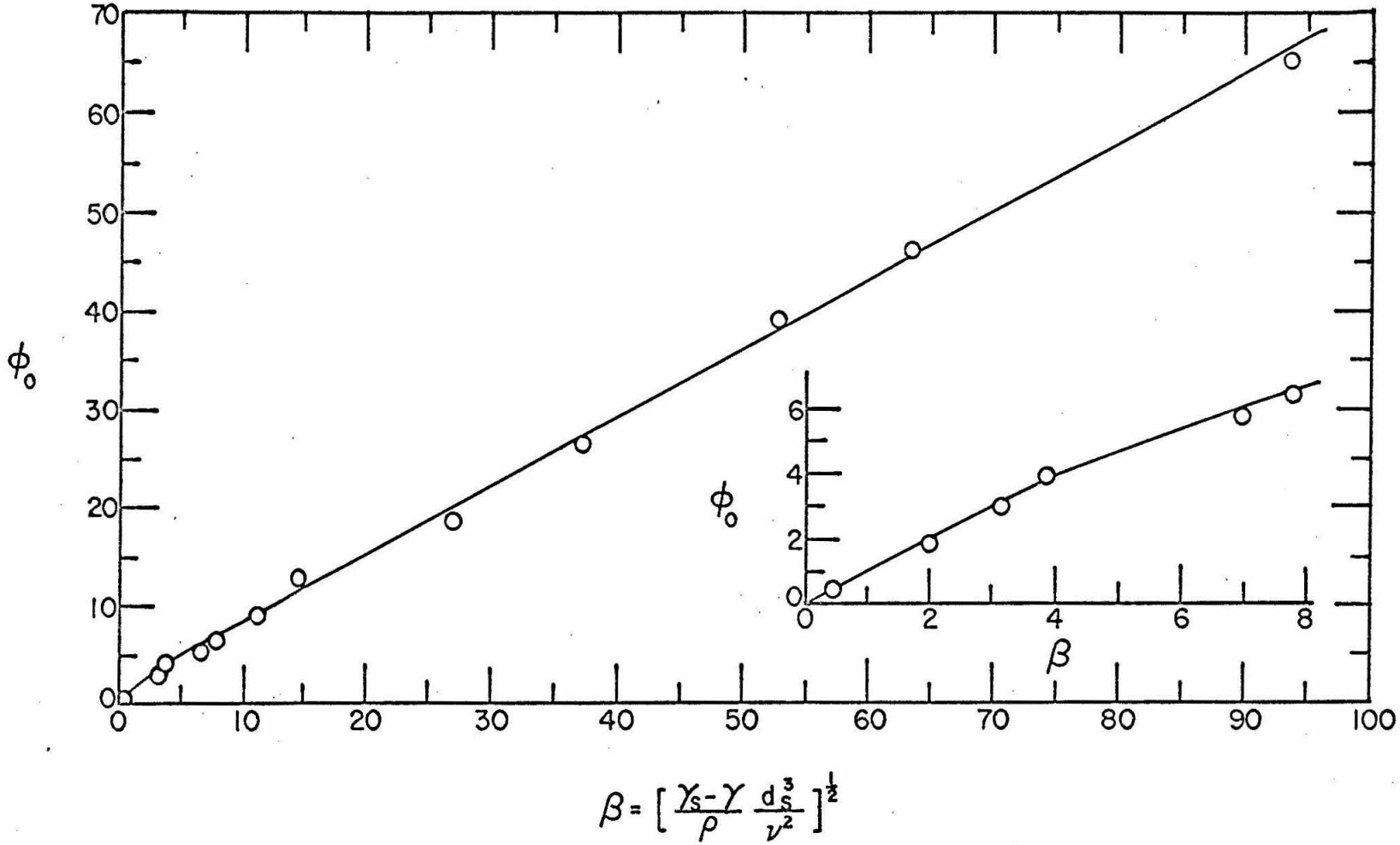

Fig. 4-18 The parameter ϕ_o as a function of $\beta = \left[\frac{\gamma_s - \gamma}{\rho} \frac{d_s^3}{\nu^2}\right]^{1/2}$.

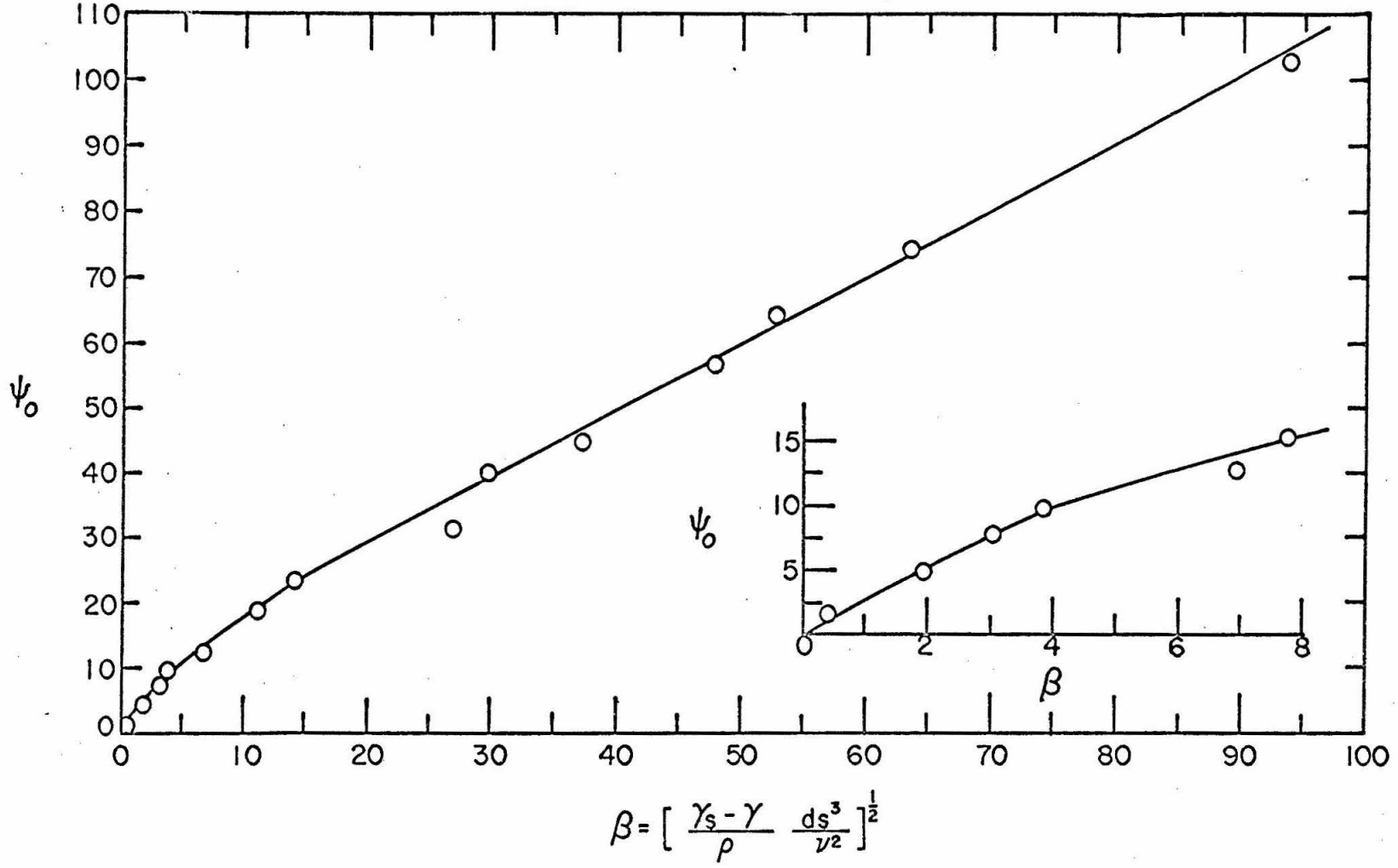

Fig. 4-19 The parameter ψ_o as a function of $\beta = \left[\frac{\gamma_s - \gamma}{\rho} \frac{d_s^3}{\nu^2}\right]^{1/2}$.

insets in each Figure) the dependence is again linear but with a different slope. A transition region exists between the two linearly dependent regions. The values of β in this transition region are approximately 4 to 5. For the Stokes range, $\beta^2 = 18R_e$ and $R_e < 1.0$ which implies that $\beta = \sqrt{18} = 4.2$ is the upper limit of this range. It is also the upper limit of the first linear portion of the relations between ϕ_o and β, and ψ_o and β.

Using Figures 4-16 and 4-17 it is possible, given values of d_s, ρ, h, ν, and $\gamma_s - \gamma$ to determine combinations of A and ω that will cause either grain motion or grain jumping. First β is computed, yielding say a value which is denoted by β^*. Using the scale of β on either Figure 4-16 or 4-17, a line of $\beta = \beta^*$ can be drawn on the diagram. It is parallel to the β = constant lines already drawn and passes through β^* on the scale of β. Any pair of values of A/h and $\frac{Ud_s}{\nu}$ which lie on this line, will determine pairs of values of either A and ω, or A and U, whichever is desired.

An alternative method which allows the jet strength to be computed directly, is as follows. Figure 4-16 shows that $\frac{A}{h} = C_1 (\frac{Ud_s}{\nu})^{x_1}$ where C_1 is a constant for a given value of β, and x_1 is the slope of the lines of constant β. Recalling that $U = 2A\omega$, we derive

$$A\omega^{\frac{-x_1}{1-x_1}} = (hC_1)^{\frac{1}{1-x_1}} (\frac{2d_s}{\nu})^{\frac{x_1}{1-x_1}} . \qquad (7)$$

Now $A\omega^{\frac{-x_1}{1-x_1}}$ must be equal to the jet strength of a pulse with amplitude A and frequency ω. This can be seen by realizing that for constant β and h the lines in Figure 4-16 are actually plots of pulse amplitude

against jet velocity. If they have a slope of x_1, this implies that the amplitude-frequency curves must have a slope of $\frac{x_1}{1-x_1} = s$. The jet strength is defined as $K = A\omega^{-s}$ and thus $K = A\omega^{\frac{-x_1}{1-x_1}}$ as stated above. From Figure 4-16, $x_1 = 2.11$ and $x_1/1-x_1 = -0.68$ which should be compared with the mean value, $\bar{s}_1 = -0.672$, of the slopes of the amplitude-frequency curves determined in Section IV-A-1.

The value of C_1 is known because at $\frac{A}{h} = 1$, $\frac{Ud_s}{\nu} = \phi_o$ and thus we have $C_1 = \phi_o^{-x_1}$. Substituting into equation (7)

$$K_1 = h\left[\frac{2d_s h}{\phi_o \nu}\right]^{\frac{x_1}{1-x_1}}$$

$$\therefore \quad K_1 = h\left[\frac{2d_s h}{\phi_o \nu}\right]^{-0.68} \tag{8}$$

where ϕ_o is known from the value of β and Figure 4-18. It is pointed out that the units of jet strength in this relation are correct. The term in the bracket has units of time, and with $-0.68 = s$ the units of K are $\left[\text{length (time)}^s\right]$.

Similarly for the jump case we have $x_2 = -2.20$, $\frac{x_2}{1-x_2} = s_2 = -0.688$ (c.f. $\bar{s}_2 = -0.685$ in Section IV-A-1), $C_2 = \psi_o^{-x_2}$ and

$$K_2 = h\left[\frac{2d_s h}{\psi_o \nu}\right]^{-0.688} \tag{9}$$

Given values of h, ρ, ν, d_s, $\gamma_s - \gamma$, one can now calculate the required jet strength for moving and jumping, by using Figures 4-18 and 4-19. As an example, consider the problem of moving glass beads

in a 50% glycerol solution. Assume the mean diameter of the beads to be 0.305 mm. Then we have:

$$d_s = 0.305 \text{ mm} = 10^{-3} \text{ ft}$$

$$\nu = 5.71 \times 10^{-5} \text{ ft}^2/\text{sec}$$

$$\rho = 2.19 \text{ slug/cu ft}$$

$$\rho_s = 4.84 \text{ slug/cu ft}$$

Calculating β, we get $\beta = 3.44$ and thus from Figures 4-18 and 4-19, $\phi_o = 3.4$ and $\psi_o = 8.6$. Assume h = 0.1 ft.

Now, by equation (8), $K_1 = h \left[\frac{2 d_s h}{\phi_o \nu}\right]^{-0.68}$

$$= 0.1 \times (1.03)^{-0.68}$$

To get K in cin it is necessary to multiply by 12 because h was in feet. Thus $K_1 = 1.18$ cin, and similarly $K_2 = 2.24$ cin.

D. INVESTIGATION OF THE FLOW FIELD.

1. Hydrogen Bubble Techniques.

Using the equipment described in Section III-A-2, hydrogen bubbles were introduced into the flow field of the pulsating jet. The dominant feature of the flow field produced by the jet was a vortex ring, concentric with and moving along the axis of the jet towards the sediment bed. Figure 4-20 shows two photographs of the rings. The left hand picture, (a), shows the hydrogen bubble wire in a horizontal position near the end of the jet tube. Three rings can be seen. One is in the center of the photograph and the other two are very close to, or even on the bed. The right hand picture (b), was taken using the jet tube as the cathode. A Stroboscope lamp flashing at 10 cycles/sec,

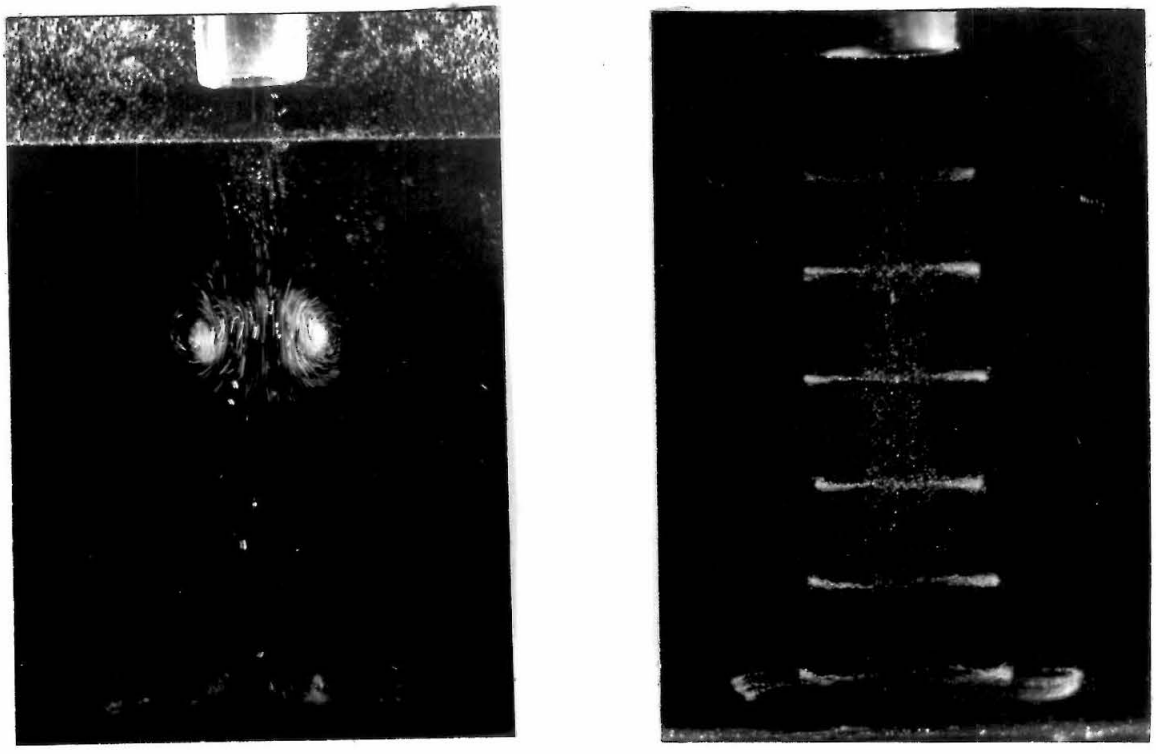

(a) (b)

Fig. 4-20 (a) Flow field of a pulsating jet. Three vortex rings can be distinguished; two adjacent to the boundary and one moving in the fluid. Scale: 1.6 x full size.

(b) Multiple exposure of a vortex ring as it moves towards a boundary. Scale: 2 x full size. Frequency of the exposures, 10/sec.

provided the illumination while the camera shutter was held open during the passage of the ring to the bed. Many images were thus obtained on the same photographic plate.

For the conditions of pulse amplitude and frequency under which these photographs were taken, the ring is not affected by the presence of a boundary until it reaches a position adjacent to that boundary. In both pictures the ring diameter appears to be constant throughout the motion towards the wall. An estimate of the translational velocity of the ring can be obtained from the spacing of adjacent images in Figure 4-20b. It is seen that the velocity is practically constant, until the ring almost reaches the wall. Adjacent to the wall the rings spread out with a corresponding decrease in the diameter of the core. Accompanying this spreading, is a great increase in the fluid velocity within the ring. These effects are very similar to those predicted for the behavior of vortex rings by the inviscid theory of classical hydrodynamics. The main difference being that in the experiments the ring had to be very close to the wall before any spreading took place. The theory predicts spreading at larger distances from the wall.

It was at low frequencies that the behavior of the ring approached that of the inviscid predictions. Here the ring would spread noticeably as the wall was approached, and would finally settle down and 'sit on the bed'. Figure 4-21 shows a photograph, taken using dye as a tracer, in which the ring appears to die at the wall and just remain on the bed. The structure of the second and third rings as they move towards the bed can also be seen. At higher frequencies the rings became 'translation dominated', in that they were completely uninfluenced by the

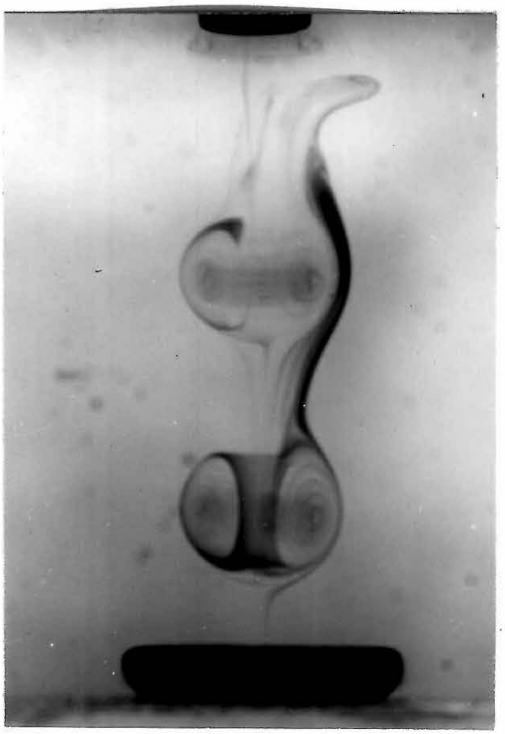

Fig. 4-21 Vortex rings approaching a boundary. Pulse amplitude 0.747 in., pulse frequency 1 cyc/sec, tube height 0.2 ft, tube diameter 0.305 in.

presence of the wall until they actually crashed into it. They then appeared to bounce back from the wall before disintegrating and mixing with the other fluid.

Those rings capable of moving sediment grains were of the small spreading and, at higher values of jet strength, of the translation dominated types. Limited measurements on photographs showed that little or no spreading took place until the ring had travelled a distance from the tube of approximately 0.9 times the tube height. Then either a rapid spreading or total disintegration occurred.

2. Studies Using Dye.

Additional studies of the flow field were made using dyed fluid to form the pulse. Photographic records of the pulse movement were made with both still and motion pictures.

The dye solution was made up using a dye powder and methyl alcohol in water in such proportions as to ensure that the dye solution had the same density as the fluid in the tank. This was accomplished by trial and error. After setting the desired amplitude and frequency, the end of the jet tube was placed in a beaker containing the dye solution. Dye was then sucked up into the tube by turning the pump through a complete suction stroke. This ensured that all the fluid ejected from the tube on the first exhaust stroke would be dyed. The tube was then transferred to the tank, and care taken to see that the pump started from the neutral position preceding an exhaust stroke.

Motion pictures were taken at 64 frames/second, using 16 mm color film, Ektachrome ERB 430, which was processed commercially.

The still pictures were taken using Kodak Royal Pan film, exposed at f5.6 for $\frac{1}{100}$ second. In both cases the flow field was lit from the back through a translucent screen. A small amount of oblique lighting from the front was used to illuminate a scale placed in the field of view.

Some excellent photographs of the formation and disintegration of vortex rings have been made by Magarvey and MacLatchy (44) and (45). They photographed the motion of a smoke jet, into still air, from the end of a tube. The disintegration of the resulting vortex ring upon impact with a boundary, perpendicular to its direction of motion, is also shown in a series of photographs.

The main purpose for the dye studies was to find an explanation of the break in slope, referred to in Section IV-A, that occurred in some of the amplitude-frequency curves. With the change in amplitude-frequency relationship that accompanies this break, one might have expected that the initial movement pattern of the grains would have been altered. However, the particles exhibited the same type of motion at critical frequencies, on both sides of the break. In some runs it was noticed that a different pattern of movement did occur when the burst amplitude was very large, e.g. Run No. 2-10 with A = 5.30 in. Here the motion did not occur spontaneously and then suddenly stop, as it did in most other cases, but the grains continued to move for an appreciable length of time after the initial disturbance. The impression given was of something being poured onto the surface rather than impacting onto it, suggesting that perhaps a continuous jet was acting for a short instant of time.

Three films were made with a view to explaining these slope changes in terms of the flow characteristics. In each film, the tube diameter and tube height were chosen to correspond to those in runs exhibiting breaks. The table below lists these conditions.

TABLE 4-3

Jet Configurations under which Motion Picture Films Were Made.

Film No.	Tube Diameter, a	Tube Height, h	Run No.
1	0.182 in	0.2 ft	2-11
2	0.244 in	0.2 ft	3-4, 2-3
3	0.305 in	0.2 ft	3-2, 12-2

Each film was made up of a number of sequences taken at different pulse amplitudes and frequencies, such that all points of interest in the amplitude frequency plane were investigated.

Four main features were observed. They can be listed as follows:

(1) At large amplitudes rings did not form at all.

(2) At intermediate amplitudes part of the dyed fluid formed into a ring.

(3) At low amplitudes rings were formed.

(4) At high frequencies the second ring caught up with and disturbed the first ring. The tube height is also an important factor in determining whether or not the rings interfere with each other.

For ease of discussion, the types of motion observed have been split into categories and will be referred to by the letter adjacent to the description below.

a. Rings form and travel unmolested to the bed.

b. Rings form and interfere with each other before reaching the bed. The second merges with the first and then impacts onto the bed.

c. Rings form and interfere with each other. The second passes through the first and separates from it before impacting onto the bed.

d. The front portion of the jet rolls up into a ring which travels to the bed. A small portion of the fluid does not go into the ring and follows as a tail.

e. An elongated jet with a well defined head forms. The flow is apparently laminar throughout.

f. An elongated jet forms and tends to break up into a turbulent jet before reaching the bed.

g. A completely turbulent jet forms.

Figure 4-21 shows an example of a type a jet. If the second ring interferes with the first ring before the wall is reached, the jet then becomes a type b or type c. Types e, f and g jets are shown in Figure 4-22. The conditions under which each was formed are noted on the Figure.

A detailed description of film No. 1 will now be given. The conditions correspond to those in Runs No. 1-8 and 2-11. The former has a very weak break on the jump curve while the latter has distinct breaks on both curves. Figure 4-23 shows the results obtained. The small letters adjacent to the circled points indicate the jet type at that particular point. Both 'move' and 'jump' curves for Run 2-11, are shown together with the 'move' curve of Run 1-8. The 'jump' curve of

TYPE e JET
A = 4.24 in ω = 0.43 cps

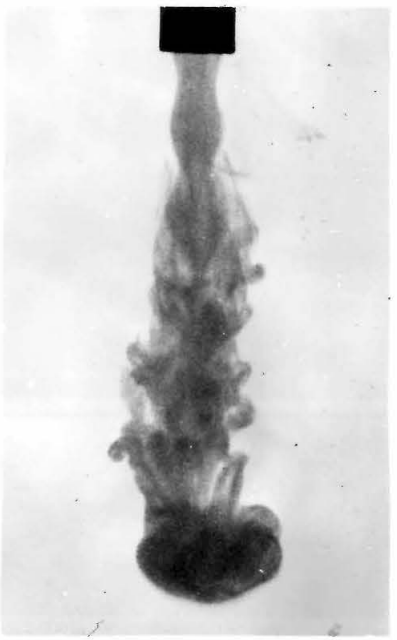

TYPE f JET
A = 3.18 in ω = 1.05 cps

TYPE g JET
A = 4.24 in ω = 1.05 cps

Fig. 4-22 Examples of jet types e, f, and g. The conditions under which each was formed are noted adjacent to each jet. Tube diameter 0.182 in. in each case.

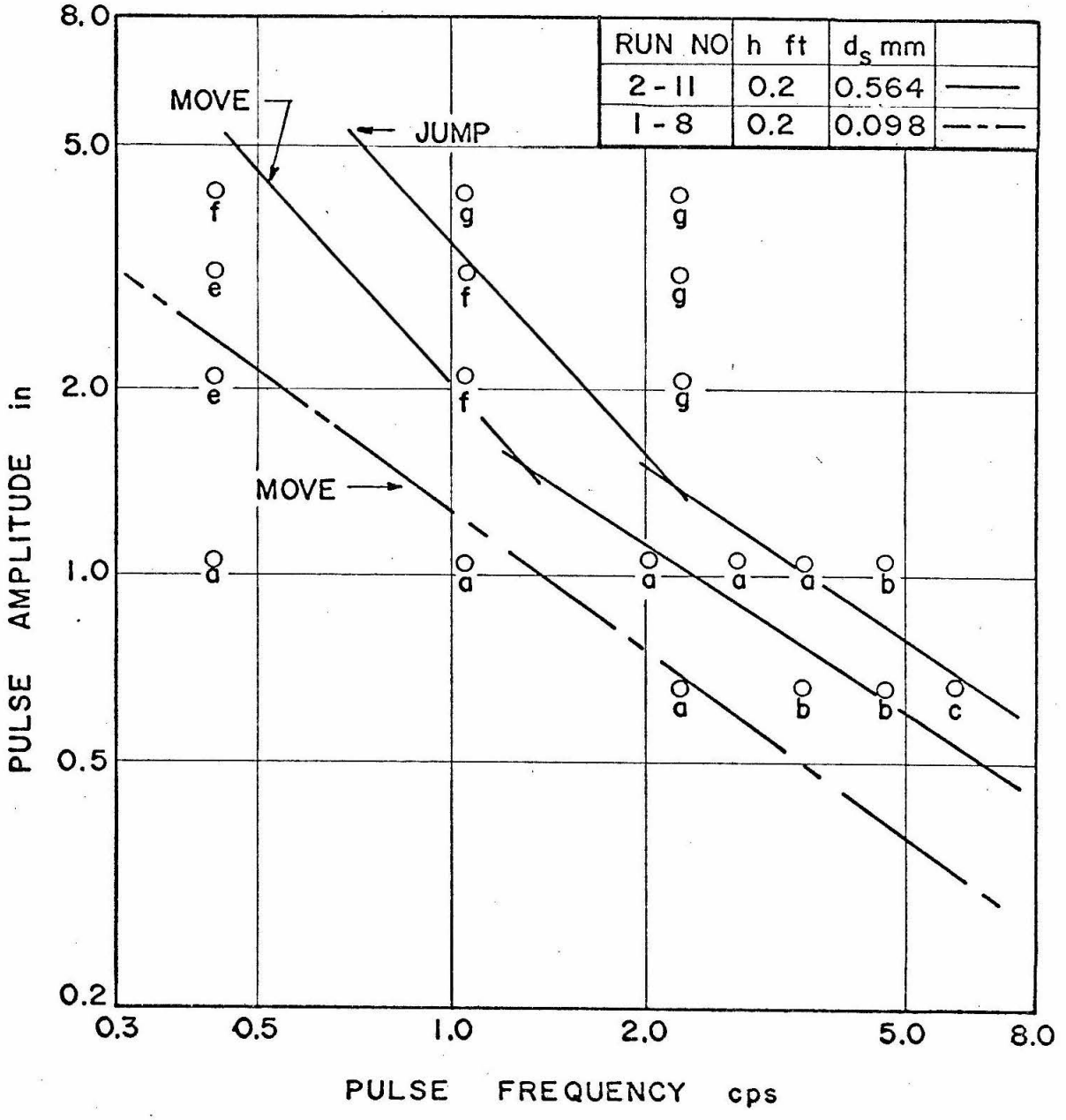

Fig. 4-23 Jet types derived from Film No. 1, plotted on the amplitude-frequency plane of Runs No. 1-8 and 2-11. Tube diameter is 0.182 in. for both runs.

Run 1-8, which has been omitted for the sake of clarity, is parallel to and displaced to the right of the 'move' curve of Run 1-8.

For fixed, small amplitude, $A < 1.2$ in. and for increasing frequency, the jet type changes from type a to type b and then to type c. This indicates that the second ring overtakes the first at an earlier stage in the sequence, if the frequency is increased. The translational velocity of the ring is considerably less than the exit velocity of the pulse. At high frequencies the first ring has not moved very far from the end of the tube by the time the second ring has formed. In such cases one ring will influence the motion of the other. Whether or not they intertwine during the sequence, then depends upon the tube height. At large amplitudes $A > 2.0$ in., as the frequency increases a transition is made from a jet with smooth appearance, type e, through type f, to one having the appearance of a turbulent jet, type g. Under these conditions the momentum of the fluid ejected from the tube, is sufficient to penetrate the ambient fluid as a continuous jet. As the exit velocity increases the jet becomes more turbulent.

Between the amplitudes of 1.1 in. and 2.0 in. there is an abrupt change of jet type with amplitude. If a finer mesh of points had been investigated, some type d jets would probably have smoothed this transition. For Run 2-11 it is in this region that the break in slope occurs. However, Run 1-8 which also passes through this region has no break on the move curve. Figure 4-23 shows that no type f or type g jets are encountered. The jump curve, which has a slight deviation at the upper end, passes through the region of type f jets.

Since the type of jet formed is independent of the tube height, with the exception of a, b and c types, it is possible to form some conclusions from this film regarding other runs with the same tube diameter but different tube height. Two such runs are 1-7 and 2-9 which both have tube heights of 0.1 ft. Figure 4-24 shows the curves for these two runs superimposed on the grid of jet types. Run 1-7 shows no breaks and passes only through regions of type a and type e jets. Run 2-9 has a break on the jump curve as it passes through the region of type f jets.

Film No. 2 was taken of sequences in which the tube diameter was 0.244 in. and tube height 0.2 ft. The same pattern of jet types in the amplitude-frequency plane was observed. Regions of type f and type g jets were smaller than those encountered in Film No. 1. Those curves from Runs 2-3, 2-4, 3-3 and 3-4 which showed breaks, did so in the type f and type g regions.

Film No. 3 was taken of sequences in which the largest tube, a = 0.305 in., and a tube height of h = 0.2 ft were used. The most interesting feature was the absence of the type g jets, and the very small regions of types e and f jets. Of the runs made with this tube diameter, only those two runs with the largest jet strength, Runs 3-2 and 12-2 showed any breaks. Both were weak breaks on the jump curve and occurred in the region of type f jets.

To summarize the results presented in this section, it may be concluded that:

(1) The explanation for the change in slope of certain of the amplitude-frequency curves lies in the fact that the jet type changes

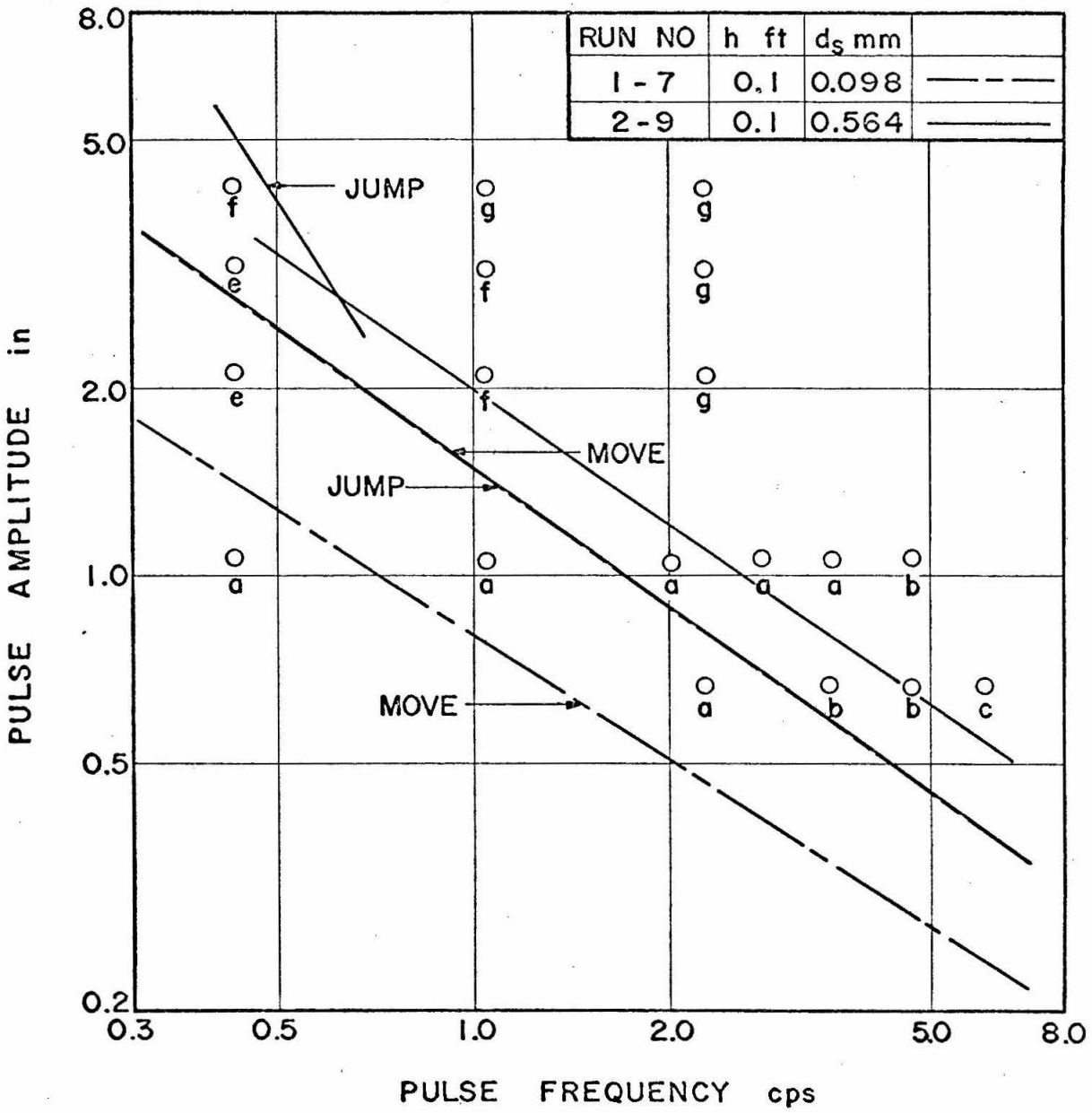

Fig. 4-24 Jet types derived from Film No. 1, plotted on the amplitude-frequency plane of Runs No. 1-7 and 2-9. Tube diameter is 0.182 in. for both runs.

from a vortex ring to an elongated jet with a turbulent appearance, as the jet strength is increased.

(2) Those amplitude-frequency curves which do not pass through the type f or type g regions, have constant slope.

(3) The type d and type e jets are a transition between the vortex ring and the turbulent jet. They have no noticeable effect on the amplitude-frequency curves.

3. Fluid Velocity Adjacent to the Bed.

It has been shown that for each sediment there is a definite critical value of the jet strength K_1 which is just sufficient to cause grain motion. For each pair of values of A and ω that combine to give the same jet strength, the flow conditions produced adjacent to the sediment bed are the same. This implies that there must be a relationship between these conditions and the jet strength. It will necessarily depend upon the fluid properties and the tube height. As representative of the flow conditions at the bed, it is proposed to use the fluid velocity produced by the pulse at the bed.

During a pulse cycle the velocity at any point on the bed is first zero, then grows to a maximum and falls to zero again as the pulse goes by. The maximum velocity that occurs at a point during this cycle will vary with the distance from the tube axis. In this investigation it is the largest of these maxima which is of interest. For it is assumed that the point at which it occurs is the point of most vigorous attack on the sediment grains. Let this maximum velocity be denoted by U_o. In Section III-C it was noted that the initial movement takes

place in an annular shaped region centered on the tube axis. Measurements showed the mean diameter of this region to be 1.5 to 1.8 times the tube diameter. Hence, in order to determine the fluid velocity at the critical conditions, it is necessary to determine the maximum velocity which occurs at a distance of 1.6 times the tube radius from the tube axis. This velocity is U_o. Accordingly the hot film sensor was placed in this position.

The hot film sensor measures the magnitude of the velocity vector at the position of the sensor. No information is given as to the direction of this vector. It is however, perpendicular to the longitudinal axis of the sensing element because the horizontal component is, by symmetry, directed radially outwards from the jet axis. For this study it is the magnitude of the velocity vector that is of interest, because this is the fluid velocity that the sediment particle experiences and the velocity that gives rise to its motion.

A typical trace of the output signal from the hot film sensor as given by the Sanborn recorder is shown in Figure 4-25. It corresponds to a jet strength of 0.85 cin and a maximum velocity of 0.23 ft/sec. Traces from three consecutive pulses are shown. The third one is squashed in a horizontal direction, because the drive motor for the recorder paper was switched off after the second pulse. There is a rapid rise to the maximum velocity and then a gradual fall, followed by another rapid rise when the second pulse reaches the bed. The three maximums have the same value which shows that at this pulse frequency, 0.75 cps, the interference of one pulse with another is negligible.

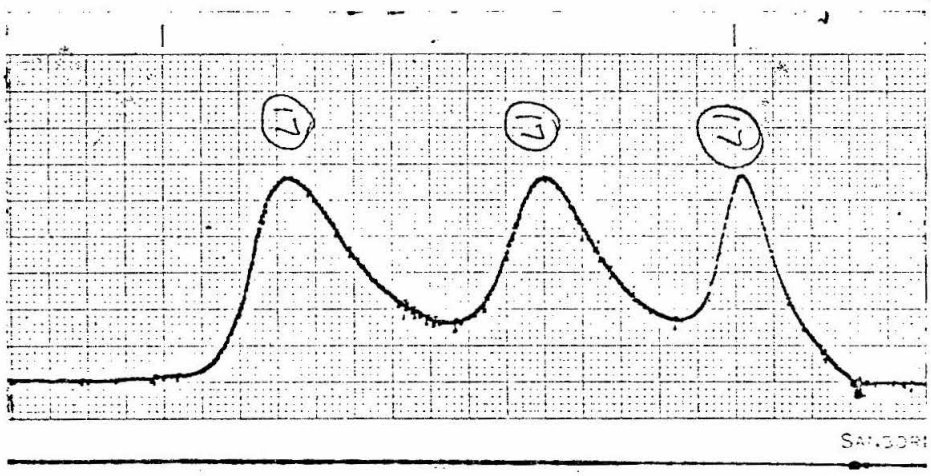

Fig. 4-25 Section of Sanborn recorder output for a jet strength of 0.85 cin and a maximum velocity at the hot film sensor of 0.23 ft/sec. Tube height, 0.1 ft; each division on the paper is 1 mm; paper speed, 25 mm/sec.

By doing a series of runs at different jet strengths, the relation between maximum bed velocity U_o and jet strength can be determined. This was done for tube heights of h = 0.1 ft and h = 0.2 ft. The results are shown in Figure 4-26. The plotted values of velocity are average values determined from nine separate trials at the corresponding jet strength. Three different combinations of pulse amplitude and frequency were used for each value of the jet strength. Three trials were made with each combination. The maximum difference between the high and low value over all the trials at a given jet strength, was about 8%.

From Figure 4-26 the bed velocity can be written as a function of the jet strength as follows:

$$U_o = 0.31\ K^{1.80} \qquad h = 0.1 \text{ ft} \qquad (10)$$

$$U_o = 0.22\ K^{1.91} \qquad h = 0.2 \text{ ft} \qquad (11)$$

where U_o is given in ft/sec when K is in cin.

For a constant value of U_o the difference in jet strengths for h = 0.1 and h = 0.2 must reflect the additional jet strength required for the pulse to travel the extra distance to the boundary. The difference increases as U_o and hence as K increases; it is 0.14 cin at U_o = 0.15 ft/sec and 0.30 cin at U_o = 1.5 ft/sec. This is in keeping with the suggestion that was made in Section IV-B-3 regarding the dissipation suffered by a pulse. That the two lines converge for larger values of U_o is understandable since, as U_o increases, the difference in jet strengths must become a smaller and smaller fraction of the total jet strength. It is unreasonable to expect the power law relation to hold for very large values of U_o, because there is a point at which the two

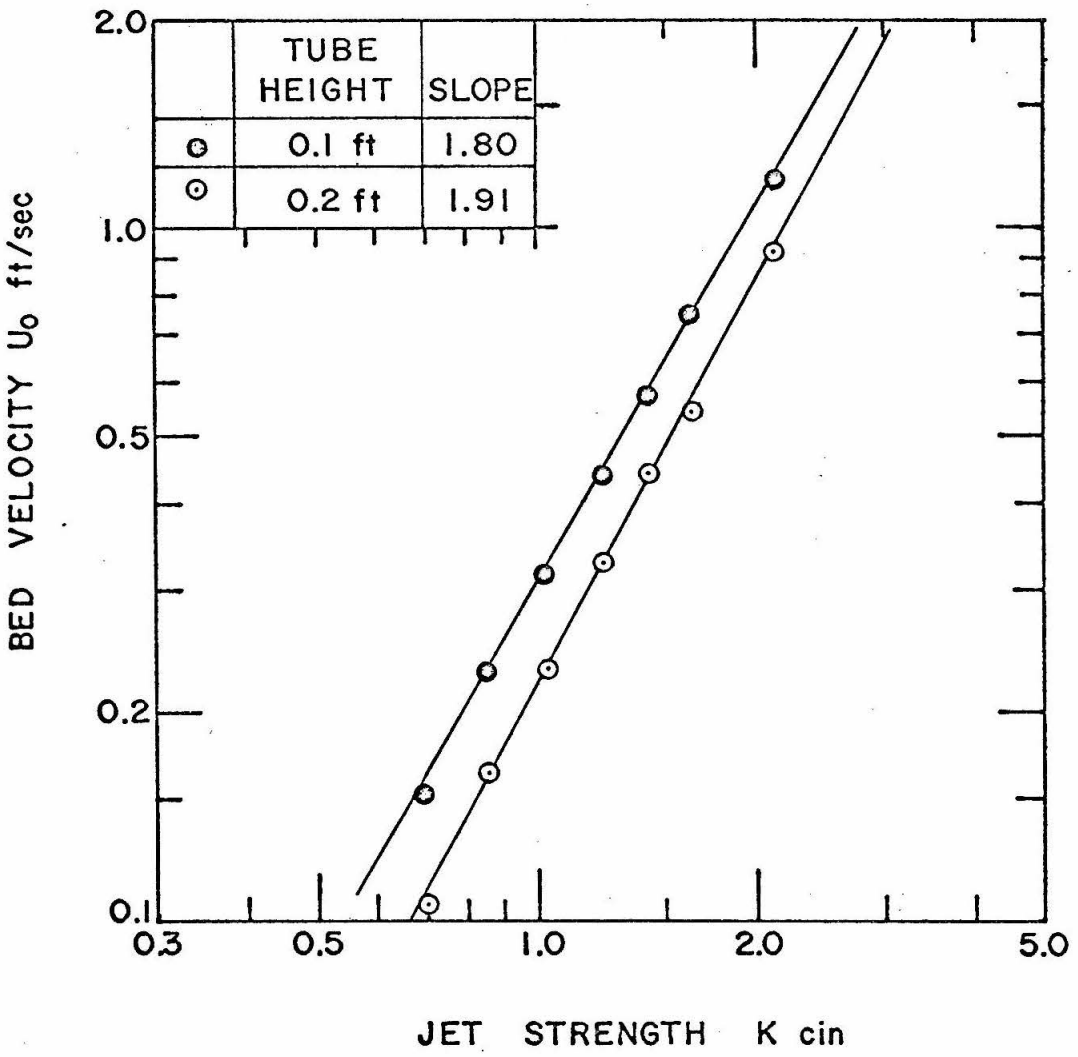

Fig. 4-26 Velocity produced at a boundary by the pulsating jet as a function of jet strength.

lines cross. To reach these velocities was beyond the capabilities of the apparatus. The power law relationship cannot hold for small values of U_o either, because as U_o tends to zero, K tends to K_h, the jet strength required for a pulse to reach the bed. This is a similar situation to that encountered in Sections IV-B-6 and 7, where a more appropriate variable for this range of jet strengths is $K-K_h$. The two points corresponding to K = 0.7 cin are below the line and probably indicate the start of this deviation.

It is concluded that for the values of bed velocity investigated, a power law relationship exists between the bed velocity and the jet strength. The constants in this relation depend upon the tube height. This rather fortuitous choice of the range of bed velocities, was dictated by the values of jet strength measured in the experiments.

4. Fluid Trajectories.

The preceding section presented results for the magnitude of the velocity vector adjacent to the sediment bed. By photographing the motion of neutrally buoyant plastic beads under the action of a pulse, an indication of the trajectory of the fluid elements can be obtained. This will then give an idea as to the direction of the velocity vector.

Figure 4-27 shows some typical pictures of the bead motion. The jet strength increases from 1.01 cin in the upper picture, to 1.42 cin in the center picture, to 2.13 cin in the lower picture. Since the frequency of the stroboscopic lights was the same for each picture, 20 flashes/second, the spacing of the beads is indicative of their relative velocities. It is clear that the velocities are higher at the higher

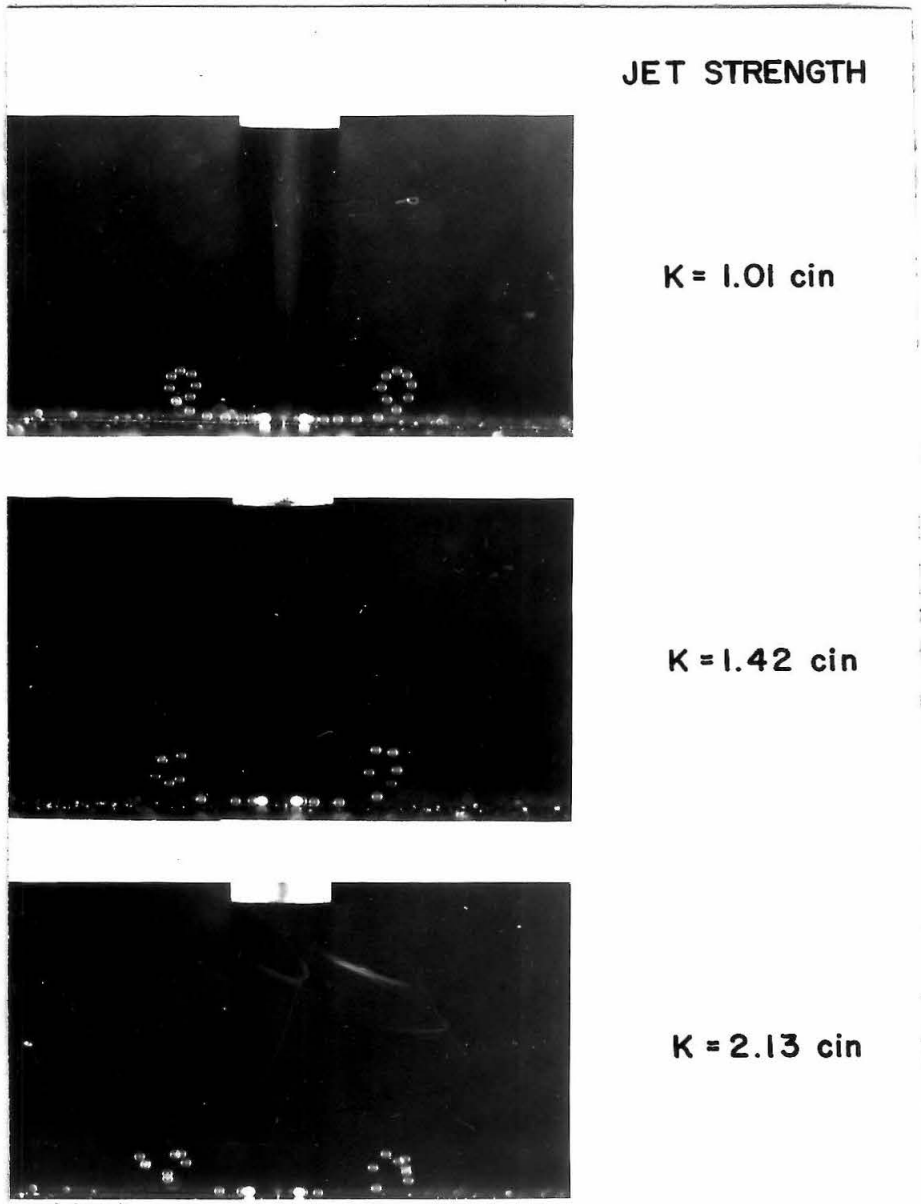

Fig. 4-27 Motion of neutrally buoyant plastic beads in the flow field of a pulsating jet. Tube height, h = 0.1 ft in each case.

jet strengths. In the lower picture the velocities are so high that it is difficult to determine exactly the path followed by the bead. The vertical velocities are much higher in this picture, where the jet strength corresponds to that required to cause 0.525 mm ilmenite to jump. The other two pictures correspond to conditions causing motion of 0.098 mm sand (upper) and motion of 0.564 mm sand (center).

The beads all follow a curved path away from the bed, confirming the existence of a vertical velocity component adjacent to the bed. The entrainment hypothesis of Section II-C assumed the existence of such a velocity component, the magnitude of which partly determined the resultant behavior of the grains. If the flow pattern produced by the simplified concept of a turbulent eddy, resembles the actual flow pattern produced by an eddy on impact with a boundary, then the existence of a vertical velocity component near the boundary can be inferred. The laboratory model would be a better representation of the natural conditions, if a horizontal velocity component were superimposed onto the flow field. This would not affect the vertical velocities however. The question is really whether or not the structure of an eddy is similar to that of the pulse. In the laboratory model, the vertical velocity component arises from the spinning motion in the vortex ring, which is intensified as the ring spreads near the wall. It is not unreasonable to expect a turbulent eddy to have a structure which would permit a spinning motion. It would certainly not be as regular a structure as that of a vortex ring, but parts of the resultant flow pattern may well be similar. In Chapter V investigations in a laboratory flume, which examine this point more thoroughly are detailed.

In Figure 4-27 the two particle paths on each photograph are not always symmetrical, because one bead may initially have been slightly further from the jet axis than the other and thus starts its motion at a different time. Each path finishes at the same instant, i. e. when the camera shutter was closed.

The vertical velocity of the beads can be determined from the photographs. However this velocity is not the maximum experienced by the grain, because the plastic bead starts to move before the maximum is reached. This happens in spite of the fact that the time required to reach the maximum, see the previous section, is very small. Two different experiments served to make this clear. Firstly, measurements of the horizontal velocity of the beads gave results that were only $\frac{1}{4}$ to $\frac{1}{3}$ of the maximum values recorded by the hot film sensor. Secondly, an experiment was done with both the hot film sensor and a bead in the flow field. The record from the hot film was marked when the bead started to move. Inevitably this mark was made during the time of velocity increase. In effect, the bead was displaced by the first portion of the pulse and was not exposed to the highest velocities.

The most important aspect of this set of experiments is the proof that a pulsating jet of the type used, is capable of producing a vertical velocity component adjacent to the bed.

E. THE MECHANISM BY WHICH THE PULSATING JET ENTRAINS SEDIMENT GRAINS.

1. Initiation of Motion.

Pulses with strengths slightly greater than the critical value for grain motion cause the grains to roll across the bed in radial lines centered on the jet axis. Motion is brief and occurs each time a pulse reaches the bed. Grains move because the force exerted on them by the fluid motion within the pulse exceeds the restraining forces. The immersed weight of the grain and the forces arising from the interference of neighboring grains make up these restraining forces.

When the pulse passes over the grains it exerts a shear stress upon them. This is not shared equally by all the surface grains because the sediment bed is not a plane boundary. Those grains which are more exposed by virtue of their position in the bed are the ones which start to move. They do so by rolling about their point of support. Under these conditions the resultant force on the grain is a drag force arising primarily from the pressure distribution over the grain's exposed surface combined with the skin friction forces.

2. Suspension of Grains.

Pulses with strengths exceeding the second critical value, K_2, cause grains to jump from the bed. To see how this is accomplished, the motion of the neutrally buoyant particles described in Section IV-D-4 is first considered in greater detail. Under the action of the pulse, these particles followed a curved path leading away from the bed.

Since the lucite base of the tank is impervious, there can be no vertical velocity right at the boundary. However, the beads have a finite diameter (approximately $\frac{1}{2}$ mm), and thus only a small portion of the bead is in direct contact with the boundary. Close examination of the pictures in Figure 4-27, shows that the bead first rolls across the boundary and then is lifted from it. This indicates that the direction of the fluid velocity vector in the immediate neighborhood of the particle changes as the pulse approaches the bed. The pulse from the tube is actually a vortex ring. First the fluid disturbed by the approaching ring moves away from the jet axis parallel to the bed. This is indicated diagrammatically in Figure 4-28a. As the ring approaches the boundary the bead is rolled until it reaches a position where the spinning motion within the ring gives rise to a velocity vector, in the neighborhood of the bead, which is inclined to the boundary. See Figure 4-28b. At this point the bead starts to rise from the bed.

Experiments with only five or six sediment grains on a solid boundary produced the same result. Namely, the grains first roll across the boundary and then are projected up into the fluid. Because of their greater inertia, the sediment grains do not necessarily loop around as the neutrally buoyant particles do. If the jet strength is large enough, however, they can be made to follow a path similar to that of the lighter particles.

On a sediment bed, there are always grains in a position at which the velocity vector adjacent to the bed becomes inclined to be horizontal when the ring reaches the bed. These are the ones which are projected up into the flow. The grains in this region which project

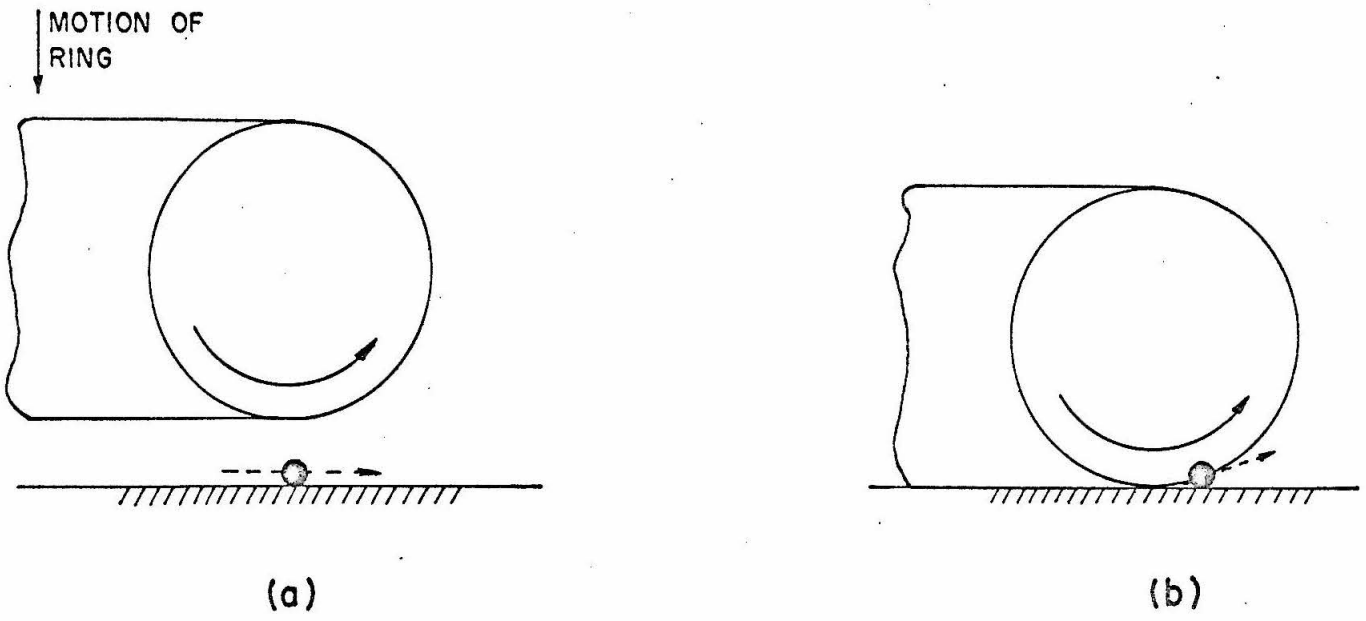

Fig. 4-28 (a) Diagrammatic representation of flow about a particle on a solid boundary as a vortex ring approaches.

(b) Diagrammatic representation of flow about a particle on a solid boundary under the action of a vortex ring.

The dashed arrows indicate the velocity vector of the fluid motion near the particle.

above the mean bed level, are in the same situation as the grains on a flat surface, i. e. they experience the greater portion of the boundary shear. The resultant force on these grains will be greater than that required to move them, because the jet strength, K_2, is greater than the critical value for grain motion. In moving, the grain must necessarily roll up onto its neighbor. This increases the exposure of the grain and places it further above the mean bed level. In this position, the inclined velocity vector adjacent to the bed can act on the grain.

The vertical component of this vector increases with jet strength, see Figure 4-27. At the critical jet strength for jumping, it must reach a value greater than the fall velocity and then the grain is projected away from the bed. Once a few grains have left the bed, the remaining ones are more exposed and can be lifted by the same process until the ring has moved over them.

Other effects can aid the suspension of grains from a sediment bed. One is the presence of hydrodynamic lift which arises from the asymmetry of the flow over a grain. Jeffreys (1) showed that a cylinder in potential flow would lift from the bed. In the case of sediment in water, there is neither potential flow nor a cylinder on which it can act. There will however be some lift exerted on the grain. That it is insufficient to lift a grain is shown by the fact that grains on a solid surface roll first before they are projected from the bed. The author feels that vertical forces arising in this way, can at most aid the process by which a grain is suspended.

Another possibility is that the fluid from the ring actually penetrates into the bed and then flows from between the grains. This is not necessary for grain suspension as shown by the experiments with a few grains on a solid boundary. It may however be pertinent in the case of high velocity flow over a flat bed. In such a system the layers of grains near the surface may well be in a very loose state and any fluid flowing out from the bed would have a definite effect upon their motion. Section V-F discusses this flow regime in greater detail.

CHAPTER V

SEDIMENT ENTRAINMENT BY TURBULENT FLOWS

A. INTRODUCTORY NOTE

The process of sediment entrainment by turbulent flows will now be considered in detail. The validity and appropriateness of the pulsating jet model proposed and explored in previous chapters is fully discussed. To do this the flow structure adjacent to the bed must first be examined, and then compared to that which results from the action of the pulsating jet.

The essential features of the pulsating jet model were the intermittent nature of its action, which gave sudden, brief increases in the velocity around the grains, and the existence of a vertical velocity component adjacent to the bed. Section V-B presents evidence which shows these two effects to be present in a turbulent flow in a laboratory flume. A discussion of previous workers' results is given, together with some photographic evidence obtained by the writer. The resultant picture of the flow structure is then matched with that assumed in the entrainment hypothesis.

The remaining sections of this chapter discuss the various flow regimes that occur in conjunction with a sediment bed. Section V-C treats the problem of initiation of motion on a flat bed of sediment grains; V-D, the initiation of motion on a dune covered bed; V-E, the suspension of sediment from a dune covered bed; V-F, the suspension of grains from a flat bed by the action of a high velocity turbulent flow. The applicability of the impinging eddy hypothesis is discussed in each case.

B. FLOW STRUCTURE ADJACENT TO A BOUNDARY

The flow structure next to a boundary depends strongly on the shape of the boundary. If the boundary is composed of loose sediment grains there are two contrasting cases; a flat bed and a dune covered bed. We consider first the structure of a turbulent boundary layer over a flat bed.

1. Discussion of Previous Work.

Section B, Chapter II, presented a brief survey of the published literature on the flow adjacent to a boundary. It was shown that flow within the sublayer ($y^+ = y \frac{U_*}{\nu} < 10$) was intermittent, and that velocity variations did exist adjacent to the bed. Little was said about the structure of the flow. One paper that treats this aspect in great detail is that of Runstadler, Kline and Reynolds (21). They investigated a fully developed turbulent boundary layer, with a constant free stream velocity, over a flat plate in a free surface water flow. Free stream velocities ranged from 0.2 ft/sec to 0.75 ft/sec and gave rise to boundary layers with a thickness of approximately 3 or 4 inches. Both dye injection and hydrogen bubble techniques were used for flow visualization.

From their observations of the flow near the wall they concluded that in the wall layers ($y^+ < 10$), the flow was highly three-dimensional with large fluctuations existing very near the wall, down to $y^+ < 0.5$. The flow had a predominantly longitudinal streaky appearance; regions of low streamwise velocity fluid alternated, in the transverse direction, with regions of higher streamwise velocity fluid. These streaks oscillated and could be seen breaking up. In addition, large fluctuations were observed in which regions of slow moving fluid were frequently

ejected away from the wall with a swirling eddy motion. The ejected fluid came almost entirely from within the wall layers. Over a long period of time the break up and ejection could be seen at all points on the wall, and it was thus possible to define and measure a mean frequency of ejection per unit area. Typical values were 0.0592 $(in^2 sec)^{-1}$ at U_∞ = 0.434 ft/sec and 0.276 $(in^2 sec)^{-1}$ at U_∞ = 0.750 ft/sec, where U_∞ is the free stream velocity.

There was no speculation as to the cause of the break up of the streaks which, it was postulated, resulted in the ejection of fluid from the wall layers. However, it was pointed out that continuity considerations imply, since there is an outflow of fluid from the wall, that there must also be an inflow to the wall. Runstadler visualized this as being a diffuse flow composed of rather large eddies which were thought to be acted on by viscous forces in the wall layer to produce new low velocity fluid (streaks). At a later time the break up and ejection cycle would start again.

Favre, Gaviglio and Dumas (41) have published the results of extensive correlation measurements made in turbulent boundary layers. Their results have some unexpected features which can be explained in terms of the flow structure just outlined. Runstadler does this in his report using the concept of a diffuse inflow and an outflow composed of eddies having an elongated streaky appearance. With a specific flow structure in mind it is possible to predict the result of correlation measurements; but, to argue in the opposite direction, and deduce a flow structure would be virtually impossible.

Favre measured the correlation between values of the streamwise velocity at two different points. He defined a correlation coefficient as $R_{11}(T, X_1, X_2, X_3)$ where T is the time delay, X_1 is the streamwise separation, X_3 is the separation in a direction perpendicular to the plate and X_2 is the separation in the lateral direction (perpendicular to X_1 and X_3), and was equal to zero for all his measurements. The subscript $_{11}$ refers to the velocity component measured at each point; in this case the streamwise velocity was measured at both points. For given values of X_1 and X_3 there is an optimum time delay that will make R_{11} a maximum. Favre has plotted his results for this value of T. The striking feature of these plots is that the locus of points of maximum correlation does not resemble a streamline at positions close to the wall ($y^+ \doteq 35$). Near the edge of the boundary layer, $y^+ = 900$, the locus is quite similar to a streamline. A point of maximum correlation is defined as a point at which the correlation coefficient reaches a maximum for a fixed separation distance and optimum time delay. The line of maximum correlation for points close to the wall bends outwards from the wall in both upstream and downstream directions. Runstadler presents arguments to explain this in terms of his flow structure. They are based upon the assumption that the structure of an eddy will determine the magnitude of the correlation coefficient in its direction of motion and also perpendicular to this direction. For example, in the ejected eddies the correlation coefficient in the direction of motion will be greater than that in the direction of motion of an incoming eddy. In the perpendicular directions the incoming eddy may be expected to have the larger coefficient. See Figure 5-2, page 155.

Another result of Favre's that is unexpected, is the existence of a non zero optimum time delay for points separated a distance that is perpendicular to the wall, i.e. $X_1 = 0$, $X_2 = 0$. When the movable point is further from the wall than the fixed point, the delay is negative; it is positive when the points are reversed. The diffuse inflow eddies, being more highly correlated perpendicular to the direction of motion than are the ejected eddies, will exert a greater influence on the correlation coefficients along a line perpendicular to the plate. When the movable point is further from the wall than the fixed point, the time delay would be negative if the diffuse eddies were flowing towards the wall. The diffuse inflow/elongated outflow structure is thus consistent with these effects deduced from measured correlations.

In making these arguments, a number of liberties have been taken by the authors. Only one component of velocity has been correlated and this could have led to some over-simplification. Measurements of fluctuations that have been made so close to the wall, $y^+ < 100$, must be interpreted with some reservation because the fluctuations are comparable in magnitude to the mean velocity. In spite of these restrictions, by being able to explain measurements of velocity correlations in terms of a flow structure based on observations, Runstadler has made a significant contribution. Evidence for the existence of the flow structure, proposed in his wall layer hypothesis, is strengthened by Favre's results.

Runstadler, having observed the ejection of fluid from the wall, has assumed the presence of an inflow which he visualized as being one of diffuse eddies. The writer would like to reverse this argument and

postulate that the ejection of fluid is linked more strongly to the incoming eddy; actually, that it is the result of the incoming eddy. The argument then becomes the following: turbulent eddies impinge onto the boundary and continuity implies that there must be an outflow from the boundary, which may take place in the form of streaks as observed by Runstadler. The impinging eddies will have the structure that is predominant in the core of the boundary layer.

General considerations of turbulent flow lead to the conclusion that eddies are regions of the flow in which the turbulent motions bear some relation to each other. They are usually pictured as being fluid balls or lumps (see Schlichting (36) page 458). Actual details of their shape are not known, but the terminology suggests that a rounded or oval shape might be expected. Eddies of this type would be called diffuse by Runstadler, so there is no contradiction with the structure he proposed. A slightly different interpretation has however been placed upon it.

It has been assumed above that the flow conditions outside the wall layer affect those inside the layer. Additional evidence for this assumption has been provided by Townes (33). He conducted an investigation on the flow over sets of square cavities ranging in size from $\frac{1}{8}$ in. to 1 in. The flow could be classified in terms of a roughness parameter defined as $\epsilon^* = \epsilon \frac{U_*}{\nu}$ where ϵ is the cavity depth, U_* is the shear velocity and ν is the kinematic viscosity of the fluid.

At low values of ϵ^* the flow in the cavities was unsteady and changed in a random way among four different flow patterns. The patterns ranged from one of gentle inflow to the cavity, to one termed "strong exchange" in which a large part of the fluid in the cavity was ejected. Two phenomena observed by Townes during the unsteady cavity flow suggest the importance of outside velocity fluctuations. First, successive cavities often had the same flow pattern at the same time, which indicated that the disturbance probably originated in the main flow and was not bound to the cavity. Secondly, patterns sometimes appeared to travel to successive downstream cavities as if they were being transported by the outside flow.

At high values of ϵ^*, ($\epsilon^* > 200$), the flow became more stable. In this range the cavity depth was larger, and turbulent bursts from the main flow could not penetrate deeply enough into the cavity to change the flow pattern. Only fluid near the opening was disturbed by bursts; the main cavity flow was, according to Townes "a fairly steady vortex driven by shear forces at the interface with the external flow".

Townes, in his concluding summary, states his belief that the disturbances responsible for the unsteady flow at low values of ϵ^*, come from the boundary layer flow outside the cavities. This writer endorses Townes's belief.

2. Dye Studies.

Experiments in which dye was injected into the sublayer of a turbulent flow over a sediment bed, were done by the author in the flume described in Section III-A-5. Dye flowed slowly from a reservoir

through a $\frac{1}{16}$- in. diameter tube placed beneath the grain surface. The end of the tube was inclined slightly upwards. The flow rate was adjusted so that dye emerged very slowly from between the grains. At zero free stream velocity the dye remained as a layer on the grain surface, showing no tendency to rise from the bed. At non zero free stream velocities the dye moved downstream as a sheet, the main body of which remained adjacent to the grains. Viewed from above, the dye cloud had a pronounced streaky appearance. These streaks wavered intermittently and at times quite violently, indicating the presence of lateral velocity fluctuations adjacent to the bed.

When viewed from the side the dye layer could be seen breaking up and portions of it moving into the main flow in intermittent gusts. Between these bursts the dye cloud remained adjacent to the grains as it moved downstream. Dye left the bed in the form of long wavy filaments. Sometimes two or more would coalesce to form a wider band. The head of the filament lifted from the bed and was immediately carried downstream by the higher velocity in the core of the boundary layer. Combined with the upward motion this caused the dye to follow a curved path. Most of the paths were inclined to the bed at angles between 10° and 20°, approximately. There were some which had much greater inclinations, the dye streak being projected a considerable distance from the bed in a short time. A strong initial impetus must have been given to the dye particles in such cases. Filaments did not always leave the bed in planes parallel to the mean flow. Some were seen to move laterally before being turned downstream by the mean velocity. Many of the filaments left the bed with a swirling motion about an axis

parallel to the downstream direction. There did not appear to be any consistency in the direction of the swirl. This was observed also from directly above the dye cloud and it contributed to the wavy appearance mentioned earlier. Further from the bed, in the more fully turbulent region of the flow, the dye filaments were distorted and broke up into a diffuse cloud of dye.

Figures 5-1-a and 5-1-b show a series of frames from a 16 mm motion picture taken of the dye streaks. The mean flow velocity was 0.741 ft/sec and the depth was 0.332 ft. The sand used for the boundary was Sediment No. 2 with d_s = 0.239 mm. Grain motion was critical under the flow conditions given above. The film was taken at 16 frames/second and the scale is 0.4 x full size. The flow direction is from left to right. In the first and second frames a burst has just left the bed. The dye streak, which is the dark portion across the center of the field of view, then remains close to the bed for the next four frames. The first frame in the second column, Figure 5-1-a, shows the start of a violent burst. Filaments appear over the whole width of the frame, approximately 4 inches. The next two frames show the dye cloud rising further from the bed to a maximum elevation which exceeds half an inch. The disturbance can then be seen dying down, and the dye streak returns to a position adjacent to the grains in the third frame of Figure 5-1-b. In the remaining frames a much weaker burst can be seen. It appears as a single filament which rises from the bed and disappears in the downstream direction. Such a burst has little observable effect upon the sediment grains.

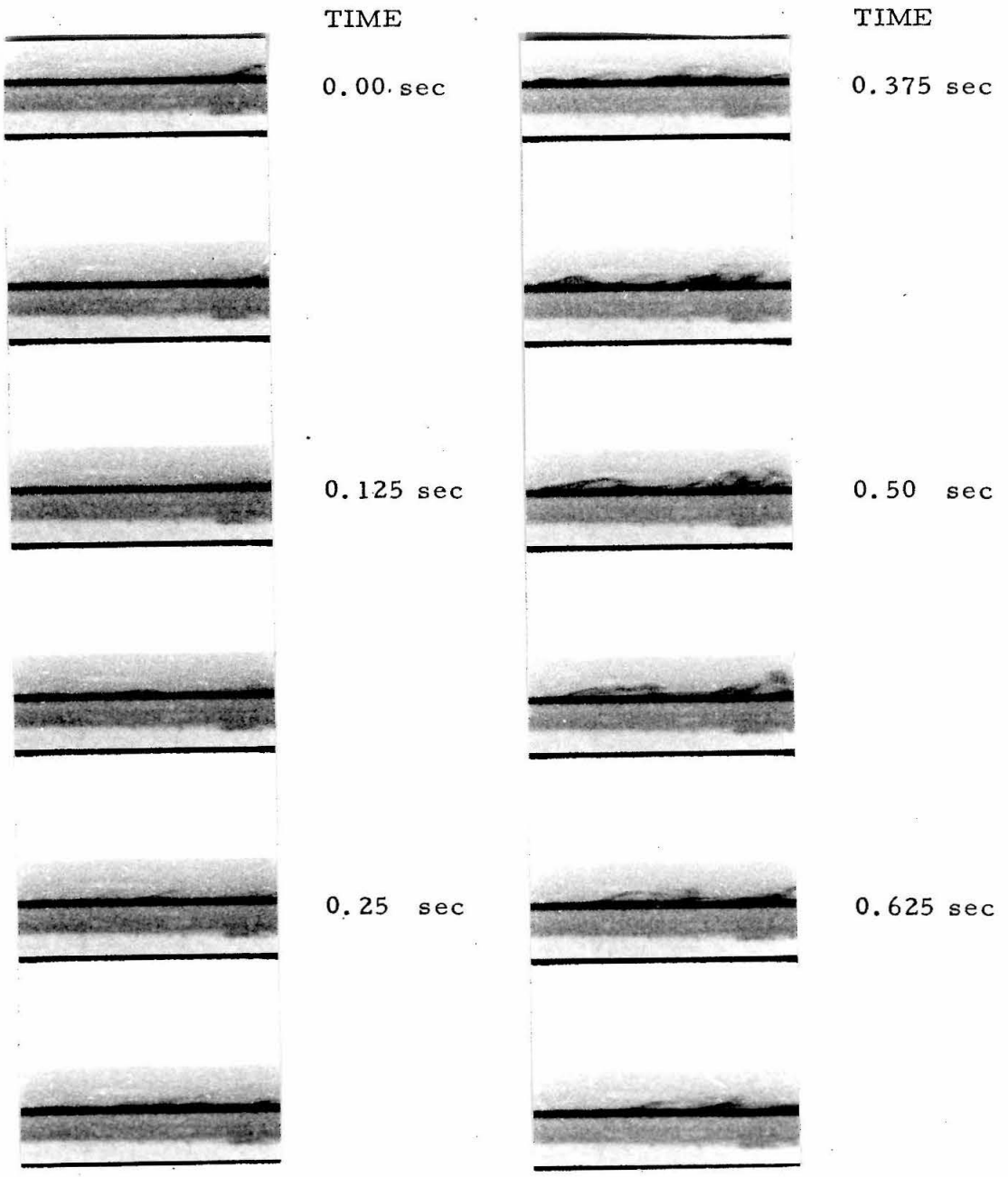

Fig. 5-1-a 16 mm motion picture frames of a dye stream injected into the sublayer of a turbulent flow over a sediment bed. Film speed: 16 frames/sec, mean flow velocity: 0.741 ft/sec, depth, 0.322 ft. Scale: 0.4 x full size. Flow direction is left to right.

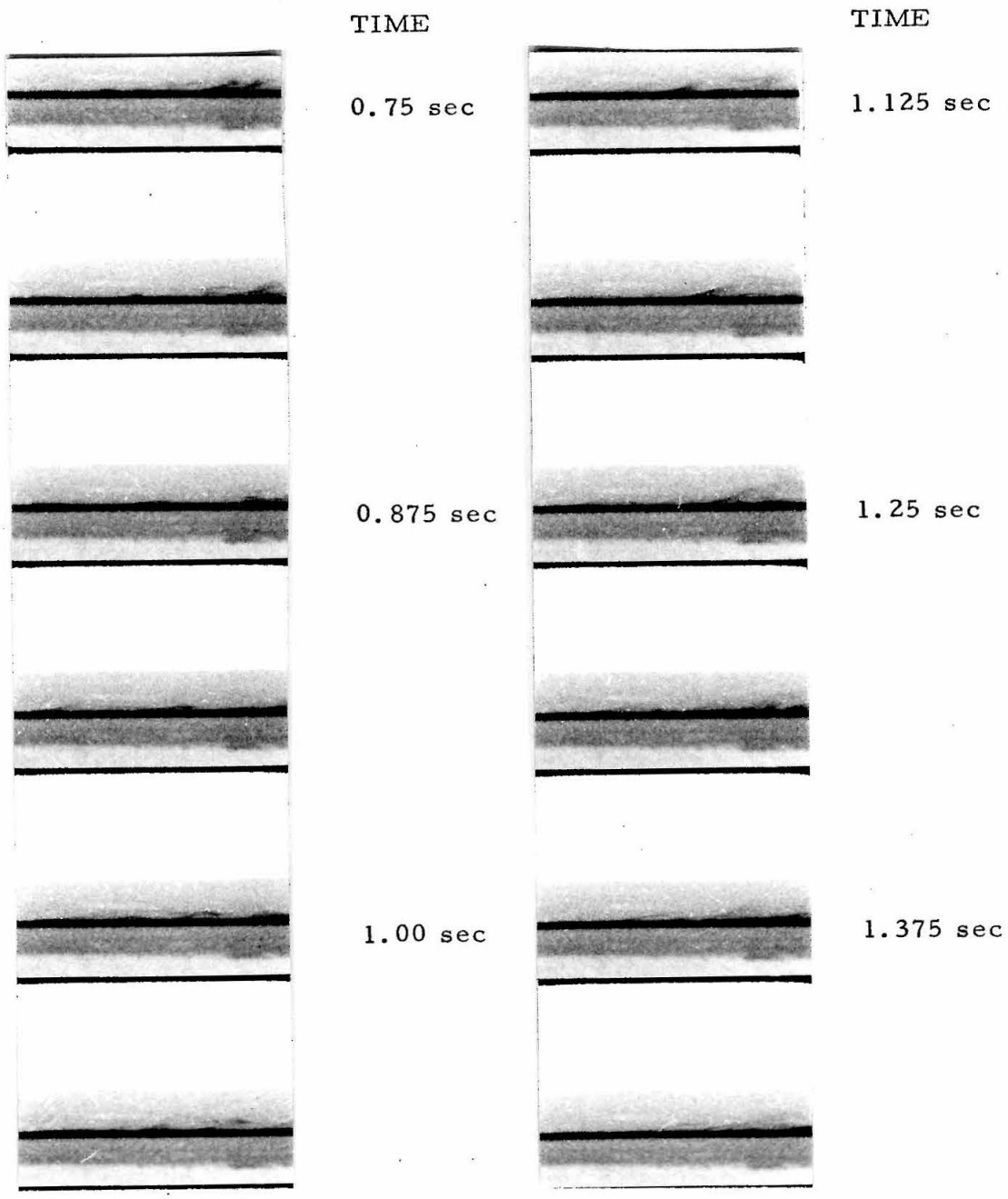

Fig. 5-1-b 16 mm motion picture frames of a dye stream injected into the sublayer of a turbulent flow over a sediment bed. Film speed: 16 frames/sec, mean flow velocity: 0.741 ft/sec, depth 0.322 ft. Scale: 0.4 x full size. Flow direction is left to right.

Figure 5-1-a shows that the time required for the dye to rise from the bed is very small, e.g. the time interval between the sixth and seventh frames is $\frac{1}{16}$ second and the dye has been projected to a height of approximately $\frac{1}{2}$ inch in this time. Neither the intermittency, nor the rapidity with which the dye rises, is consistent with the process of molecular diffusion through the sublayer to the turbulent flow. Observation of grain motion as the dye is ejected from the wall layers provides an insight into the process. At the critical conditions for 0.239 mm sand, shown in Figure 5-1, the frequency with which dye was ejected from bed was such that the grain motion at each burst could be observed. Grains moved only during the larger bursts. At flow velocities in excess of critical, the grains moved with a jerky but continuous motion. This motion is described in detail in the next section. Under these conditions the more violent grain motions could be correlated with the stronger dye ejections.

The presence of a boundary composed of loose grains gives these observations an important advantage over those of Runstadler (21). Both experiments show dye streaks leaving the wall. However, in the present experiments it is possible to establish a link between the dye ejection and the large disturbances which occur in the sublayer. Earlier in this section it was suggested that the dye ejections were a result of the intrusion of turbulent eddies into the sublayer. Further support for this concept is provided by the correlation between grain motion and dye ejections.

3. The Writer's Concept of Grain Entrainment.

The fluid motion near a wall is visualized, as a result of the above discussion, as an interchange of incoming and outgoing eddies superimposed onto a mean flow. The outflow is typified by concentrated bursts of low momentum fluid, while the inflow is typified by eddies of a somewhat larger size which are composed of relatively high momentum fluid from the outer flow. Figure 5-2 shows, in a pictorial way, the writer's concept of the predominant eddy structure near a wall. The figure is similar to one which appears in Runstadler's report (21). Eddies are shown approaching and leaving the wall along curved paths. The eddy shapes are inferred from arguments made in explaining Favre's results. The entrainment hypothesis, Section II-C, was based upon the existence of such a structure. Figure 2-1, which shows only one eddy and its interaction with the sediment grains, is actually a simplified form of Figure 5-2.

Section IV-E discussed the mechanism that the author suggests is responsible for grain entrainment by the pulsating jet. In the turbulent boundary layer the pulse of the jet is replaced by a turbulent eddy which makes contact with the bed. It is postulated that the mechanism of grain entrainment in the boundary layer is the same as that outlined for the jet. At the initiation of motion the eddy, as it impacts onto the bed, increases the shear stress on the exposed portions of the grains causing them to roll. In suspending grains the action of the eddy is two-fold. First, in conjunction with the mean flow velocity, it rolls the grain into a position in which the vertical velocity components near the bed can influence it. Dye studies, reported above, showed that these

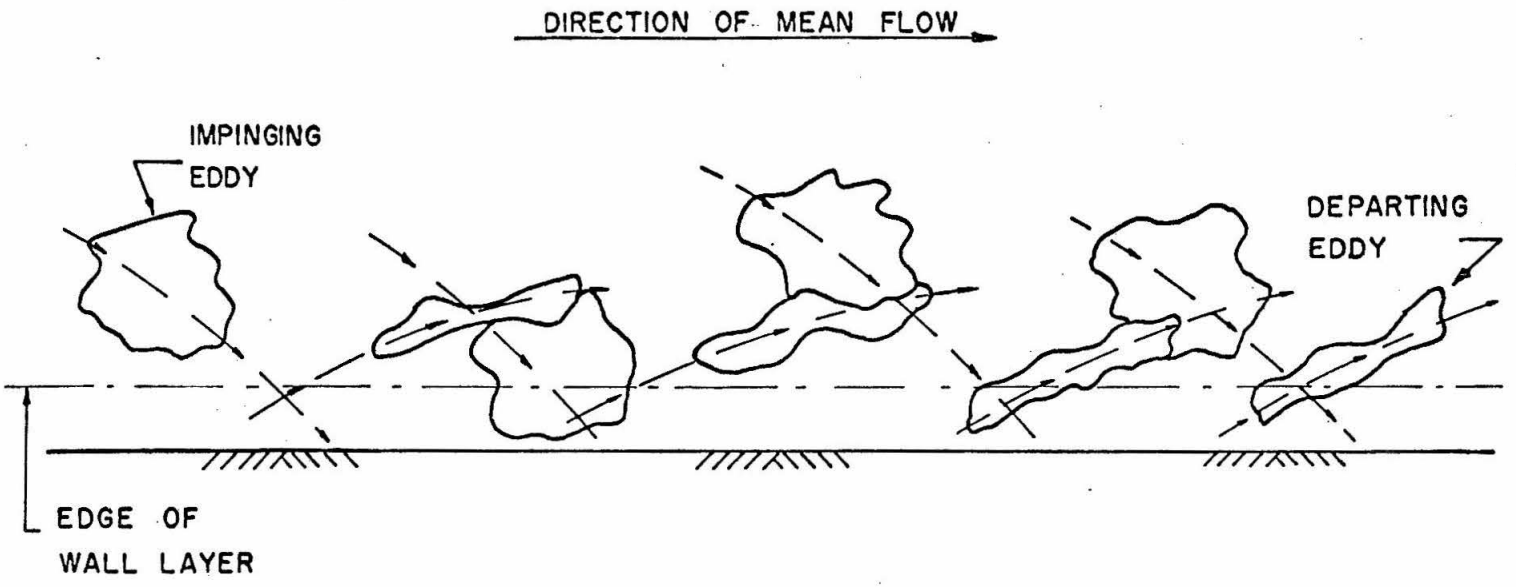

Fig. 5-2 Idealized concept of the predominant eddy structure in the wall region of a turbulent boundary layer.

components were present very close to the grain surface. Secondly, the eddy, as a result of its internal fluid motion, provides the vertical velocity component adjacent to the bed. When the magnitude of this component is comparable with the fall velocity of the sediment, those grains which are sufficiently above the mean bed level to be affected by it, can be suspended.

It can be asked whether the pulse of fluid formed by the pulsating jet provides a sufficient representation of an incoming eddy. To answer this fully would require a knowledge of the actual structure of the impinging eddy. Unfortunately such information is not available. It is unreasonable to expect the vortex ring (see Section IV-D-1) of the pulsating jet to represent an eddy exactly. However, the gross features of each may be similar. Since the pulsating jet is at best a simplified version of the actual conditions in a boundary layer, similarity of the important features of each system is all that is necessary. The important features of an eddy are: its identity as a fluid region having an intrinsic and coherent motion, and the brief period of time for which it can interact with the bed. A vortex ring possesses both of these properties. The motions within the eddy will not be as regular as those in the vortex ring. A swirling motion that resembles, at least in part, that of a vortex ring, can however be expected. In such cases the two structures are similar and the pulsating jet is a sufficient representation of the eddy action.

A difference between the pulsating jet experiments and the conditions in a stream flow is the presence of a horizontal velocity in the latter. Superimposing a horizontal velocity field onto the pulsating jet

has two major effects. Firstly, it is more difficult for the pulse to reach the bed and secondly, at the bed there is a mean shear stress caused by the horizontal flow which can assist the pulse in its action on the sediment grains. Section V-C, below, gives a more complete discussion of these effects together with a brief report on experiments performed with a jet in a cross current. Addition of this horizontal flow will not alter either of the important characteristics of the jet, namely its intermittency and its ability to cause vertical velocities adjacent to the bed.

In summary, Section V-B has presented evidence of velocity fluctuations in the wall layers and of the existence of vertical velocity components near the wall. A flow structure which would give rise to these effects has been presented and the entrainment mechanism outlined. The structure is consistent with the entrainment hypothesis of Section II-C. It is perhaps not the only structure which fits the experimental observations, but physically it is a reasonable one and it also has the advantage of being able to explain measurements of velocity correlations.

The ability of turbulent eddies to disrupt the sublayer and make contact with the wall is basic to the entrainment hypothesis and the resultant pulsating jet model. The ideas discussed above do not prove conclusively that eddies can reach the bed, but the writer feels that the evidence in favor of such an hypothesis is very strong.

C. INITIATION OF MOTION ON A FLAT BED

Consider the action of a turbulent flow over a levelled bed of loose sediment grains. At very low velocities the flow is unable to move individual grains and the bed remains undisturbed, acting as a rigid boundary. By increasing the flow velocity a critical value can be reached at which the grains start to move. The critical velocity depends upon the fluid and sediment properties, and the flow depth. A detailed discussion of the initial motion is given later in this section.

1. Pulsating Jet Experiments.

The experimental results, obtained with the pulsating jet, which are relevant to this problem are those found under the conditions referred to as 'move'. Briefly reviewing the main features of these results, it is recalled that: (1) Pulses with values of jet strength, K, less than a critical value K_1, do not disturb the grains. The jet strength was defined as $K = A\omega^{-s}$, where s is the slope of a plot of log A against log ω, A is the pulse amplitude, and ω the pulse frequency. Pulses with $K > K_1$ cause grains to move from a small area of the bed with a rolling motion.

(2) The value of the critical jet strength K_1 is a function of the properties of the sediment and fluid, and of the tube height.

(3) The flow field created by the pulse adjacent to the sediment grains is one in which the fluid velocity is first zero, then rises rapidly to a maximum and falls off to zero again. The maximum value of the velocity is dependent not only upon the value of K, but also upon the position relative to the jet axis at which it was measured. Grains rolled across the bed under the action of the drag forces exerted by the

fluid when its velocity was greatest. A vertical velocity component, directed upwards, was induced adjacent to the bed by the spinning motion within the pulse. Under the 'move' conditions it was insufficient to cause grains to leave the bed.

In Section IV-D-3 the relation between jet strength and maximum bed velocity was developed. By using it together with the relation between critical jet strength and grain size, the bed velocity at critical conditions can be found as a function of grain size. Table 5-1 compares these values with some results obtained from the field and from experiments in laboratory flumes.

TABLE 5-1

Comparison of Critical Bed Velocities in the Pulsating Jet Model with Results Obtained in Laboratory Flumes.

Sand Size d_s mm	Jet Strength K, cin	Critical Bed Velocity ft/sec		
		Sutherland	Shields	Mavis and Laushey
0.098	1.01	0.308	0.279	0.226
0.239	1.23	0.439	0.410	0.338
0.564	1.42	0.575	0.625	0.495
0.825	1.64	0.729	0.722	0.589

Values listed under Shields were computed by Vanoni from the data given on Shield's diagram. Vanoni assumed a velocity profile of the form $\frac{U}{U_*} = 5.75 \log y/k_s + a_r \left(\frac{U_* k_s}{\nu}\right)$ where k_s is the sand grain roughness, assumed to be equal to the mean grain size, and a_r is a known function of the boundary Reynolds number. The velocity quoted is that

at an elevation of $y = k_s = d_s$ or $y = \delta = 11.6 \frac{\nu}{U_*}$, whichever was the larger. Values listed under Mavis and Laushey were computed from a formula for critical bed velocity presented by them in reference (37).

Velocities measured by the author are close to those of Shields and higher than those of Mavis and Laushey. The quoted values, being mean velocities, are certainly less than the velocity adjacent to the particle when it moves under the action of a turbulent burst. Even without this reservation, the agreement between the critical velocities derived from the pulsating jet experiments and those observed in turbulent flows is very good.

In Section IV-B-7 the relation between jet strength K, and the parameter $(\gamma_s - \gamma)\, d_s$ was derived. It could be written

$$K = 2.21 \left[(\gamma_s - \gamma)\, d_s\right]^{0.286} \qquad \text{for } h = 0.1 \text{ ft} \tag{4}$$

and

$$K = 2.39 \left[(\gamma_s - \gamma)\, d_s\right]^{0.263} \qquad \text{for } h = 0.2 \text{ ft} \tag{5}$$

where $(\gamma_s - \gamma)$ is in lb/cu ft, d_s is in ft, and K is in cin. The relation between jet strength and bed velocity is known for these two values of h from Section IV-D-3, viz

$$U_o = 0.308\, K^{1.79} \qquad \text{for } h = 0.1 \text{ ft} \tag{10}$$

$$U_o = 0.226\, K^{1.90} \qquad \text{for } h = 0.2 \text{ ft} \tag{11}$$

where U_o is in ft/sec and K is in cin. Combining equations (4) and (10) and equations (5) and (11) the bed velocity as a function of $(\gamma_s - \gamma)d_s$ can be found:

$$U_o = 1.27 \left[(\gamma_s - \gamma) d_s \right]^{0.51} \text{ for } h = 0.1 \text{ ft} \tag{12}$$

$$U_o = 1.18 \left[(\gamma_s - \gamma) d_s \right]^{0.50} \text{ for } h = 0.2 \text{ ft.} \tag{13}$$

Since the bed velocity required to move grains is independent of the bed distance, these two equations must have the same constants. Taking mean values:

$$U_o = 1.23 \left[(\gamma_s - \gamma) d_s \right]^{0.50} \tag{14}$$

with $(\gamma_s - \gamma)$ in lb/cu ft and d_s in ft.

This relation can now be compared with those published by investigators who did their work in the field or in laboratory flumes. Since the weight of the particle, W, is proportional to its diameter cubed, we have that $d_s^3 \alpha W \alpha U_o^6$ which is the sixth power law proposed by Brahms and Airy in 1753. They stated that the heaviest particle of a given specific gravity which a flow is capable of moving, is proportional to the sixth power of the velocity.

Mavis and Laushey (37) published a formula for critical bed velocity, viz

$$U_o = \frac{1}{2} d_s^{4/9} (s-1)^{1/2} \text{ ft/sec}$$

where s is the specific gravity of the sediment, and d_s, the sediment size, is in mm. This is the formula used in compiling Table 5-1. It can be written

$$U_o = 0.8\,(\gamma_s-\gamma)^{1/2}\,d_s^{4/9} \text{ ft/sec}$$

with the same units as equation (14). Mavis and Laushey's formula agrees well with the data for coarser sediments ($d_s > 1.0$ mm), and gives values too low for sediments in the range $d_s < 1.0$ mm, where the pulsating jet experiments were done. Taking this into account the two relations are comparable.

White (7) determined that $\frac{\tau_o}{(\gamma_s-\gamma)d_s} = 0.18 \tan\theta$ for conditions of laminar flow about the grain. Here, τ_o is the critical bed shear stress and θ is the angle of repose of the sediment. He suggests turbulence factors of up to 4 or 6 when the flow is turbulent. If one assumes that $\tau_o \alpha U_o^2$, then we get $U_o \alpha \left[(\gamma_s-\gamma)d_s\right]^{1/2}$. The numerical factor cannot be determined without making further assumptions. White made his experiments under many different conditions; here we will consider only those made with a horizontal sand bed under a turbulent boundary layer. Two of the experiments which fit these conditions have boundary Reynolds numbers of 480 and 1280. Flow in both cases is thus in the completely rough regime. The velocity profile is then given by

$$\frac{u}{U_*} = 5.75 \log \frac{y}{d_s} + 8.5.$$

Also, $\tau_o = \rho U_*^2$ and if we compute the value of u at $y = d_s$ we get

$$u = U_o = 8.5\, U_*.$$

Taking White's results for these two experiments, $\tau_o = 0.102\,(\gamma_s-\gamma)d_s$, and $\tan\theta = 1$ we find,

$$U_o = 1.9\left[(\gamma_s-\gamma)d_s\right]^{1/2} \text{ ft/sec}$$

The constant is higher than that deduced from the pulsating jet.

A qualitative study with the pulsating jet in a cross current was made with sediment number 3, a sand with $d_s = 0.564$ mm and $\sigma_g = 1.14$. The flume described in Section III-A-5 was used. A mean flow velocity, considerably less than that required to cause grain motion, was established over a levelled sand bed in the flume. The jet tube was inserted into the flow and a run performed in exactly the same way as reported for the experiments in still water. Two critical jet strengths were obtained; one for moving sediment and the other for causing the grains to jump. Both were in excess of those found when the current was zero. As the mean flow velocity was increased the jet strength required to attain critical conditions also increased. At first glance these observations seem illogical, but the reason for them is easily found.

In Section IV-B-3 it was suggested that the jet strength consisted of two parts. One was that portion required to overcome the resistance offered to the pulse as it travels to the bed, and the other is the remainder which acts upon the sediment grains. With a cross current it is much more difficult for the pulse to reach the bed. One effect of the current is to distort the shape of the pulse both as it is being formed and during its motion through the fluid. It thus loses some of its vortex ring structure and its ability to move parallel to its axis. The pulse is also swept downstream following a longer path, and decaying more, before reaching the bed. For increased mean flow velocities both effects become more pronounced, resulting in increased critical jet strengths. At the bed, the pulse has merely to add to the mean bed velocity in order to move the grains. At this stage of its motion it will in fact be weaker than the corresponding pulse in the no current case.

Weaker is used here in the sense that the increase in bed velocity caused by the pulse is less.

Figure 5-3 shows the pattern of grain motion in the flume at jet strengths just in excess of the critical value. The view is from directly above the bed. Grains are disturbed in a region which is downstream of the jet axis an amount determined by the cross current and the tube height. It has a rounded upstream boundary and is ill-defined at the downstream end. At low current velocities there was a considerable amount of lateral grain motion as indicated in Figure 5-3. With increasing velocities this motion was decreased, the grains moving in a predominantly downstream direction. When the current was close to the critical velocity for grain motion, some of the grains moved by the pulse continued rolling downstream for a distance much greater than the pulse dimensions. Often these were the larger grains which, being more exposed, were kept in motion by the current. Some smaller grains continued to move for a short period under the action of bursts from the flow. This indicates that it requires larger bursts to initiate motion and smaller bursts to maintain it.

At critical conditions for jumping the grains left the bed and were carried in a downstream direction by the cross flow. They all returned to the bed at points away from the region influenced by the pulse. By increasing the frequency of the jet so that $K > K_2$, the strength to cause jumping, grains could be made to jump upstream. In such cases the pulse arrived at the bed with sufficient strength to momentarily reverse the flow direction. This did not occur at either of the critical jet strengths.

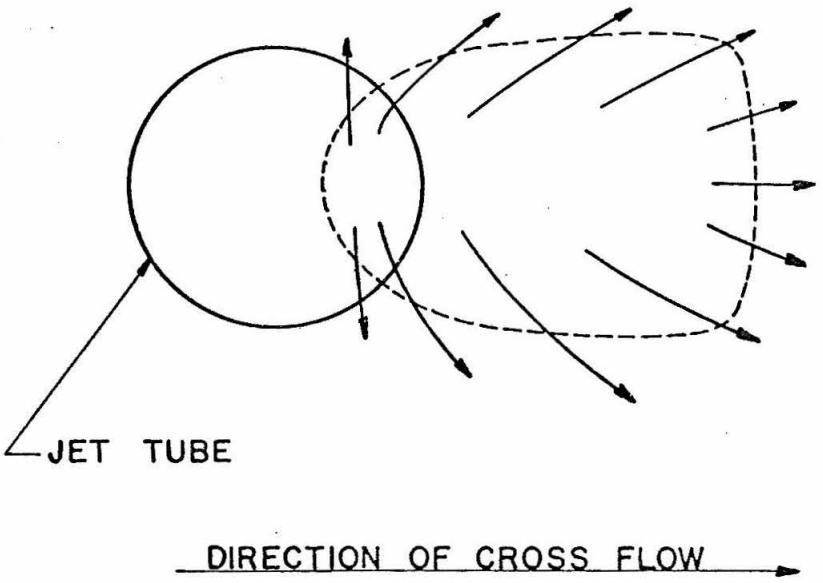

Fig. 5-3 Plan view of the grain motion produced by a pulsating jet in a cross flow.

2. Initiation of Motion by a Turbulent Flow.

Using the flume described in Section III-A 5, observations were made of grain motion at critical conditions. Sediments Nos. 2 and 3 were used. They were both sands with the following properties: d_s = 0.239 mm and σ_g = 1.12; d_s = 0.564 mm and σ_g = 1.14 respectively.

After carefully levelling the bed a flow was started. By adjusting both the downstream and upstream gate valves, a constant depth of flow was maintained as the velocity was increased. After each increase in velocity, a time interval of approximately 10 minutes was allowed for the flow to become steady. Observations were then made to determine if any grains were in motion. A section of the flume, approximately 1 ft in length and 10 ft from the inlet, was chosen as the test section. At this point the boundary layer was fully turbulent. The type of boundary layer present was determined by dropping potassium permanganate crystals into the flow and noting the streak left by the crystal. In the laminar portion the streak remained as a line until after the crystal had reached the bed, while in the transition and turbulent regions the streak broke up into a diffuse cloud of dye before reaching the bed.

Grain motion first became apparent in isolated spots. At this stage most of the grains in motion were the largest ones. Because of their size these grains project above the mean bed level and are more exposed to the action of the flow. If this flow velocity is maintained they are either swept out of the system or they settle into a hollow left by the levelling process, and the motion ceases.

At slightly higher velocities grain motion resumed. It occurred intermittently at isolated places on the bed. Grains at a particular location would move and then come to rest. The number of grains in motion at each burst varied, but was always less than twenty. Both the duration of the motion and the distance moved varied from grain to grain. Motion was always brief, with maximum excursions being approximately one or two inches. Bursts of motion were observed to occur from positions all over the bed, with frequencies that appeared to be constant from one location to another. Because of the brief duration of the motion, it was difficult to define either the shape or size of the regions from which motion occurred. They were small, however, being in general less than one inch in diameter.

The critical conditions were judged to have been reached when grain motion occurred about every two seconds at any chosen spot on the bed. Grains, under these conditions, generally moved in the downstream direction. However, at each burst there were some grains that had a lateral component to their motion. This was less than the streamwise component and the grains moved in a direction making a small angle with the mean flow. The overall appearance of the motion at each burst was similar to that of the motion produced by the pulsating jet in a stream. The magnitude of the lateral motions, which was large at low stream velocities, was the essential difference between the two cases. At higher stream velocities the patterns caused by the pulsating jet resembled more closely those observed in the flume.

If it is assumed that a grain will move in a given direction only if the velocity past the grain in that direction exceeds a critical value,

then the presence of the lateral motions becomes significant. By moving laterally, the grain shows that the velocity has a finite component, in the lateral direction, at least for the duration of the movement. Let U_c be the velocity necessary to cause grain motion, $\overline{U}$ be the main stream velocity adjacent to the grains and u', w' be the velocity fluctuations near the grains in the streamwise and perpendicular directions respectively. The grains will move when the magnitude of the velocity vector, $|\overline{U} + u' + w'|$, exceeds U_c. The direction of motion will be that of the velocity vector. Hence the angle between the path followed by the grains and the streamwise direction is an indication of the relative magnitude of w' and $\overline{U} + u'$. Larger angles would indicate larger values of the ratio $w'/\overline{U} + u'$.

A turbulent eddy disrupting the sublayer could generate this w' in two ways. First, the intrinsic motion of the eddy may be such as to induce a lateral velocity component and second, the fluid within the sublayer must flow away from the path of the incoming eddy. The former, which is certainly present in the pulsating jet experiments, is probably responsible for the grain motion. The latter would be a diffuse flow of low velocity and could only aid the lateral motion.

Vanoni (24) recently reported the results of some experiments which determined the critical values of boundary shear stress for the entrainment of fine sediments. Detailed observations of the motion of grains on a sediment bed were made using an optical apparatus which magnified the grains and also confined attention to a very small area of the bed, about 15 mm in diameter. He reported that near conditions of critical motion, sediment grains appeared to move in gusts or bursts

produced by the turbulence, many grains being moved by each burst. From measurements and observations with sand grains, d_s = 0.102 mm and glass beads d_s = 0.037 mm he was able to establish a criterion for critical movement which involved the frequency of these bursts. Table 5-2 below, taken directly from Vanoni's report (24), gives his criterion.

TABLE 5-2

Vanoni's Criterion for Classifying Sediment Movement.

Burst Frequency Bursts per Sec	Rate of Movement
Less than $\frac{1}{10}$	Negligible
$\frac{1}{10}$ to $\frac{1}{3}$	Small
$\frac{1}{3}$ to 1	Critical
Larger than 1	General

In the author's experiments, reported above, the critical stage was judged to have been reached when bursts occurred about every two seconds at any given position on the bed. This is in accord with Vanoni's criterion (see Table 5-2) and is the reason for what may have appeared to be an arbitrary choice.

There was a difference in the number of grains set in motion by the bursts in the two sets of experiments. Vanoni reports that between 20 and 40 grains were set in motion, in the small area observed, at each burst. In the author's experiments approximately 10 grains, with the larger sand, and 15 to 20 grains, with the smaller sand, were set in motion at each burst. The difference between the two cases is

probably due to the large difference in the grain sizes, $d_s = 0.102$ mm as compared with $d_s = 0.564$ mm and $d_s = 0.239$ mm. Although at what was taken as critical conditions by the author, the number of grains in motion was considerably less, the transport rates in terms of weight of sediment per unit time may well have been comparable.

Vanoni notes that for boundary Reynolds numbers $Re_* = \frac{U_* d_s}{\nu}$ less than 2, there is a wide range of mean bed shear stress less than the critical value for which some sediment movement occurs. This is apparent from Table 5-2 where the rate of movement is characterized as small for burst frequencies between $\frac{1}{10}$ and $\frac{1}{3}$. That some motion occurs at conditions less than critical is understandable in terms of the entrainment hypothesis proposed in Section II-C. It is the effect of those turbulent eddies which are considerably 'stronger' than the average eddy in a particular flow. Their frequency of occurrence is low and thus the number of grains affected is small, too small to constitute critical motion.

One further important conclusion can be inferred from Vanoni's measurements. He notes that the thickness of the sublayer, defined as $\delta = 11.6 \frac{\nu}{U_*}$, during the experiments ranged from 7 to 50 grain diameters. Hence the grains were well embedded in the sublayer. Since they were not in continuous motion, the mean velocity in the layer was insufficient to cause movement. One must conclude that the layer was intermittent in nature, being broken up by a turbulent burst each time grain motion occurred.

Grain motion,which occurs over a flat bed at conditions in excess of critical, is also interesting. Vanoni's criterion (Table 5-2)

would classify the motion as 'general'. The movement is almost continuous at all places on the bed with many grains moving together as groups. Periods of rapid motion will alternate with periods of relative calm. Some of the larger grains roll through the whole field at average velocities considerably greater than those of the smaller grains. This is a result of their greater exposure. Only the topmost layer of grains is affected by the flow; the lower layers remain stationary as the surface grains roll over them. Lateral motions are more pronounced under these conditions. A factor which can contribute to lateral motion under these conditions is glancing collisions between a moving grain and a stationary one. However when a number of grains moved laterally together, the cause must have been a sudden gust of fluid in their vicinity, i. e. an impinging eddy. Lateral motion in groups occurred at all points on the bed with some regularity.

Further discussion of grain motion over a flat bed is given in Section V-E where the problem of suspension from the bed is treated.

This section has presented a discussion of the initiation of motion on a flat bed, the main points of which can be summarized as:

(1) Grain motion was observed to occur first in intermittent bursts. The author suggests that it does so as a result of turbulent eddies from within the flow interacting with the bed.

(2) A representation of a turbulent eddy, the pulsating jet, determined an expression relating critical bed velocity to the sediment properties. It had the same form as those derived by other investigators from turbulent flows over sediment beds, and predicted critical velocities close to those observed in the field.

D. INITIATION OF MOTION ON A DUNE COVERED BED

Consider now beds that are more likely to occur in natural streams. These beds, as a result of grain motion, are deformed into features, called ripples or dunes, which have the appearance of a series of waves, each being somewhat triangular in profile. The upstream face is a gently sloping one and the downstream face forms a steep drop from a sharp crest. As time progresses they build up into a three-dimensional array of crests and hollows; the system is then referred to as a dune covered bed. A photograph of such a bed appears in Figure 5-4. By reducing the flow velocity over a dune bed until grains no longer move, it is possible to determine, as the velocity is increased again, the critical conditions for motion. Also of interest is the position on the bed at which motion first takes place.

The presence of the dune has a marked effect upon the local velocity distribution. Fluid on the upstream side of the dune is in a region of converging flow and is thus accelerated as it moves towards the crest. It then separates from the crest and decelerates as a result of the flow expansion. A separation stream line must extend from the crest to the point at which the flow reattaches to the bed. The location of this point will vary slightly with time but a mean position can be determined by measurements of the local velocity, U_o, at points on the dune surface. Hwang (38) measured the velocity adjacent to the surface of a stabilized dune bed. A few of his results, normalized with respect to the mean flow velocity $\overline{U}$, are shown in Figure 5-5. Values of $\frac{U_o}{\overline{U}}$ increase from near the stagnation point, i.e. where the separation stream line, shown as a series of dashes, meets the dune surface, to

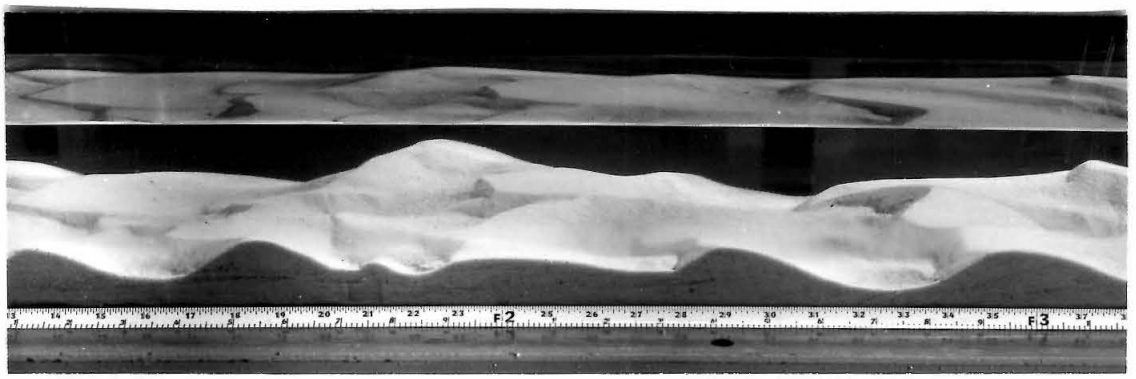

Fig. 5-4 A dune covered bed in a laboratory flume. Sediment size: 0.23 mm, mean flow velocity: 0.749 ft/sec, flow depth 0.231 ft. Photograph taken by Hwang (38).

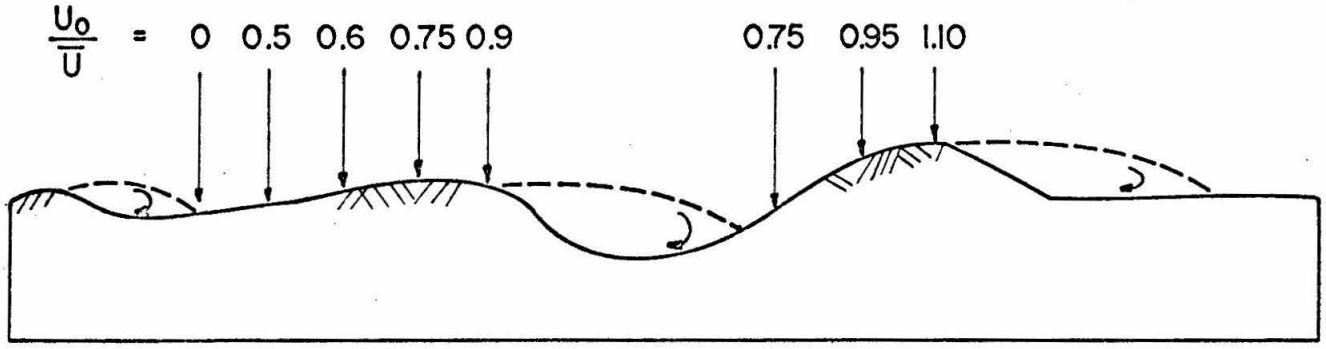

Fig. 5-5 Velocity distribution over the surface of a dune. (Taken from Hwang (38)). Scale: 1/3 x full size.

a maximum at the crest. These values are mean velocities at the point of measurement, and were determined by a pitot tube connected to a pressure transducer.

In view of Hwang's results, one might expect to observe the first signs of grain motion near the crests where the velocity is greatest. However, in accordance with the proposed mechanism of sediment movement, it is suggested that as the mean flow velocity is increased, the first signs of movement will be at those positions at which the eddying motion is most pronounced. In order to move grains, the local velocity must reach a value close to that given by equation (14) above. It is postulated that this will be achieved first by the superposition of the mean flow at a point and the more severe motion associated with eddy impingement.

Consideration of the flow pattern over a dune surface will allow a prediction to be made as to where the eddy motion will be most severe. The region around the stagnation point is one such region. Here the flow is being turned abruptly from its initial direction and swept either into the trough or up the back slope of the dune. Eddies being carried in the flow near the separation streamline, have an excellent chance of actually impacting directly onto the bed. This situation is parallel to that existing in the jet. The direction of rotation of the eddy will determine the direction in which the grains will move. It can be expected that the direction of movement will vary and even at times be upstream. The dune trough is another region where successful eddy action may be anticipated. It is probable that eddies cross the separation streamline and thus enter a comparatively quiet section of the flow field.

Here the mean velocities are quite small and the eddy can move towards the bed almost unhindered. In other words, once an eddy enters this region the chances of it impacting onto the bed are high.

Experiments were performed in the flume to determine the critical conditions for grain motion and the position at which motion first occurred. A dune covered bed of sand grains, d_s = 0.564 mm, was developed by running the flume for 30 minutes at a mean velocity of 1.13 ft/sec at a depth of 0.347 ft. Under these conditions the bed transport rate was high with bed features forming rapidly. There was only a small amount of material in suspension. The dunes had developed to an average height of approximately $\frac{1}{2}$ in. before the flow was stopped.

The flow was then started again at a very low mean velocity and increased in small steps until motion was observed. It occurred first in the troughs and at the base of the upstream slope of the dune. Motion was intermittent with 5 or 6 grains moving simultaneously from a small area. In the trough there did not appear to be any preferred direction of motion even within one burst. Grains appeared to move away from a center as in the jet experiments. On the dune slope the preferred direction was downstream, but there were many instances in which grains moved laterally and upstream.

The dye injection technique outlined in Section V-B-2 can yield further information about the structure of the flow over the dunes. A flow over a dune bed which can move the sediment grains, also moves the dunes. By placing a dye tube beneath such a bed, the flow structure at all points on the dune profile can be observed as the dune moves over the end of the tube. A typical dune velocity is 1 inch in 10 or 15 minutes,

which allows ample time for observations at each point on the profile. Four distinct regions will be discussed; the trough, the dune crest, the upstream slope and the region near the stagnation streamline.

(i) The Trough. Dye appeared at the grain surface as a circular patch approximately $\frac{3}{4}$ in. in diameter. From this patch filaments of dye could be seen rising from the bed. Each filament twisted as it rose. Often filaments would disperse quite suddenly and disappear into the main flow. Some moved slowly up the face of the dune towards the crest. Those that reached the crest bent over in a downstream direction and were swept away. The intrusion of fluid from the main flow into the lee of the dune could be clearly seen. Dye filaments would all move rapidly sideways, some to the left and some to the right, and then be turned towards the bed or be dispersed. When this occurred, the grains in the trough could be seen moving rapidly across the bed, some even jumping from the bed and being carried away. The observations showed convincingly that the lee of a dune is not a region of quiescent fluid, but one in which frequent bursts of motion occur. These bursts had a very definite effect on the sediment grains. More detail is given in Section V-D.

It is not clear why the dye filaments formed. The dye could have left the bed from all points of the patch formed on the surface. Instead it preferred to flow across the surface, concentrate in spots, and then leave the bed from these spots. A possible explanation is that the dye concentrates in places where the vorticity is high. These would be the ends of vortex lines which extend out into the flow. Another possible reason is the existence of very local pressure fluctuations which suck the dye out from between the grains and cause a filament of dye to form.

(ii) The Crest. In this region the mean velocity of the flow is high, and the dye was swept across the grain surface as soon as it appeared. There was a tendency for the dye to move in streaks which were carried over the dune crest. Some of the streaks tended to curl downwards forming small regions of high dye concentration which resembled shed vortices. Others curled upwards and disappeared in the main flow. Occasionally all of the streaks would dip sharply into the trough, showing the intrusion of an eddy into the lee-side region of the dune.

(iii) The Upstream Slope. Dye moved up the slope, remaining in close proximity to the grain surface. When viewed from above, the dye sheet had a streaky appearance which was similar to that observed with a flat bed, (see Section V-A). Occasionally dye filaments could be seen rising from the bed and mixing with the main flow. This motion was infrequent and always accompanied by intensified grain motion.

(iv) The Stagnation Region. As the dune moves downstream, the dye patch on the grain surface moves from the crest towards the trough. As it nears the stagnation region the frequency with which dye filaments leave the bed increases. The stagnation region is reached when the filaments start to move radially from a center at each burst. At this stage the eddy action is vigorous and frequent, the dye patch often appearing to erupt from the bed in a cloud. Between the larger bursts, some of the dye moved downstream towards the next crest and some moved into the trough region. Even this motion was intermittent and punctuated with ejections of dye streaks from the bed.

These dye studies emphasized the importance of the dune configuration in determining the flow structure over a dune bed. They also established that the two regions in which eddy action is most pronounced are the stagnation zone and the region in the lee of the dune face.

Another aspect of the sediment fluid interaction was revealed by the initiation of motion experiments on a dune bed. The critical mean velocity of flow was less with a dune covered bed than with a flat bed. Two runs gave values of 0.606 ft/sec and 0.591 ft/sec with a depth of 0.347 ft. For the flat bed a velocity of 0.847 ft/sec was required at the same depth. The sand size in each case was 0.564 mm. Mennard (42) has reported this effect and mentions values of about 5 cm/sec difference in the two cases. In the author's experiments the difference is $7\frac{1}{2}$ cm/sec.

Reasons for the lower mean velocity over the dunes can be found in the hypothesis of impinging eddies. At the base of the dune the flow is directed at an appreciable angle to the bed instead of being parallel to it. This not only has the effect of increasing the chances of an eddy striking the bed, but also aids its progress to the bed. In the trough region, those eddies which impinge onto the bed do so without encountering much resistance from a mean flow and without having to disrupt a sublayer. The dune also aids in another way; that of intensifying the turbulent fluctuations near the bed. It is a case of flow over a rough boundary as opposed to flow over a smooth one. Together these effects suggest that over a dune covered bed, flows with smaller mean velocities can provide the eddy activity required for grain motion.

Summarizing this discussion of initiation of motion on a dune covered bed, it can be said that

(1) The initial grain motion is intermittent in nature and occurs in those regions in which eddy action has been shown to be a maximum.

(2) A dune covered bed acts as an aid to the mechanism of grain motion, enabling flows of lower mean velocity to initiate movement. The reason for this is thought to be the resultant flow pattern which assists eddies to impinge onto the sediment bed.

These two statements are indicative that a mechanism involving the interaction of turbulent eddies and the sediment grains is of importance in the entrainment process.

E. SUSPENSION OF GRAINS FROM A DUNE COVERED BED

Consider now the conditions created adjacent to a dune covered bed by a flow transporting sediment in suspension. The mean flow velocity is considerably in excess of that required to initiate motion. Because the sediment has a finite fall velocity and the impulses given to it by turbulence act downwards as well as upwards, many grains are returned to the bed. However, the concentration profile in a flume remains essentially unchanged with distance along the flume, which implies that sediment is being continually entrained from the bed.

There are four possible places for this entrainment to occur; from the troughs, from the crests, from the upstream slopes of the dunes, and from the stagnation region.

(1) The trough is a region of strong eddy motion. This was discussed in the previous section where it was shown that eddies leave

the main flow, cross the separation streamline and impact onto the bed. Since the dune pattern is not two dimensional, there is the possibility of fluid entering this region from the side in the form of a jet or, possibly, as a series of bursts. Interaction with the eddies, mentioned above, results in a highly unsteady flow pattern. Grains in this region are observed to be in a state of continual jerky motion, and very seldom are they stationary. The movement is in no preferred direction and is often oscillatory. From time to time a large disturbance of short duration appears and grains, as in the 'jump' experiments of the pulsating jet, are lifted from the bed in a cloud. The trajectories of these grains are radial from the center of the disturbance and are curved away from the bed. A scour mark of somewhat circular shape can be seen on the bed after each burst. It is obliterated almost immediately by the continual motion of grains in the trough. Some of the grains lifted by the burst return to the bed in the trough; others are caught up in the main flow and are suspended. The bed geometry, which determines the flow pattern, is important in this process, e.g. jet-like flow between two dunes will suspend any grains that are projected up into it. Grains are sometimes thrown well up the back slope of a dune, from where they are swept away.

Flow conditions in the trough parallel those of the pulsating jet because there is no mean cross flow through which an eddy must pass. The mechanism by which grains leave the bed in this region is the same as that which causes jumping in the pulsating jet experiments. See Section IV-E-2. The most violent eddies caused grains to jump almost vertically from the bed. This could be done with the pulsating jet by

using a jet strength much greater than the critical jet strength for jumping. Flow conditions in the trough are probably represented more accurately by the pulsating jet, than those in any other region of the bed.

(2) The back slope of the dune is a region in which the flow is parallel to the grain surface and conditions are thus similar to those on a flat bed. However, the probability of there being a thick viscous sublayer is small because there is not sufficient distance over which one can develop. Eddies being carried along in the flow can then impact very effectively onto the surface.

Flow conditions which suspend sediment are such that grains on the backs of the dunes are in constant motion. It is a jerky, wavy motion in which grains often move in a streaky pattern. The effect of an eddy is to disrupt this pattern. If the eddy is a violent one, grains move in groups which are suddenly accelerated or even lifted from the bed. These effects can be easily observed in a laboratory flume.

(3) The dune crests act mainly as launching devices for the grains which are rolling up the dune slope. Many grains which roll to the crest tumble down the lee side, which results in a forward movement of the dune as a whole. Those grains which arrive at the crest with a sufficiently high velocity are, as a result of their inertia, launched from the crest into the main flow. Once over the crest they can be either suspended or returned to the bed. It is proposed that the high velocity of the grains launched from the crest is achieved with the help of eddy action in the region behind the dune crests. Observations of grain motion, both up the dune slope and from the crest, leave no doubt that this is the case. Suspension of grains from the dune crests

is thus dependent upon eddy action. The dependence is less direct than in other regions of the bed.

(4) The stagnation region is that part of the dune profile where the separated flow from the previous crest impinges directly onto the sediment surface. It was noted in Section V-D that the flow in this region was very unsteady, with large fluctuations occurring frequently. This is demonstrated clearly by the action of the sediment grains. Motion is very similar to that described in connection with the trough region, but it is more violent and extensive. The bursts are not nearly as symmetrical as the ones in the trough. Most of the grains move downstream or laterally, and only a few are seen moving upstream. Most bursts cause grains to leave the bed. Many of the grains are projected right over the crest and are immediately suspended. This is the only region on the bed where more than just the topmost layer of grains is affected. The intensity of the fluid motion is often such that considerable scour occurs. Any depression left on the surface by this action is quickly covered by grains from adjacent areas of the bed. The fluid flow pattern is very similar to that of the pulsating jet because the eddies carried by the flow impact directly onto the bed. On impact they are turned sharply and move either into the trough or up the dune slope. In so doing they exert large drag forces on the grains, causing their motion.

Discussion in this section has described conditions which are parallel to those in Section V-D. The essential difference is that flow velocities are higher and eddy motions are more intense. The same conclusions can be drawn as to the importance of the impinging eddies.

It is suggested that grains are suspended from the four regions discussed above primarily as a result of turbulent eddies interacting with the bed.

F. SUSPENSION FROM A FLAT BED

With increasing flow velocities the sediment bed changes from a dune bed to a flat bed. The bed is level except for two narrow bands at the side walls of the flume where small dunes are found. The sediment transport rate is high with grains being moved both as suspended load and bed load. In elevation the flow appears as a dense cloud of sediment grains moving over a flat bed. It is equivalent to a dust storm caused by high winds over a desert.

The high concentrations of suspended load make it impossible to observe any details of grain motion. One can only engage in speculation concerning the entrainment mechanism and the applicability of the impinging eddy hypothesis. Observations made of grain motion at low flow velocities over a flat bed must form the basis for any such speculation and are reported at the end of Section V-C on page 171. This discussion actually bears the same relation to Section V-C as the last section did to V-D.

At these high velocities the grains will be rolling over the surface under the action of the mean velocity. The sublayer, which has a nominal thickness of $y = 10\frac{\nu}{U_*}$, is thinner than that at critical conditions on a flat bed. Grains rolling along will tend to disrupt the layer, and in all probability the layer will have a small effect upon the conditions at the bed.

Increased flow velocities imply higher turbulence intensities. Thus, both the motion of the eddies through the fluid and also the motion within the eddies, will be increased. As a counter to the effect of increased turbulence the higher shear stresses in the fluid near the boundary will cause greater distortion and perhaps disintegration of some eddies before the wall is reached. The relative importance of these two opposing effects can only be estimated. Comparison of observations made of critical conditions with those made at higher velocities over a flat bed, show that noticeable increases in grain agitation take place as the flow velocity is increased. Based on this, it seems that the effect of increased turbulence intensity would be more important than the increased resistance to eddy impingement by the faster flow. The author believes that the impinging eddy hypothesis is applicable at these high velocities, although its effects upon a sediment bed have not been observed directly.

Grains on the bed, because of their continual motion, are in a very loose state and encounter little interference from their neighbors. An eddy coming into contact with such a dispersed system would have a pronounced effect upon it. Fluid motion within the eddy will increase the forces acting on the grains and those that are sufficiently exposed will experience a vertical force component which, if large enough, will cause grains to leave the bed. The high mean velocity will carry them downstream a considerable distance before they can settle back to the bed. During this time, the probability of the turbulent fluctuations in the flow projecting the grain further from the bed and suspending it, is high.

If the vertical component of the force on the grain is less than the grain's submerged weight, there is another mechanism which can project grains from the flat bed. Locally, when the eddy makes contact with the bed, the grains are accelerated and will overtake and collide with those that are moving ahead of them. As a result the direction of motion of the grain can be inclined to the bed, and if the velocity increase is sufficient the grain will be projected away from the neighborhood of the boundary. For this mechanism to be effective, the fluctuating nature of the velocities adjacent to the bed is essential. If the flow velocity was constant in this region, then no grain could overtake another and be deflected into the flow.

Until a method is devised to observe the motion next to a flat bed, the points outlined above must remain speculation. They have however, been based on observations made at lower velocities and are reasonable extensions of the conclusions drawn from these observations.

CHAPTER VI

SUMMARY AND CONCLUSIONS

This study has attempted to clarify the process by which sediment grains are first moved and then lifted from the bed of an alluvial stream. The main conclusions that may be drawn are:

A. From dye studies in the flume.

1. Fluid motion in the sublayer of a turbulent boundary layer over a flat sediment bed is irregular and unsteady.

2. Bursts of fluid leave the sublayer and mix with the fluid in the boundary layer.

3. Continuity implies that when bursts of fluid leave the bed, there must be a flow towards the bed.

4. On a dune bed the most unsteady regions of flow are the trough, and that region near the stagnation point on the back slope of the dune.

5. Fluid enters the lee side region of a dune from the main flow over the crest, in irregular bursts.

6. Bursts of fluid rise from the back slope of the dune and mix with the main flow in a manner similar to that observed over a flat bed.

B. From observations of grain motion.

1. Under critical conditions for grain motion on a flat bed, the motion occurs in intermittent bursts over small areas of the bed.

2. As the flow velocity over a dune bed is increased from below the critical value, the grains which move first are those in regions where the unsteadiness of flow was shown to be a maximum. (See A-4 above.)

3. The critical mean flow velocity for initiation of grain motion, at the same flow depth, is less for a dune bed than for a flat bed. The reason for this is thought to be that the flow pattern over the dunes assists the entrainment process.

4. Suspension from a dune bed occurs at all points on the dune profile. The manner in which grains leave the bed differs from one region of the profile to another. At each point the grain motion can be explained in terms of the observed flow pattern at that point. (See A-4, 5, and 6 above.)

C. From the pulsating jet experiments.

A piston pump and a cam mechanism were used to produce a pulsating jet with a range of amplitudes and frequencies. The jet issued from a tube placed vertically in a tank of still water, the base of which was covered with a bed of loose sediment grains. The distance from the end of the jet tube to the sediment bed ranged from 0.1 ft to 0.3 ft. Pulse amplitude was defined as the volume of fluid in the pulse divided by the cross sectional area of the jet tube. The following conclusions may be drawn from the jet experiments:

1. There are two critical values of jet strength: one at which grains start to roll across the bed, and one at which grains are projected up from the bed. Jet strength is defined in Section IV-B-1, equation No. 3.

2. Data from all the experiments can be correlated in terms of three parameters formed from the experimental variables. When plotted in the form A/h against $\frac{Ud_s}{\nu}$, the data define a family of curves, each of which corresponds to a particular value of $\left[\frac{\gamma_s - \gamma}{\rho} \frac{d_s^3}{\nu^2}\right]$. Definitions of all the symbols can be found in the list starting on page 192. Figure 4-16 presents the data determined from critical conditions for grain movement, and Figure 4-17 shows the data from critical conditions for grain jumping. The critical jet strength at a given tube height, and for a specified fluid and sediment combination, can be calculated directly from Figure 4-18 ('move') or Figure 4-19 ('jump').

3. The relation between the maximum velocity produced adjacent to a boundary by the pulsating jet, and the jet strength, can be written as a power law.

4. Based on (3), an expression relating critical bed velocity to sediment and fluid properties, can be deduced. It has the same form as those derived by other investigators from experiments with turbulent flows over sediment beds, and predicts critical velocities close to those observed in the field.

5. The velocity produced adjacent to the sediment bed by the pulsating jet has a vertical component. The fluid elements follow trajectories inclined at an angle to the mean bed level.

6. Under the action of the jet, grain motion is brief, intermittent, and occurs only on a small portion of the bed.

7. The pulse moves sediment grains by increasing the bed shear stress to a value exceeding the critical value for grain motion.

8. The pulse lifts grains from a sediment bed by rolling them to a position in which they are exposed to the action of the vertical component of velocity described in C-5, above. When this component is of the order of the fall velocity of the grain, the grain can leave the bed.

From the conclusions listed in A and B above, it is hypothesized that turbulent eddies impinge directly onto the sediment bed. An entrainment hypothesis based on this concept of impinging eddies was proposed and investigated using a pulsating jet to simulate the action of a turbulent eddy upon a sediment bed. The hypothesis is presented in detail in Section II-3.

If the effect of a turbulent boundary layer upon a sediment bed is to be adequately represented by the pulsating jet experiments, the characteristic features of one must be reproduced in the other. For the jet these features are:

(i) The existence of two critical jet strengths, (C-1),

(ii) the intermittent and local nature of the grain motion, (C-5), and

(iii) the introduction of a vertical component of velocity adjacent to the bed, (C-6).

The equivalent of the two critical jet strengths, mentioned in (i) above, can be inferred from the existence of a flow velocity for which motion occurs by rolling and sliding, and the requirement of a considerably higher velocity for grain suspension from a bed by a turbulent flow. They may be interpreted as two critical levels of eddy activity. The presence at the boundary of a turbulent flow, of the

effects mentioned in points (ii) and (iii) above, was established by observations of grain motion and the movement of dye filaments, see B-1 and A-2.

From these observed similarities it is inferred that the entrainment mechanism in the two cases is the same. Hence the mechanism by which a turbulent eddy, upon impact with a sediment bed, moves and then suspends sediment, is the same as that outlined for the pulsating jet in Section IV-E and summarized in C-8 above.

The author does not claim to have completely solved the problem of fluid and grain interaction, or even to have proved that the proposed mechanism is the only one which can result in the entrainment of sediment grains. An entrainment hypothesis has, however, been proposed. Evidence in favor of its validity has been presented and may be summarized in three points:

1. The flow structure implied by the hypothesis is consistent with that reported by other workers after extensive investigations.

2. Simultaneous observations of dye filaments and grain movement give a visual correlation between the violent disturbances in the sublayer, and the grain motion.

3. The hypothesis can explain many of the observed features of grain motion on sediment beds.

An important consequence of the entrainment hypothesis is that grains cannot be lifted from the bed without the presence of turbulent fluctuations adjacent to and directed towards the bed.

LIST OF SYMBOLS

A	pulse amplitude
A'	constant used in King's Law
a	diameter of jet tube
B'	constant used in King's Law
C	sediment concentration
C_a	sediment concentration at $y = a$
C_D	drag coefficient
C_L	lift coefficient
D^*	diffusivity
$d_{84.1}$	grain size for which 84.1% by weight of sediment is finer, (similarly for $d_{15.9}$)
G_1, G_2	functions of $\gamma_s - \gamma$, h, ν
h	tube height
I	current flowing in hot wire
K	jet strength
K_h	jet strength required to overcome the resistance offered to the pulse by the fluid
K_s	jet strength required at the bed to cause grain motion
k	von Karman constant
R_e	Reynolds number based on fall velocity
R_{e*}	Reynolds number based on shear velocity
R_w	electrical resistance of hot wire
R_g	electrical resistance of hot wire at temperature of fluid
S	Shield's parameter

LIST OF SYMBOLS (Cont'd)

S. G.	specific gravity
s	slope of amplitude-frequency curve when plotted on logarithmic paper
T	period of bursts of grain movement
U	exit velocity of pulse = $2A_{\omega}$
U_*	shear velocity
U_o	maximum velocity that occurs at the bed during the passage of a pulse
U_c	critical velocity for grain motion
u	velocity of fluid over hot film sensor
u'	streamwise velocity fluctuation
V	voltage output from hot film sensor
w	fall velocity
w'	lateral velocity fluctuation
x	slope of lines of constant β in Figures 4-16 and 4-17
y	elevation above the bed
y^+	dimensionless coordinate $y^+ = y \frac{U_*}{\nu}$
α_1, α_2	numerical coefficients
β	parameter characterizing sediment and fluid = $\left[\frac{\gamma_s - \gamma}{\rho} \frac{d_s^3}{\nu^2}\right]^{1/2}$
γ	specific weight of fluid
γ_s	specific weight of sediment
δ	sublayer thickness = $11.6 \frac{\nu}{U_*}$
ϵ	cavity depth

LIST OF SYMBOLS (Cont'd)

ϵ^*	roughness parameter
ϵ_s	diffusion coefficient for sediment
θ	angle of repose
ν	kinematic viscosity
ρ	density of fluid
ρ_s	density of sediment
σ_g	geometric standard deviation
τ_o	bed shear stress
τ_c	critical value of bed shear stress
ϕ	dimensionless parameter $= \frac{U_1 d_s}{\nu}$
ψ	dimensionless parameter $= \frac{U_2 d_s}{\nu}$
ω	pulse frequency
Δp	pressure difference
$\Delta\rho$	density difference
$-_1$	subscript $_1$ refers to critical conditions for moving
$-_2$	subscript $_2$ refers to critical conditions for jumping

BIBLIOGRAPHY

1. Jeffreys, H. J., "On the Transport of Sediments by Streams", Proc. Camb. Phil. Soc., Vol. 25, pp. 272-6, (1929).

2. Chepil, W. S., "The Use of Evenly Spaced Hemispheres to Evaluate Aerodynamic Forces on a Soil Surface", Trans. AGU, Vol. 39, pp. 397-404, (1958).

3. Einstein, H. A. and El-Samni, E. A., "Hydrodynamic Forces on a Rough Wall", Revs. Mod. Phys., Vol. 21, pp. 520-4, (1949).

4. Leliavsky, S., "An Introduction to Fluvial Hydraulics", Constable and Co. Ltd., London, (1955).

5. Gilbert, G. K., "Transportation of Debris by Running Water", U. S. Geol. Survey Prof. Paper No. 86, (1914).

6. Shields, A., "Anwendung der Aehnlichkeitsmechanik und der Turbulenzforschung auf die Geschiebebewegung", Mitt. der Preuss. Versuchsanstalt fur Wasserbau und Schiffbau, Berlin, (1936).

7. White, C. M., "The Equilibrium of Grains in the Bed of a Stream", Proc. Roy. Soc., A, Vol. 174, pp. 324-38, (1940).

8. O'Brien, M. P., "Review of the Theory of Turbulent Flow and Its Relation to Sediment Transportation", Trans. AGU, pp. 487-491, (1933).

9. Rouse, H., "Experiments on the Mechanics of Sediment Suspension", Proc. 5th Int. Cong. Appld. Mech., (1938).

BIBLIOGRAPHY (Cont'd)

10. Rouse, H., "Modern Conceptions of the Mechanics of Fluid Turbulence", Trans. ASCE, Vol. 102, pp. 463, (1937).

11. Anderson, A. G., "Distribution of Suspended Sediment in a Natural Stream", Trans. AGU, pp. 678-683, (1942).

12. Vanoni, V. A., "Transportation of Suspended Sediment by Water", Trans. ASCE, Vol. 111, pp. 67-133, (1946).

13. Kalinske, A. and Pien, C. L., "Experiments on Eddy Diffusion and Suspended Material Transportation in Open Channels", Trans. AGU, pp. 530-35, (1943).

14. Vanoni, V. A., Brooks, N. H., Kennedy, J. F., "Lecture Notes on Sediment Transportation and Channel Stability", Report No. KH-R-1, W. M. Keck Laboratory of Hydraulics and Water Resources, California Institute of Technology, (1961).

15. Kalinske, A., "The Movement of Sediment as Bed Load in Rivers", Trans. AGU, Vol. 28, pp. 615-20, (1947).

16. Chepil, W. S., "Equilibrium of Soil Grains at the Threshold of Movement", Proc. Soil Sci. Soc. of Am., Vol. 23, pp. 422-28, (1959).

17. Chepil, W. S., "The Use of Spheres to Measure Lift and Drag on Wind Eroded Soil Grains", Proc. Soil Sci. Soc. of Am., Vol. 25, pp. 343-5, (1961)

18. Deacon, G. F., Proc. Inst. Civ. Eng., Vol. 118, pp. 93-6, (1894).

19. Fage, A. and Townend, H., "An Examination of Flow with an Ultramicroscope", Proc. Roy. Soc., A, Vol. 135, (1932).

BIBLIOGRAPHY (Cont'd)

20. Nedderman, R. M., "The Measurement of Velocities in the Wall Region of Turbulent Liquid Pipe Flow", Chem. Eng. Sci., Vol. 16, pp. 120, (1961).

21. Runstadler, P. W., Kline, S. J., Reynolds, W. C., "An Experimental Investigation of the Flow Structure of the Turbulent Boundary Layer", Report MD-8, Dept. of Mech. Eng., Stanford University, (1963).

22. Einstein, H. A. and Li, H., "The Viscous Sublayer along a Smooth Boundary", Trans. ASCE, Vol. 123, pp. 293-313, (1958).

23. Laufer, J., "The Structure of Turbulence in Fully Developed Pipe Flows", Tech. Note 2945, NACA, (1953).

24. Vanoni, V. A., "Measurements of Critical Shear Stress for Entraining Fine Sediments in a Boundary Layer", Report No. KH-R-7, W. M. Keck Laboratory of Hydraulics and Water Resources, California Institute of Technology, (1964).

25. Danckwerts, P. V., "Significance of Liquid-Film Coefficients in Gas Absorption", Ind. and Eng. Chem., Vol. 43, pp. 1460, (1951).

26. Hanratty, T. J., "Turbulent Exchange of Mass and Momentum with a Boundary", A.I.Ch.E., Vol. 2, pp. 359, (1956)

27. Hanratty, T. J., and Reiss, P. L., "An Experimental Study of the Unsteady Nature of the Viscous Sublayer", A.I.Ch.E., Vol. 9, pp. 154, (1963).

BIBLIOGRAPHY (Cont'd)

28. Hanratty, T. J. and Shaw, van P., "Fluctuations in the Local Rate of Turbulent Mass Transfer to a Pipe Wall", A.I. Ch. E., Vol. 10, pp. 475, (1964).

29. Lin, C. S., Moulton, R. W., and Putnam, G. C., "Mass Transfer between Solid Wall and Fluid Streams", Ind. and Eng. Chem., Vol. 45, pp. 636, (1953).

30. Bacalso, A., "Report on the Determination of the Critical Shear Stress from the Measured Velocity Profile of a Flow Initiating Motion on a Bed of Fine Particles", Tech. Memo No. 62-4, W. M. Keck Laboratory of Hydraulics and Water Resources, California Institute of Technology, (1962).

31. Hill, M. J., "On a Spherical Vortex", Phil. Trans., A, Vol. 185, (1894).

32. Hinze, J. O., "Turbulence", McGraw Hill, (1959).

33. Townes, H. W., "Flow over a Rough Boundary", Doctoral thesis at California Institute of Technology, (unpublished), (1965).

34. Tsien, Hsue-Shen, "On the Design of the Contraction Cone for a Wind Tunnel", Jour. Aero. Sci., Vol. 10, No. 2, pp. 68-70, (1943).

35. Otto, G. H., "A Modified Logarithmic Probability Graph for the Interpretation of the Mechanical Analysis of Sediments", Jour. of Sedimentary Petrology, Vol. 9, No. 2, pp. 62-76, (1939).

36. Schlichting, H., "Boundary Layer Theory", McGraw Hill, (1960).

BIBLIOGRAPHY (Cont'd)

37. Mavis, F. T. and Laushey, L. M., "Formula for Velocity at Beginning of Bed-Load Movement is Reappraised", Civ. Eng., Vol. 19, No. 1, pp. 38-39 and 72, (1949).

38. Hwang, L. S., "Flow Resistance of Dunes in Alluvial Streams", Doctoral thesis, California Institute of Technology, (1965).

39. Bagnold, R. A., "Some Flume Experiments on Large Grains but Little Denser than the Transporting Fluid and their Implications", Proc. Inst. Civ. Engrs., Vol. 4, pp. 174-205, (1955).

40. Bagnold, R. A., "The Physics of Blown Sand and Desert Dunes", Methuen and Co. Ltd., London, (1941).

41. Favre, A., Gaviglio, J., and Dumas, R., "Further Space-time Correlations of Velocity in a Turbulent Boundary Layer", Journal Fluid Mechanics, Vol. 3, p. 344, (1958).

42. Menard, H. W., "Sediment Movement in Relation to Current Velocity", Journal Sedimentary Petrology, Vol. 20, No. 3, pp. 148-160, (1950).

43. Einstein, H. A., "Formulas for the Transportation of Bed Load", Trans. ASCE, Vol. 107, pp. 561-577, (1942).

44. Magarvey, R. H. and MacLatchey, C. S., "Formation and Structure of Vortex Rings", Canadian Jour. of Physics, vol. 42, p. 678, (1964).

45. Magarvey, R. H. and MacLatchey, C. S., "The Disintegration of Vortex Rings", Canadian Jour. of Physics, Vol. 42, p. 684, (1964).